Synthesis and Photoreaction Behavior of Photo-Cross-Linkable Polymer and Its Application for Photoalignment Layer

Kohei Goto

2013

Contents

General Introduction

Liquid crystal materials are well known as a representative self organization material. The combination of long range orientational ordering and relatively free movement of anisotropic molecules in liquid crystals (LCs) makes these materials unique. Since this combination leads to exceptional sensitivity of LCs to electric and magnetic fields, liquid crystal science and development of liquid crystal display (LCD) industries has initiated in the 1970s and grew up so far. Then, among the flat panel display technologies, LCD has been the most dominant. In such devices, aligning the LCs on the substrate is the most important technology. Generally, in order to obtain initial alignment of LCs, alignment layers made of organic materials are utilized and alignment is usually set by a rigid substrate with anisotropic surface. In order to generate an anisotropy on the polymer surface for making alignment layers, a mechanical rubbing with a cloth has been commonly used both, in small scientific labs, as well as large LCD factories.[1-5] This method is still actively used in the LCD industry for the alignment treatment of LCD substrates even with a linear size exceeding 3 meters. With respect to the type of alignment materials, conventional polyimides are widely used as alignment layers at present and they can lead to parallel alignment of LCs along to the rubbing direction.

Despite the apparent achievements of the rubbing technology, it has some serious issues, such as generation of fine dust particles, generation of static charge accumulation and poor uniformity of rubbing, which has been clear from the first step of its application and appeared to be crucial for the production of last generation LCDs including high resolution and high contrast devices. These drawbacks come from the contact type characteristics of the rubbing method and they can diminish the fundamental characteristics of the devices and, consequently, decrease productivity of LCD manufacturing.

As the limitation of the rubbing technique is getting obvious, alternative methods for LC alignment have been widely searched. Among the developed methods, the alignment technique by exposure of linearly polarized (LP) light, called “photoalignment”, shows the greatest industrial prospect.[6-42] As photoalignment technology is based on an anisotropic photoreaction of photoreactive polymeric layers by the use of polarized light in order to acquire the ability to align liquid crystals, the substrate must be covered with a layer containing photoreactive moieties. After LP irradiation to the photoreactive polymer is performed, absorption of irradiating LP light by photosensitive moieties is achieved under exclusive requirements including coincidence of the electric vector (**E**) of actinic

light with the electric dipole transition moment of ground-state chromophores. Consequently, axis-selective light absorption takes place to induce the generation of optical anisotropy such as dichroism and birefringence. This photoreaction is called "axis-selective photoreaction". This optical anisotropy caused by anisotropic distribution of the photoreacted molecules controls the LC alignment because the interaction between the photoreacted molecules and LCs are different from the interaction between unphotoreacted molecules and LCs.

The photoalignment effect was first reported in 1988 by Ichimura et al.[6] In this report, it was described that by exposure of a substrate grafted with azobenzene monolayers, the ability to control LC alignment from homeotropic to planar due to *trans-cis* isomerization of azobenzene moieties was achieved. Shortly after publication of Ichimura's results, Gibbons et al. reported an unidirectional in-plane LC alignment on a polymer film comprising azobenzene moieties[12] and, in 1992, Schadt et al. found that the LCs align on poly(vinyl cinnnamate) film, in which anisotropic photo-cross-linking was carried out by LP ultraviolet (UV) light irradiation.[5] The latest results has received much attention since it provided relatively stable LC alignment due to photo-cross-linking. The advantages of photoalignment (which is a contact less technology) are evident compared to rubbing technique.

Possible benefits for using this technique include:

1. Elimination of electrostatic charge and impurities as well as of mechanical damage of the surface.
2. A controllable pretilt angle and alignment direction of LCs
3. Providing uniform alignment of LCs, especially in LCDs with the pixels of a high resolution.

Therefore, photoalignment technique became one of the hottest topic because of the possibility to realize a contactless technology from the view point of practical use and, in this way, several types of photoreactive material for the photoalignment layer have been investigated. They are usually categorized in three groups according to prevailing photochemistry of their photosensitive groups. The first group is includes materials undergoing *trans-cis* photoisomerization.[6,12-17] This reaction is reversible; *cis*-isomers can be transferred back to the *trans*-state either by irradiation with a proper wavelength or by thermal activation. This group of materials mainly includes azo-compounds in the form of small molecules as dopants in polymer matrices and azobenzene containing polymers and stilbene

derivatives. The second group comprises materials photoreactable based on photo-degradation represented by chain scission reaction of polyimides (PIs).[35-40] The third group includes various photo-cross-linkable moieties, which can be used in the form of small molecules as well as polymers. The majority of these materials undergo [2 + 2] cycloaddition type photoreaction.[5,7,16-36] The typical materials that undergo photo-cross-linking are represented by cinnnamate,[5,7,18,21-28] coumarin,[34-36] chalconyl[31] and maleimide[45,46] groups. In addition, the photoalignment ability of anthracenyl containing polymers due to [4 + 4] cycloaddition was investigated.[47] Recently, good photoalignment properties of methacrylamidoarylmethacrylates were reported.[48.49] Cross-linkings in these materials are formed due to radical photopolymerization of methacryloyl groups accompanied with photo-Fries rearrangements.[50] With respect to cinnamate and chalcone derivatives, [2 + 2] cycloaddition is accompanied with *trans-cis* isomerization. On the other hand, in the materials with rigid structure, such as coumarin and maleimide, *trans-cis* isomerization does not occur and at high exposure doses their photodegradation becomes an issue.

From a practical view point, these photoreactive materials have advantage as well as disadvantages. The azobenzene moieties show good LC alignment at low exposure dose, which can be less than 50 mJ cm^{-2}. However, this alignment is not stable enough against heat and light because of the reversible photochemistry and orientational disordering of azobenzene fragments. In contrast, photodegradation of PIs give sufficiently alignment stability and high anchoring energy since photoinduced optical anisotropy of PI film based on the photodegradation of the materials along parallel direction to the polarization of LPUV light seems to be quite large as in the case of mechanical rubbed film. However, large exposure energy is generally required to achieve sufficient LC alignment on PI films because it needs sufficient amount of axis-selective photodegradation of the materials. Photo-cross-linkable materials may combine good photosensitivity and alignment stability of LC due to irreversible photochemistry and strongly restricted molecular motion.

In this way, alignment materials which can induce large optical anisotropy and its stability with high photosensitivity are strongly required.

The controlled alignment of molecules in photoreactive polymer films induced by photoreaction can afford large optical anisotropy because molecules in polymer films align in a direction either parallel or perpendicular to the **E** of LP light. This phenomenon is usually observed after irradiating polymer films with LPUV, in which photoreactive mesogenic side

groups are connected to poly-(meth) acrylate backbone through a spacer. Several types of materials have been reported, including azobenzene-containing polymers and photo-cross-linkable polymers, which can generate optical anisotropy on their films upon irradiation with LP light.[51-66] In particular, numerous studies of azobenzene containing polymers have been performed to characterize the axis-selective *trans-cis* photoisomerization reaction which leads to in-plane, high molecular reorientation in a direction perpendicular to **E** of LP light as in the case of using as a photoalignment layer. Alternatively, we have studied a photo-cross-linkable polymer liquid crystal (PLC) containing a cinnamoyloxyethoxybiphenyl side group and its copolymers which exhibit thermally stable reorientation of mesogenic side groups by the use of LPUV light and subsequent annealing as shown in **Figure 1**.[67-69] This phenomenon is called "Thermally enhanced photoinduced reorientation".

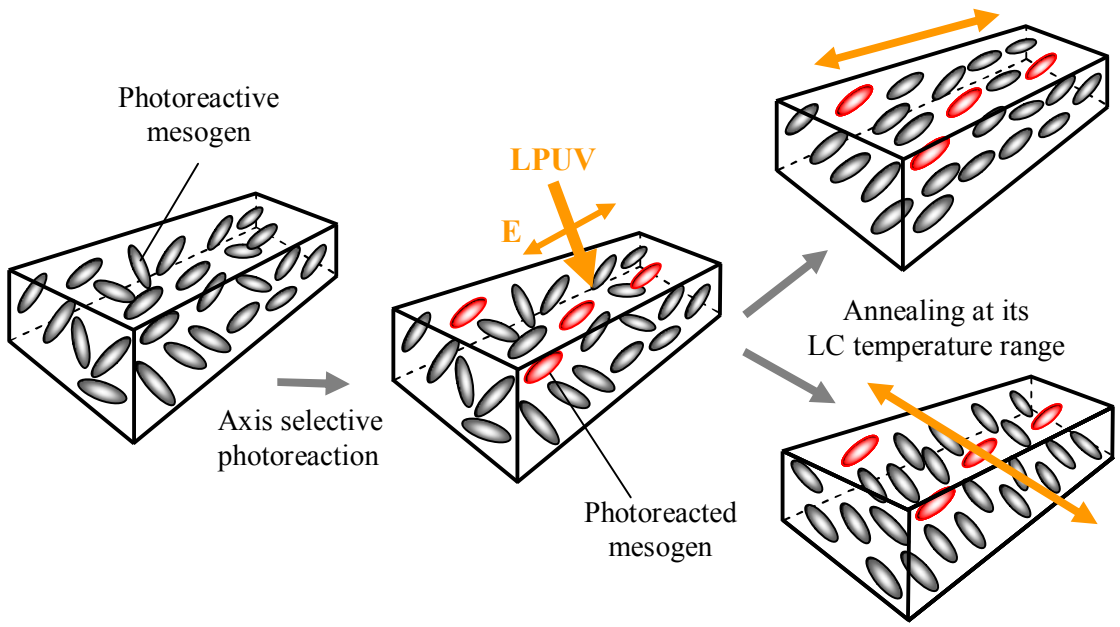

Figure 1 Concept illustration of thermally enhanced photoinduced reorientation

In this thesis, I firstly focused on the photoalignment of LCs and its mechanism on the photo-cross-linkable polymers because, in the case of cinnamate and chalcone derivatives, it is not clear which kind of photoreaction, photo-cross-linking or photoisomerization, affect the photoalignment of LCs. Next I studied the development of PLCs having large and reversible orientation order of mesogenic side groups. The molecularly oriented films may prove to be useful in birefringent optical devices, optical memories, holographic elements, phase retarders

and photoalignment layer for LCD. As I described above, molecularly oriented structure is expected to improve photoalignment properties, especially anchoring energy and alignment stability of LCs, and therefore, I investigated its photoalignment performance from a practical standpoint. In addition, I designed and synthesized new type of polyamic-ester (PAE) derivatives comprising photo-cross-linkable groups in the polymer main chain. In this way, the anisotropic photoreaction of PAE by LPUV light irradiation was performed and the photoinduced optical anisotropy of the resultant films as well as their photoalignment behavior were investigated.

Chapter 1 deals with a novel photo-cross-linkable polymer liquid crystal comprising coumarin-containing side group. After describing the design, synthesis and thermal properties of the novel methacrylate polymer having photo-cross-linkable coumarin moieties at the end of the mesogenic groups, anisotropic photoreaction at a various conditions by LPUV light irradiation are carried out. Then, it is described the photoinduced optical anisotropy and LC alignment behavior on the resultant films.

In Chapter 2, novel photo-cross-linkable methacrylates with a 4-methoxycinnamoyloxy-biphenyl side group were synthesized and reversion of the in-plane reorientation direction of the mesogenic groups of PLC films generated by irradiation with LPUV light and subsequent annealing was demonstrated. The orientational behavior of the film was studied using polarization UV-vis and FT-IR spectroscopies. In order to investigate the photoproduct influence on reorientational behavior, spectral analysis of mesogenic group synthesized in this study was performed.

In chapter 3, it is described a new photoalignment layer for LCs containing photo-cross-linkable mesogen and a photosensitizing group which exhibits high photosensitivity, high azimuthal anchoring, tilt-angle formation of LCs, and high thermal stability.

Chapter 4 deals with the new photoreactive LC polymer which was prepared via polymer reaction. After design and synthesis of polymers, thermally enhanced photoinduced reorientation behavior was investigated.

Chapter 5 deals with the new photoreactive PAE derivative containing *p*-phenylene diacrylate in the polymer main chain. After design and synthesis of the PAE, the influence of the exposure condition on its photoreactivity and LC alignment behavior were investigated.

In chapter 6, the photoalignment performance of larger molecularly oriented film made of PLC comprising photo-cross-linkable group was investigated from the practical stand point using In Plane Switching LC cell.

References

1) J. Cognard: Mol. Cryst. Liq. Cryst. Suppl. Ser., **1982**, *1*, 1.

2) K. W. Lee, S. H. Peak, A Lien, C. During, H. Fukuro: *Macromolecules*, **1996**, *29*, 8894.

3) k. Sakamoto, R. Arafune, N. Ito, S. Ushioda, Y. Suzuki, S. Morokawa: *J. Appl. Phys.*, **1996**, *80*, 709.

4) M. Schadt and W. Helfrich: *Appl. Phys. Lett.*, **1971**, *18*, 127.

5) M. Schadt, K. Schmitt, V. Kozinkov and V. Chigrinov: *Jpn. J. appl. Phys.*, **1992**, *31*, 2155.

6) K. Ichimura, Y. Suzuki, T. Seki, A. Hosoki and K. Aoki: *Langmuir*, **1988**, *4*, 1214.

7) M. Schadt, H. Seiberle and A. Schuster: *Nature*, **1996**, *381*, 212.

8) K. Ichimura: *Chem. Rev.*, **2000**, *100*, 1847.

9) M. O'Neill and S. M. Kelly: *J. Phys. D, appl. Phys.*, **2000**, *33*, R67.

10) O. Yaroshchuck and Y. Reznikov: *J. Mater. Chem.* **2012**, *22*, 286

11) K. Ichimura: *Polymers as Electrooptical and Photooptical Active Media*, edited by V. Shibaev (Berlin: Springer), **1996**, p. 138.

12) W. M. Gibbons, P. J. Shannon, S. T. Sun and B. J. Swetlin: *Nature*. **1991**, *351*, 49.

13) W. M. Gibbons, T. Kosa , P. P. Muhoray, P. J. Shannon and S. T. Sun: *Nature*. **1995**, *377*, 43.

14) S. T. Sun, W. M. Gibbons and P. J. Shannon: *Liq. Cryst.* **1992**, *12*, 869.

15) V. A. Barachevsky: *Proc. SPIE*, **1991**, *1559*, 184.

16) K. Ichimura, H. Aliyama, N. Ishizuki and Y. Kawanishi: *Macromol. Chem. Rapid Commun*. **1993**, *14*, 813.

17) K. Ichimura: *J. Photopolym. Sci. Technol.*, **1995**, *8*, 343.

18) M. Schadt, H. Seiberle, A. Schuster and S. M. Kelly: *Jpn. J. appl. Phys.*, **1995**, *34*,

3240.

19) Y. Iimura, T. Saitoh, S. Kobayashi and T. Hashimoto: *J. photopolym. Sci. Technol.*, **1995**, *2*, 257.

20) X. T. Li, D. H. Pei, S. Kobayashi and Y. Iimura: *Jpn. J. appl. Phys*., **1997**, *36*, L432.

21) K. Ichimura, Y. Akita, H. Akiyama, K. Kudo and Y. Hayashi: *Macromolecules*, **1997**, *30*, 903.

22) K. Ichimura, Y. Akita, H. Akiyama, Y. Hayashi and K. Kudo: *Jpn. J. appl. Phys.*, **1996**, ***35***, L992.

23) D. Shenoy, K. Gru¨ eneberg, J. Naciri and R. Shashidhar: *Jpn. J. appl. Phys.*, **1998**, *37*, L1326.

24) M. Schadt, H. Seiberle, A. S. Schuster and M. Kelly: *Jpn. J. appl. Phys.*, **1995**, *34*, L764.

25) Y. Akita, H. Akiyama, Y. Hayashi and K. Ichimura: *J. photopolym. Sci. Tech.*, **1995**, *8*, 75.

26) M. Obi, S. Morino and K. Ichimura: *Jpn. J. appl. Phys.*, **1999**, *38*, L145.

27) H. Kim and J. Park, *Jpn. J. appl. Phys.*, **1999**, *38*, 201.

28) J. Liu, X. Liang and H. Gao: *Jpn. J. appl. Phys.*, **2000**, *39*, L1221.

29) N. Kawatsuki, H. Ono, H. Takatsuka, T. Yamamoto and O. Sangen: *Macromolecules*, **1997**, *30*, 6680.

30) N. Kawatsuki, H. Takatsuka, T. Yamamoto and H. Ono: *Jpn. J. appl. Phys.*, **1997**, *36*, 6464.

31) N. Kawatsuki, H. Takatsuka, Y. Kawakami and T. Yamamoto: *Polym. Adv. T echnol.*, **1999**, *10*, 429.

32) N. Kawatsuki, K. Matsuyoshi, M. Hayashi, H. Takatsuka and T. Yamamoto: *Chem. Mater.*, **2000**, *12*, 1549.

33) Y. Makita, T. Natsumi, S. Kimura, S. Nakata, M. Kimura, Y. Matsuki and Y. Takeuchi: *J. Photopolym. Sci.* **1998**, *11*, 187.

34) M. Obi, S. Morino and K. Ichimura: *Chem. Mater.*, **1999**, *11*, 656.

35) M. Obi, S. Morino and K. Ichimura: *Macromol. rapid Commun.*, **1998**, *19*, 643.

36) P. O. Jacson, P. Hindmarsh, S. M. Kelly and M. O'Neill: *in Abstracts of the 18th International Liquid Crystal Confonference*, *Sendai*, *Japan*, **2000**, p. 85.

37) M. Hasegawa and Y. Taira: *J. Photopolym. Sci.* **1995**, *8*, 241

38) J. L. West, X. Wang, Y. Ji, and J. R. Kelly: *Dig. Tech. Pap. SID.* **1995**, *26*, 703.

39) H. Endo, Y. Miyama, T. Nihira, H. Fukuro, E. Akiyama and Y. Nagase: *J. Photopolym. Sci.* **2000**, *13*, 277.

40) M. Nishikawa, T. Kosa and J. L. West: *Jpn. J. Appl. Phys.* **1999**, *38*, L334.

41) C. J. Newsome and M. O'Neill: *J. Appl. Phys.* **2000**, *88(12)*, 7328.

42) S. -K. Park, U. -S. Jung, S. –B. Kwon, M. Yi, Ahn, J. –S. Kim, Y. Kurioz and Y. Reznikov: *J. Soc. Inf. Disp.* **2010**, *18/3*, 199.

43) S. W. Lee, T. Chang and M. Lee: *Macromol. Rapid Commun.* **2001**, *22*, 941.

44) W. C. Lee, C. S. H and S. T. Wu: *Jpn. J. Appl. Phys.* **2000**, *39*, L471.

45) L. O. Vretik, V. G. Syromyatnikov, V. V. Zagniy, E, A. Savchuk and O. V. Yaroshchuk: *Mol. Cryst. Liq. Cryst.*, **2008**, *486*, 57.

46) H. Murai, T. Nakata and T. Goto: *Liq. Cryst.*, **2002**, *29(5)*, 669.

47) N. Kawatsuki, T. Arita, Y. Kawakami and T. Yamamoto: *Jpn. J. Appl. Phys.* **2000**, *39*, 5943.

48) L. Vretik, V. Syromyatnikov, V. Zagniy, L. Paskal, O. Yaroshcuk, L. Dolgov, V. Kyrychenko and C. Lee: *Mol. Cryst. Liq. Cryst.*, **2007**, *479*, 121.

49) L. Vretik, L. Paskal, V. Syromyatnikov, V. Zagniy, O. Savchuk, L. Dolgov, O. Yaroshcuk and C. Lee: *Mol. Cryst. Liq. Cryst.*, **2007**, *468*, 173.

50) V. Kyrychenko, G. Smolyakov, V. Zagniy, L. Vretik, L. Paskal, V. Syromyatnikov and O. Yaroshcuk: *Mol. Cryst. Liq. Cryst.*, **2008**, *496*, 278.

51) (a) Fischer, T.; La¨sker, L.; Stumpe, J. *J. Photochem. Photobiol. A: Chem.* **1994**, *80*, 453. (b) Andrews, S. R.; Williams, G.; La¨sker, L.; Stumpe, J. *Macromolecules* **1995**, *28*, 8863, (c) Fischer, T.; La¨sker, L.; Czapla, S.; Ru¨ bner, J.; Stumpe, J. *Mol. Cryst. Liq. Cryst.* **1997**, *298*, 213.

(52) (a) Holme, N. C. R.; Ramanujam, P. S.; Hvilsted, S. *Appl. Opt.* **1996**, *35*, 4622. (b) Ramanujam, P. S.; Holme, C.; Hvilsted, S.; Pedersen, M.; Andruzzi, F.; Paci, M.; Tassi,

E.;Magagnini, P.; Hoffman, U.; Zebger, I.; Siesler, H. W. *Polym. Adv. Technol.* **1996**, *7*, 768.

(53) (a) Wu, Y.; Zhang, Q.; Kanazawa, A.; Shiono, T.; Ikeda, T. *Macromolecules* **1999**, *32*, 3951. (b) Wu, Y.; Demachi, Y.; Tsutsumi, O.; Kanazawa, A.; Shiono, T.; Ikeda, T. *Macromolecules* **1998**, *31*, 4457. (c) Wu, Y.; Demachi, Y.; Tsutsumi, O.; Kanazawa, A.; Shiono, T.; Ikeda, T. *Macromolecules* **1998**, *31*, 1104. (d) Wu, Y.; Demachi, Y.; Tsutsumi, O.; Kanazawa, A.; Shiono, T.; Ikeda, T. *Macromolecules* **1998**, *31*, 349.

(54) Meng, X.; Natansohn, A.; Rochon, P. *Supramol. Sci.* **1996**, *3*, 207.

(55) Labarthet, F.; Freiberg, S.; Pellerin, C.; Pe´zolet, M.; Natansohn, A.; Rochon, P. *Macromolecules* **2000**, *33*, 6815.

(56) Ruslim, C.; Ichimura, K. *Macromolecules* **1999**, *32*, 4254.

(57) Han, M.; Morino, S.; Ichimura, K. *Chem. Lett.* **1999**, 645.

(58) Han, M.; Ichimura, K. *Macromolecules* **2001**, *34*, 82.

(59) Han, M.; Ichimura, K. *Macromolecules* **2001**, *34*, 90.

(60) Han, M.; Morino, S.; Ichimura, K. *Macromolecules* **2000**, *33*, 6360.

(61) (a) Meier, J. G.; Ruhmann, R.; Stumpe, J. *Macromolecules* **2000**, *33*, 843. (b) Stumpe, J.; Fischer, T.; Rutloh, M.; Meier, J. G. *Proc. SPIE* **1999**, *3800*, 150.

(62) Kidowaki, M.; Fujiwara, T.; Morino, S.; Ichimura, K.; Stumpe, J. *Appl. Phys. Lett.* **2000**, *76*, 1377.

(63) Date, R. W.; Fawcett, A. H.; Geue, T.; Haferkorn, J.; Malcolm, R. K.; Stumpe, J. *Macromolecules* **1998**, *31*, 4935.

(64) Kawatsuki, N.; Takatsuka, H.; Yamamoto, T.; Sangen, O. *J. Polym. Sci., Part A: Polym. Chem.* **1998**, *36*, 1521.

(65) (a) Kawatsuki, N.; Suehiro, C.; Yamamoto, T. *Macromolecules* **1998**, *31*, 5984. (b) Kawatsuki, N.; Matsuyoshi, K.; Yamamoto, T. *Macromolecules* **2000**, *33*, 1698.

(66) (a) Kawatsuki, N.; Suehiro, C.; Shindo, H.; Yamamoto, T.; Ono, H. *Macromol. Rapid Commun.* **1998**, *19*, 201. (b) Kawatsuki, N.; Yamamoto, T.; Ono, H. *Appl. Phys. Lett.* **1999**, *74*, 935.

(67) Kawatsuki, N.; Takatsuka, H.; Yamamoto, T.; Sangen, O. *J. Polym. Sci., Part A: Polym. Chem.* **1998**, *36*, 1521.

(68) (a) Kawatsuki, N.; Suehiro, C.; Yamamoto, T. *Macromolecules* **1998**, *31*, 5984. (b) Kawatsuki, N.; Matsuyoshi, K.; Yamamoto, T. *Macromolecules* **2000**, *33*, 1698.

(69) (a) Kawatsuki, N.; Suehiro, C.; Shindo, H.; Yamamoto, T.; Ono, H. *Macromol. Rapid Commun.* **1998**, *19*, 201. (b) Kawatsuki, N.; Yamamoto, T.; Ono, H. *Appl. Phys. Lett.* **1999**, *74*, 935.

Chapter 1

Photoinduced Anisotropy and Photoalignment of Nematic Liquid Crystals by a Novel Polymer Liquid Crystal with a Coumarin-Containing Side Group

1-1. Introduction

Linearly polarized ultraviolet (LPUV) light induces an optical anisotropy in photo-cross-linkable polymer films because of an angular-selective photoreaction, and the resultant films are applied as the alignment layer for liquid crystals (LCs).[1–5] Typical materials are based on cinnamate derivatives such as poly(vinyl cinnamate) (PVCi). PVCi is a well known negative-type photoresist, and a negative optical anisotropy is induced by the LPUV light irradiation.[1,6] The LC aligns on the photoreacted PVCi films in a direction perpendicular to the electric vector (**E**) of the incident LPUV light.[1,3–10] The LC alignment behavior on the photoreacted PVCi film is induced by two kinds of angular selective photoreaction, viz. a [2 + 2] photocycloaddition reaction and *trans-cis* photoisomerization.[10–12] In this way, several kinds of cinnamate-containing polymers used for the LC alignment layer have been reported.[10,11,13–18] We have also studied polymethacrylates with a cinnamoyloxyalkoxybiphenyl side group (**p*m*B*n*Ci** in **Figure 1-1**) for the LC alignment layer.[19–22] In this case, the 'whole' photo-cross-linked side mesogenic group controls the parallel LC alignment,[20,21] although it was difficult to clarify the effect of the photoisomerization of the cinnamoyl group on the LC alignment, because the spectrum of the cinnamoyl group overlaps with that of the biphenyl group.

Coumarin derivatives also undergo angular-selective photoreaction and polymer films with coumarin side groups have been applied as LC alignment layer.[2,23-25] Since the coumarin exhibits no photoisomerization, the LC alignment on a coumarin-containing polymer film can be brought about only by the [2 + 2] photocycloaddition reaction.[23] Shadt *et al*. reported that the LC aligns in a direction parallel to **E** of the incident LPUV light on a polymer film comprising coumarin side groups.[2] Ichimura et al. made systematic studies on the effect of the spacer length using methacrylates with coumarin side groups and investigated the reversion of the LC alignment direction.[23,24] With respect to the photochemistry of coumarin derivatives, it is well known that they can produce four regioisomeric photodimers, viz. *syn*- and *anti*-

head-to-head (H-H) dimers, and *syn*-and *anti*-head-to-tail (H-T) dimers.[26-29] The type of photodimer depends on the nature and the position of the substituents in the solid state. Therefore, it is important to study the influence of the type of photodeimer on the LC photoalignment behavior using coumarin-containing photopolymers.

In this work, I synthesized a novel methacrylate polymer liquid crystal (PLC: **P6MBC**) with a coumarin moiety at the end of the mesogenic groups as illustrated in **Figure 1-1**. This polymer comprises a biphenyl side group connected to a coumarin group instead of a cinnamate group as in **p*m*B*n*Ci**, resulting in elimination of the influence of photoisomerization. The photoreaction of a thin film was carried out by using LPUV light under various conditions. In this chapter, it is concluded that the photoinduced optical anisotropy of the films and the LC alignment behavior on the resultant films are greatly dependent on the irradiation conditions, the type of photodimer and the orientation of the mesogenic side groups.

1-2. Experimental Section

1-2-1. Materials and Monomer Synthesis

All starting materials were used as received from Tokyo Kasei Chemicals. 2,2'–Azobis(2–methylpropionate) (AIBN) was recrystalized from ethanol and stored at 0 °C. Monomers and the polymer were synthesized according to the reaction scheme in **Figure 1-1**, and the chemical structures of the synthesized monomers and polymer were confirmed by ^{1}H-NMR and FT-IR spectroscopy.

4-(6-Methacryloyloxyhexyloxy)-4'–hydroxybiphenyl was synthesized from 4'-(6-Bromohexyloxy)-4'–hydroxybiphenyl and Lithium methacrylate by using a previously reported method.[30] Yield, mp, NMR, and IR spectroscopic characteristics are as follows: Yield; 67.8 %, mp 68-70 °C, ^{1}H-NMR ($CDCl_3$): δ (ppm) 1.51-1.58 (m, 4H, -O-$(CH_2)_2$-(CH_2)$_2$-$(CH_2)_2$-O-), 1.70-1.85 (m, 4H, -O-CH_2-CH_2-(CH_2)$_2$-CH_2-CH_2-O-), 1.95 (s, 3H, CH_2=C(CH_3)), 3.99 (t, 2H, J = 6.43 Hz –COO-CH_2-), 4.17 (t, 2H, J = 6.11 Hz CH_2-O-Ph), 4.85 (s, 1H, PhO*H*), 5.55 (s, 1H, -CH_2=C(CH_3)), 6.1 (s, 1H, -CH_2=C(CH_3)), 6.86-6.95 (dd, 4H, Ph). IR (KBr): 3336, 2934, 1719, 1608, 1248, 1171, 830 cm^{-1}.

6-[4'-(6-Methacryloyloxyhexyloxy)biphenyl-4-yloxy]methyl coumarin (6MBC) was synthesized from 4-(6-Methacryloyloxyhexyloxy)-4'–hydroxybiphenyl and 6-Bromo coumarin in Yield; 59.9 %, mp 123-126 °C, ^{1}H-NMR ($CDCl_3$): δ (ppm) 1.45-1.55 (m, 4H,

-O-CH_2-CH_2-(CH_2)$_2$-CH_2-CH_2-O-), 1.72 (m, 2H, -COO-CH_2-CH_2-), 1.82 (m, 2H, -(CH_2)$_4$-CH_2-CH_2-O-), 1.94 (s, 3H, CH_2=C(CH_3)), 3.99 (t, 2H, J = 6.4 Hz –COO-CH_2-), 4.16 (t, 2H, J = 6.11 Hz CH_2-O-Ph), 5.13 (s, 2H, Ph-O-CH_2-Ph), 5.54 (s, 1H, CH_2=C(CH3)), 6.1 (s, 1H, CH_2=C(CH3)), 6.94 (d, 2H, J = 8.63 Hz Ph-Ph), 7.02 (d, 2H, J = 8.64 Hz, Ph-Ph), 7.37 (d, 1H, J = 8.37 Hz, Ph(coumarin)), 7.48 (m, 4H, Ph-Ph), 7.6-7.62 (m, 2H,Ph(coumarin)), 7.73 (d, 1H, J = 9.52 Hz, -C*H*=CH- coumarin)). IR (KBr): 2940, 1731, 1606, 1574, 1502, 1237, 1179, 825 cm^{-1}.

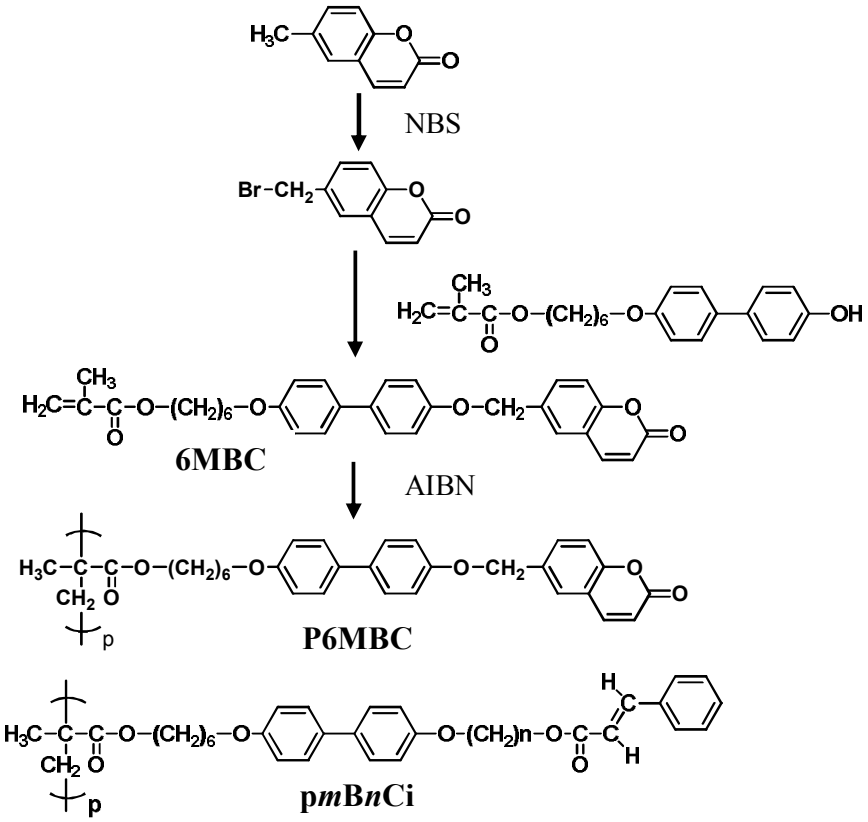

Figure 1-1 Chemical structure and synthetic route to the polymer liquid crystal.

P6BC: ^{1}H-NMR ($CDCl_3$): δ (ppm) 0.9-1.8 (m, 10H, -OCH2-(CH2)4-CH2-O-Ph, CH_2=C(CH_3)COO-), 1.67 (brs, 2H, CH_2=C(CH_3)COO-), 3.9-4.0 (m, 4H, -COO-CH_2-CH_2, -CH_2-CH_2-O-Ph), 4.95 (brs, 2H, -O-CH_2-Ph (coumarin)), 6.35 (m, 1H, CH=C*H*-CO), 6.8-6.9 (m, 4H, Ph-Ph), 7.27 (m, 1H, Ph (coumarin)), 7.4-7.5 (m, 6H, Ph-Ph, Ph (coumarin)), 7.63 (m, 1H, C*H*=CH-CO (coumarin)). IR (KBr): 3035, 2940, 1735, 1607, 1573, 1497, 1234, 1174, 822 cm^{-1}.

1-2-2. Characterization, Photoreaction and LC Alignment

^{1}H-NMR spectra were measured with a Bruker DRX-500 FT-NMR apparatus. The molecular weight of **P6MBC** was measured by GPC (Tosoh HLC-8020 GPC system with Tosoh TSK gel column; eluent, THF) calibrated using polystyrene standards. Thermal properties were examined using a polarization optical microscope (Olympus BHA-P) equipped with a Linkam TH600PM heating and cooling stage in addition to differential scanning calorimetry (DSC; Seiko-I SSC5200H) analysis at a heating and cooling rate of 10 K/min. Polarization FTIR spectra were recorded through a JASCO FTIR-410 system with an attached wire-grid polarizer. Polarization UV-vis spectra were measured using a Hitachi U-3030 spectrometer equipped with Glan-Taylor polarizing prisms.

1-2-3. Photoreaction

Thin film of **P6MBC** was prepared by spin-coating a methylene chloride solution of polymers (~3 wt %) onto a quartz or CaF_2 substrate. The film thickness was 0.2-0.5 μm, which was determined by the stylus contact method using Taly-Step (Rank Taylar Hobson). Photoreaction was performed by irradiating light from a 250 W Xe-Hg UV lamp after passing through Glan-Taylor polarizing prisms with a cutoff filter under 290 nm. The light intensity was about 12 mW cm^{-2} at 365 nm. Optical anisotropy of the film was measured by polarizing microscopy and polarization UV-vis and FT-IR spectra. Optical anisotropy measured by polarization UV-vis spectra is expressed as following eq :

$$\Delta A = A_{\parallel} - A_{\perp}$$

where $A_{\parallel}$ and $A_{\perp}$ are the absorbances parallel and perpendicular to **E** of the LPUV light. The LC alignment behavior was evaluated by dichroic absorption measurements utilizing the guest-host effect of a dye-doped nematic LC (ZLI 4792: Merck, T_i = 102 °C) as previously described in literature 19, 20. The order parameter, S, of a dye is expressed in the form of following eq :[23]

$$S = (A_p - A_s) / (A_{(large)} + 2A_{(small)})$$

where A_p and A_s are the absorbances parallel and perpendicular to **E**, respectively, while $A_{(large)}$ is taken to be the larger of A_p and A_s, while $A_{(small)}$ is taken to be the smaller. S was calculated by polarized UV-vis spectroscopy.

1-3. Results and Discussion

1-3-1. Photo induced Reorientation

P6MBC exhibited a liquid crystalline phase as summarized in **Table 1-1**. Polymer films were irradiated by using LPUV light at various temperatures. After exposure, all films became insoluble in organic solvents due to the [2 + 2] photo-cross-linking reaction of the coumarin group. Photoreaction and photoinduced optical anisotropy of the film were examined by obtaining a polarization UV absorption spectrum.

Table 1-1 Molecular Weight and Thermal Properties of **P6MBC**.

Polymer	Molecular Weight (g/mol) [a]		Phase Trandition Temperature (°C) [b]			
	$M_w \times 10^{-3}$	$M_n \times 10^{-3}$	T_g	T_m	Phase	T_i
P6MBC	49.1	34.4	61	145	LC	220

a Determined by GPC, Polystylene standards, THF as eluent
b Determined by polarization microscopy observation and DSC
T_g = glass transition, T_m = melting point, T_i = clearing point

Figure 1-2-1-4. shows the changes in the absorption spectra and the induced ΔA when films were irradiated at room temperature, 180 °C and 220 °C, respectively. When a film was irradiated at room temperature (**Figure 1-2**), the absorption decreased and shifted to shorter wavelentgth with increasing dose of irradiation due to the photo-cross-linking of the coumarin group, and a small negative dichroism corresponding to the angular-selective photoreaction of the coumarin group was observed. However, when the irradiation energy was 3.6 J cm^{-2} or more, the absorbance around 270 nm still decreased, suggesting a side photoreaction of the biphenyl group besides the photocycloaddition reaction.[20] In contrast, when a film was irradiated at 180 °C (LC temperature range), the shape of the spectrum changed and the induced dichroism was very small as shown in **Figure 1-3**. The absorption maximum shifted from 270 to 285 nm, and the absorbance around 330 nm increased after the irradiation using the range 0.0036 – 0.18 J cm^{-2}. The shape of the spectrum became similar to that in **Figure 1-2(a)** when the irradiation energy was 3.6 J cm^{-2} or more. In addition, a strong decrease in the absorption and a red shift of the absorption maximum were observed even though the film was annealed at 180 °C without UV light exposure. The red shift and the decrease in the

absorption would be a consequence of a head-to-tail aggregation or an out-of-plane alignment of the mesogenic side groups.[31,32] The detailed orientational behavior of the mesogenic side groups at elevated temperature is discussed later.

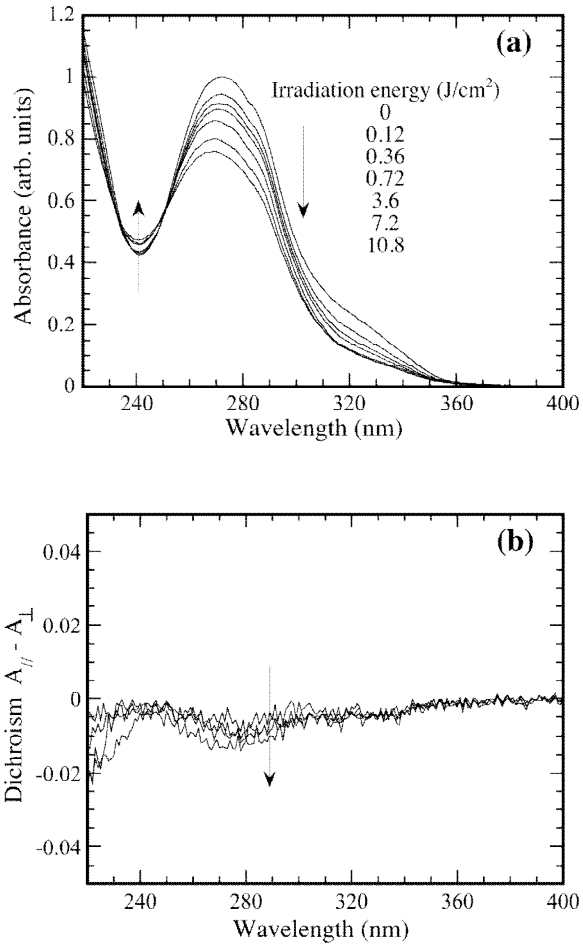

Figure 1-2 Change in absorbance (a) and induced dichroism (b) of **P6MBC** film irradiated at room temperature.

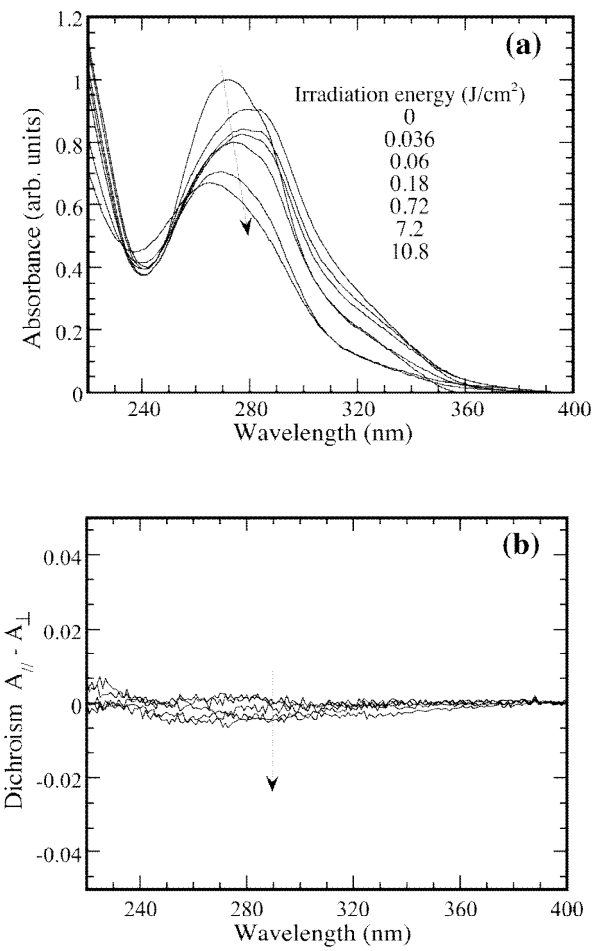

Figure 1-3 Change in absorbance (a) and induced dichroism (b) of **P6MBC** film irradiated at 180 °C.

When the film was irradiated at 220 °C (near T_i), the change in the UV spectrum was similar to that for a film irradiated at room temperature. However, the induced dichroism was positive at the beginning of the photoirradiation and decreased when the exposure energy was 3.6 J cm^{-2} or more, as shown in **Figure 1-4(b)**. The positive dichroism is due to a thermally enhanced photoinduced orientation of the mesogenic groups in a direction parallel to **E**, This phenomenon is similar to that observed for polymer liquid crystal films of **p*m*B*n*Ci** derivatives when they are irradiated by LPUV light around T_i.[20,33,34]

1-3-2. FT-IR Study

To investigate the type of photoproduct from the coumarin group, FT-IR spectroscopy measurements were carried out. **Figure 1-5** shows the change in FT-IR spectrum after UV light irradiation of 3.0 J cm^{-2} at various temperatures. The peak at 1730 cm^{-1} before exposure is assigned to the C=O stretching of both coumarin and ester units of polymethacrylate chains, and the peak at 1574 cm^{-1} is the cis-C=C stretching of the coumarin group. After exposure, the intensity of the cis-C=C stretching band decreased in all cases due to the dimerization of the coumarin group.

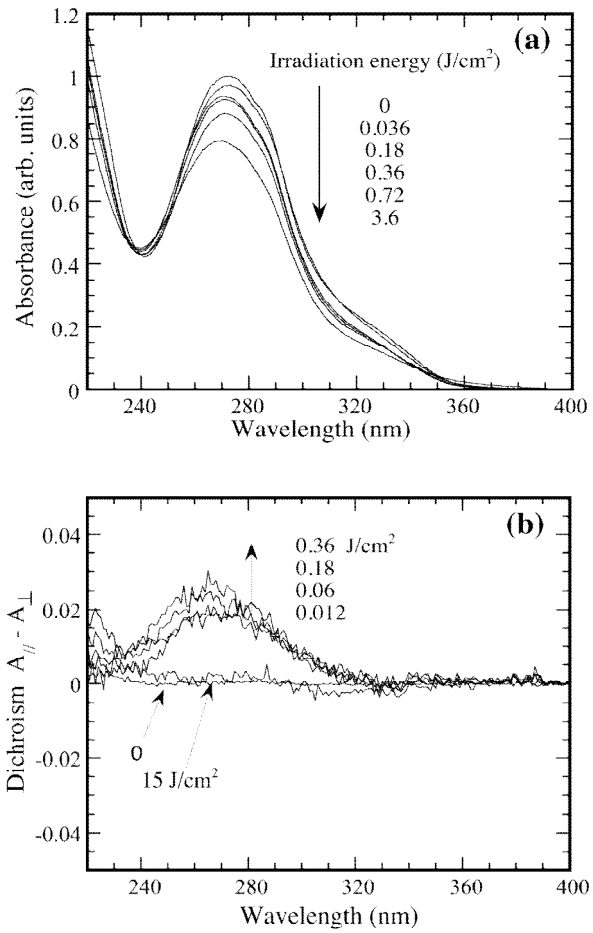

Figure 1-4 Change in absorbance (a) and induced dichroism (b) of **P6MBC** film irradiated at 220 °C.

It has been reported that the difference in the isomerism of cyclobutane adducts can be distinguished by a spectral shift of the C=O stretching band of a coumarin group.[28,29] According to the literature, the shift to higher wavenumbers is attributed to the formation of an H-H dimer, while that to lower wavenumbers is due to the formation of an H-T dimer.[29] For **P6MBC**, a new band at 1775 cm^{-1} appeared when the film was irradiated at room temperature, and the absorption of the C=O stretching band became broad when the film was irradiated at 180 or 220 °C. These results suggest that the H-H dimer was the main adduct when the film was irradiated at room temperature, while the H-T dimer was the main adduct when irradiated at 180 or 220 °C. The shift to lower wavenumbers might be small and it will be overlapped by the ν(C=O) of the polymethacrylate chains.

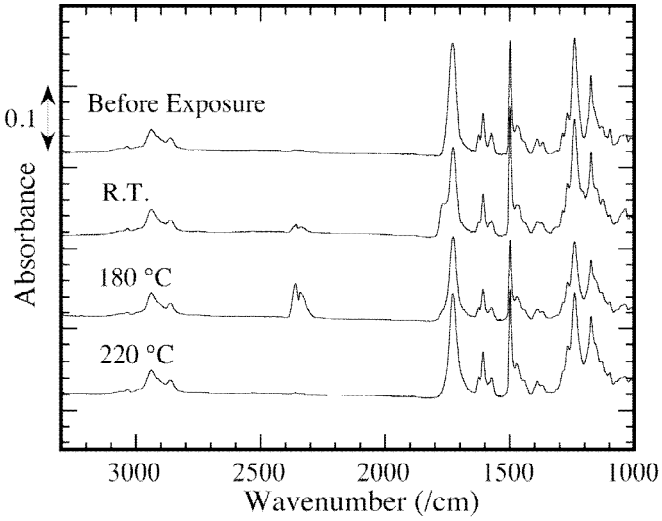

Figure 1-5 FT-IR spectra of **P6MBC** film before and after irradiation of 3.0 J cm^{-2} exposure dose at various temperatures.

1-3-3. Mesogenic Groups Behavior at Elevated Temperature

Since the UV absorption spectrum has changed after annealing in the LC temperature range of **P6MBC** as described in the above section, the orientational behavior of the mesogenic groups was investigated by polarization UV spectroscopy and FT-IR spectroscopy.

Figure 1-6 shows UV absorption spectra of films before and after annealing at 180 °C for 10 min, and also the absorption spectrum of the annealed film measured at various angles (θ_m) of the incident *p*-polarized probe light to obtain information about the three-dimentional orientation of the mesogenic groups. For normal incidence of the probe light (θ_m = 0°), the absorption decreased and red shift of the spectrum was seen after annealing. In addition, a small shoulder-like absorption band around 285 nm, as seen before exposure, was enhanced after annealing. The same absorption band was enhanced, as shown in **Figure 1-2 (a),** when the irradiation dose was 0.18 J cm^{-2} or less. This band is a consequence of mesogenic groups arranged in the head-to-tail geometry of *J*-aggregates.[31,32] Furthermore, **Figure 1-6** shows that the red shift is weakened with increasing θ_m, accompanied by an increase in the absorbance, indicating that larger amounts of *J*-aggregate are present in a plane parallel to the substrate and that the orientation of the mesogenic group is out-of-plane.

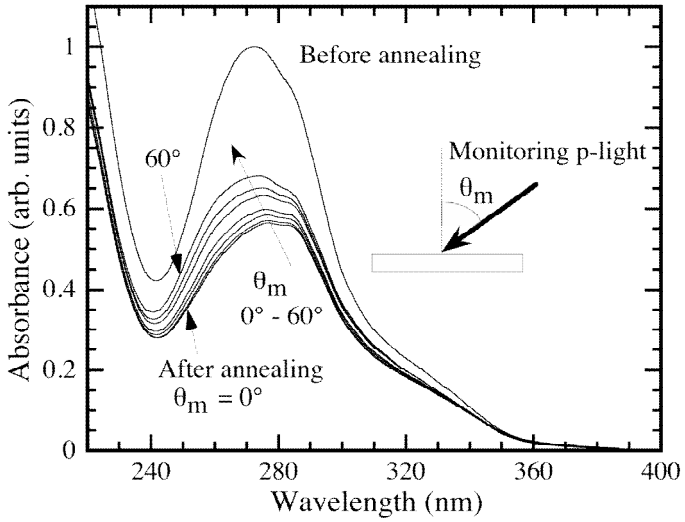

Figure 1-6 Absorbance spectra of **P6MBC** film before and after annealing at 180 °C for 10 min. followed by quenching and measuring the spectrum at various incident angle of *p*-polarized monitoring light.

Figure 1-7 shows FT-IR spectra before and after annealing at 180 °C. This indicates that ν(C=C) and ω(C=O) for the side groups are decreased, while the CH vibration around 2850 − 2950 cm^{-1} for the methylene spacer is increased after annealing. This result also supports the out-of-plane alignment of the mesogenic groups. Similar results were obtained for the film annealed at 150 °C and 200 °C (LC temperature range), but neither the red shift nor the out-of-plane alignment was observed for the film annealed in the isotropic temperature range at 240 °C. It should be noted that the decrease in the absorption was not strong when the film was irradiated at 180 °C with 0.0036 or 0.06 J cm^{-2}, as shown in **Figure 1-2 (a)**. The annealing was carried out during the UV illumination. This result suggests that UV exposure suppressed the out-of-plane alignment of the mesogenic groups even though the film was heated in the LC temperature range.

1-3-4. Photoreaction of Annealed Film

The change in the FT-IR spectrum of the annealed film after exposure is also shown in **Figure 1-7**. The shift of the C=O stretch to a higher wavenumber at 1775 cm^{-1} is clearly seen and this new band is a consequence of the H-H dimer. In the case of the annealed film, there should be a large amount of *J*-aggregate as described above, and the aggregated mesogenic groups will form H-T dimers. To investigate a source of the resulting H-H dimer, UV light

was irradiated obliquely to the annealed film, and a relationship between the photoreacted regioisomers and the orientational direction of the mesogenic groups was clarified by FT-IR. **Figure 1-8** plots the ratio of the absorption intensities at 1775/1730 cm^{-1} as a function of the incident angle of the UV irradiation. This shows that larger amounts of H-H dimer were obtained when the angle of the incident UV was large. This means that the mesogenic groups lying in a direction perpendicular to the substrate plane preferentially form H-H dimer.

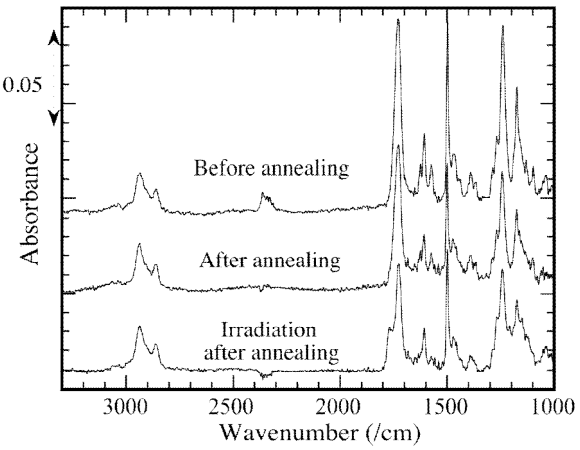

Figure 1-7 FT-IR spectra of **P6MBC** film before and after annealing at 180 °C for 10 min. followed by quenching and after irradiation of the annealed film using a 3.0 J cm^{-2} exposure dose.

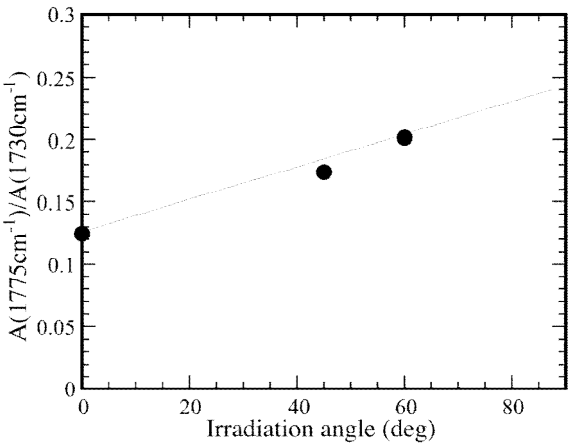

Figure 1-8 Ratio of the FT-IR absorption intensities at 1775/1735 cm^{-1} as a function of the irradiation angle.

1-3-5. LC Alignment on Photoreacted P6MBC Film

Figure 1-9 summarizes the LC alignment behavior on **P6MBC** film irradiated under various conditions. When the film was irradiated at room temperature, the LC aligned parallel to **E** and the direction changed to perpendicular to **E** with increasing exposure dose. The reversion occurred when the exposure dose was 0.36 J cm^{-2}, where the degree of photoreaction of the coumarin groups was about 30 %. The reversion of the LC alignment direction was observed for other type of polymethacrylates with coumarin side groups as studied by Ichimura *et al.*[23,24] They concluded that perpendicular LC alignment was brought about by the remaining coumarin groups in a direction perpendicular to **E**. Here, the perpendicular LC alignment will be due to the remaining mesogenic groups, as is the case of Ichimura's polymer.

On the other hand, parallel LC alignment could not be obtained when a film was irradiated

at 180 °C. The loss of the LC alignment ability may be ascribed to the aggregates of mesogenic groups formed in the LC temperature range. However, the LC aligned in a direction perpendicular to **E** when the irradiation energy was 4.8 J cm^{-2} or more. For this energy dose, the side photoreaction should occur and the aggregation of the mesogenic groups became broken. Therefore, the interaction between the remaining mesogenic groups lying in the direction perpendicular to **E** and the LC will be increased, resulting in a perpendicular LC alignment. In addition, the LC did not align on the annealed films. The associated mesogenic groups may prevent the LC alignment although H-H dimer could be formed.

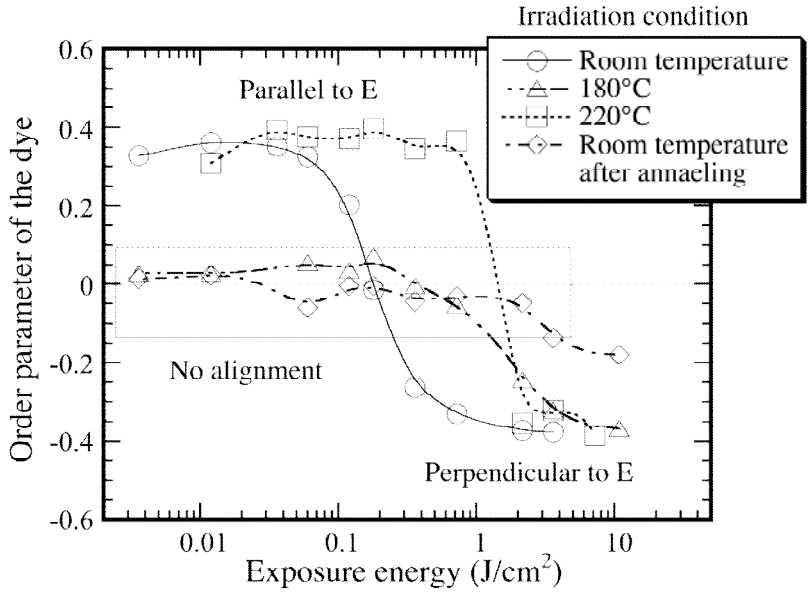

Figure 1-9 Order parameter and alignment direction of the parallel LC cell as a function of the irradiation dose.

In contrast, homogeneous LC alignment could be obtained when the film was irradiated near T_i for **P6MBC** (220 °C), and it took longer exposure doses to reverse the alignment direction from parallel to perpendicular to **E**. For the photoreaction at 220 °C, the main photoreacted product is H-T dimer and the photoindused thermal orientation of the mesogenic groups occurs as shown in **Figure 1-4**. In this case, the azimuthal anchoring energy in a direction parallel to **E** should be larger than that for the film irradiated at room temperature, since both photoreacted mesogenic groups and the mesogenic groups are aligned parallel to **E**. Therefore, longer exposure dose are needed to obtain perpendicular LC alignment.

1-4. Conclusion

It was found that H-H cycloadducts of the mesogenic side groups were formed for **P6MBC** film and the film showed negative dichroism when it was irradiated at room temperature. This H-H dimer can control the LC alignment in a direction parallel to **E**, and reversion of the LC alignment direction occurred because of the increased interaction between the LC and remaining mesogenic groups in a direction perpendicular to **E**.

On the other hand, the film exhibited a positive dichroism and H-T cycloadducts were produced when the film was irradiated near the clearing temperature of **P6MBC.** The positive dichroism was generated by the photoinduced thermal reorientation of the mesogenic groups in a direction parallel to **E**, and the LC aligned in this direction. This leads to the conclusion that both H-T dimmer and oriented mesogenic groups can control the parallel LC alignment. Reversion of the LC alignment was also observed when the dichroism became smaller, and the required energy dose for the reversion was larger than that for the film irradiated at room temperature. In this case, the reversion is due to the photodegradation of the mesogenic groups in a direction perpendicular to **E**

In addition, aggregation of the mesogenic groups was observed when the film was irradiated in the LC temperature range of the polymer, or was annealed before exposure. The type of cycloadducts was different in these two cases, and the parallel LC alignment was not achieved for both, suggesting that the aggregated mesogenic groups could not regulate the LC alignment.

1-5. References

1) M. Schadt, K. Schmitt, V. Kozinkov and V. Chigrinov: *Jpn. J. appl. Phys.*, **1992**, *31*, 2155.

2) M. Schadt, H. Seiberle and A. Schuster: *Nature*, **1996**, *381*, 212.

3) K. Ichimura: *Chem. Rev.*, **2000**, *100*, 1847.

4) M. O'Neill and S. M. Kelly: *J. Phys. D, appl. Phys.*, **2000**, *33*, R67.

5) K. Ichimura: *Polymers as Electrooptical and Photooptical Active Media*, edited by V. Shibaev (Berlin: Springer), **1996**, p. 138.

6) V. A. Barachevsky: *Proc. SPIE*, **1991**, *1559*, 184.

7) M. Schadt, H. Seiberle, A. Schuster and S. M. Kelly: *Jpn. J. appl. Phys.*, **1995**, *34*, 3240.

8) Y. Iimura, T. Saitoh, S. Kobayashi and T. Hashimoto: *J. photopolym. Sci. Technol.*, **1995**, *2*, 257.

9) X. T. Li, D. H. Pei, S. Kobayashi and Y. Iimura: *Jpn. J. appl. Phys*., **1997**, *36*, L432.

10) K. Ichimura, Y. Akita, H. Akiyama, K. Kudo and Y. Hayashi: *Macromolecules*, **1997**, *30*, 903.

11) K. Ichimura, Y. Akita, H. Akiyama, Y. Hayashi and K. Kudo: *Jpn. J. appl. Phys.*, **1996**, ***35***, L992.

12) N. J. Turro: *Modern Molecular Photochemistry* (Menlo Park CA: Benjamin/Cummings), **1978**.

13) D. Shenoy, K. Gru¨ eneberg, J. Naciri and R. Shashidhar: *Jpn. J. appl. Phys.*, **1998**, *37*, L1326.

14) M. Schadt, H. Seiberle, A. S. Schuster and M. Kelly: *Jpn. J. appl. Phys.*, **1995**, *34*, L764.

15) Y. Akita, H. Akiyama, Y. Hayashi and K. Ichimura: *J. photopolym. Sci. T ech.*, **1995**, *8*, 75.

16) M. Obi, S. Morino and K. Ichimura: *Jpn. J. appl. Phys.*, **1999**, *38*, L145.

17) H. Kim and J. Park, *Jpn. J. appl. Phys.*, **1999**, *38*, 201.

18) J. Liu, X. Liang and H. Gao: *Jpn. J. appl. Phys.*, **2000**, *39*, L1221.

19) N. Kawatsuki, H. Ono, H. Takatsuka, T. Yamamoto and O. Sangen: *Macromolecules*, **1997**, *30*, 6680.

20) N. Kawatsuki, H. Takatsuka, T. Yamamoto and H. Ono: *Jpn. J. appl. Phys.*, **1997**, *36*, 6464.

21) N. Kawatsuki, H. Takatsuka, Y. Kawakami and T. Yamamoto: *Polym. Adv. Technol.*, **1999**, *10*, 429.

22) N. Kawatsuki, K. Matsuyoshi, M. Hayashi, H. Takatsuka and T. Yamamoto: *Chem. Mater.*, **2000**, *12*, 1549.

23) M. Obi, S. Morino and K. Ichimura: *Chem. Mater.*, **1999**, *11*, 656.

24) M. Obi, S. Morino and K. Ichimura: *Macromol. rapid Commun.*, **1998**, *19*, 643.

25) P. O. Jacson, P. Hindmarsh, S. M. Kelly and M. O'Neill: *in Abstracts of the 18th International Liquid Crystal Conference*, *Sendai*, *Japan*, **2000**, p. 85.

26) R. Anet: *Chem. Ind.*, **1960**, 897.

27) G. O. Schenck, I. Wilucki and C. H. Krauch: *Chem. Ber.*, **1966**, *99*, 625.

28) Y. Chen and C. Chou: *J. polym. Sci., A, polym. Chem.*, **1995**, *33*, 2705.

29) W. Li, V. Lynch, H. Thompson and M. A. Fox: *J. Am. chem. Soc.*, **1997**, *119*, 7211.

30) N. Kawatsuki, K. Takatani, T. Yamamoto and O. Sangen, *Macromol. Chem. Phys.*, **1997**, *198*, 2853.

31) N. Kawatsuki, S. Sakashita, K. Takatani, T. Yamamoto and O. Sangen, *Macromol. Chem. Phys.*, **1996**, *197*, 1919.

32) D. Singh Creed and C. E. Hoyle, *Proc SPIE*, **1992**, *1774*, 2.

33) N. Kawatsuki, H. Takatsuka, T. Yamamoto and O. Sangen, *J. polym. Sci., A, polym. Chem.*, **1998**, *36*, 1521.

34) N. Kawatsuki, C. Suehiro and T. Yamamoto, *Macromolecules*, **1998**, *31*, 5894.

35) N. Kawatsuki, K. Matsuyoshi and T. Yamamoto, *Macromolecules*, **2000**, *33*, 1698.

Chapter 2

Achievement of Large Orientation Order and Its Reversion Control in the Thermally Enhanced Photoorientation of Photo-Cross-Linkable Polymer Liquid Crystal

2-1. Introduction

The controlled alignment of molecules in photoreactive polymer films induced by photoreaction has received much attention because this phenomenon may prove to be useful in birefringent optical devices, optical memories, holographic elements, phase retarders and photoalignment layers for liquid crystal displays (LCD).[1-6] In this respect, several types of materials have been reported, including azobenzene-containing polymers and photo-cross-linkable polymers, which can generate optical anisotropy of their films upon irradiation with linearly polarized (LP) light.[7-22] In particular, numerous studies of azobenzene containing polymers have been performed to characterize the axis-selective *trans-cis* (*E*-to-*Z*) photoisomerization reaction which leads to in-plane, high molecular reorientation in a direction perpendicular to the electric vector (**E**) of LP light.[7-15] Alternatively, we studied a photo-cross-linkable polymer liquid crystal (PLC) containing a cinnamoyloxyethoxybiphenyl side group and its copolymers which exhibit thermally stable reorientation of mesogenic side groups by the use of LP ultraviolet (LPUV) light and subsequent annealing.[20-22]

If the in-plane orientation can be controlled both parallel and perpendicular to **E** of LP light, a patterning of the direction and birefringence of the film is enabled. Reversion of the alignment direction of liquid crystal (LC) on some types of photo-cross-linkable polymer surfaces has been explored by changing exposure doses of LPUV light.[6,23-26] This may offer the multidomain alignment of LC materials. In these cases, the direction of interaction between the LC and polymer surfaces may be dependent on the exposure dose. The in-plane and out-of-plane switching of photo-orientation of polymer films has been observed in some azobenzene-containing PLCs by adjusting exposure doses of LP light or by controlling the annealing process,[16,17] although the direction of the in-plane orientation is always perpendicular to **E**. To date, there are no reports on photoreactive polymer materials which can self-induce the reversion of in-plane molecular orientation. The purpose of this chapter is to develop a novel photo-cross-linkable PLC that can generate high orientational order and

induce the reversion of the in-plane reorientational direction. The influence of the photoisomerization reaction on the reorientational behavior of the PLC containing the cinnamoyl group was then clarified. To this end, a novel photo-cross-linkable methacrylate with a 4-methoxycinnamoyloxybiphenyl side group was synthesized, and reversion of the in-plane reorientation direction of the mesogenic groups of PLC films generated by irradiation with LPUV light and subsequent annealing was demonstrated. The orientational behavior of the film was studied using polarization UV-vis and FT-IR spectroscopies. Since the mesogenic group in this study contains a 4-methoxycinnamoyl group, in which the absorption band is separated from that of the biphenyl group, spectral analysis was performed to investigate the photoproduct influence on reorientational behavior. We have determined that the thermally enhanced reorientation direction is dependent on the distribution of photoproducts and the degree of photoreaction. Furthermore, the highest orientational order of a photo-cross-linkable PLC system has been observed.

2-2. Experimental Section

2-2-1. Materials and Monomer Synthesis

All starting materials were used as received from Tokyo Kasei Chemicals. The syntheses of methacrylate monomers (nCB) and compounds **1-3** are outlined in **Scheme 2-1**.

4-Acetoxy-4′-methoxybiphenyl (1) was synthesized by a conventional method from 4-methoxy-4′-hydroxybiphenyl and acetic anhydride, while **methyl (*E*)-4-methoxycinnamate (2)** was generated from 4-methoxycinnamoyl chloride and methanol. The structures of these compound were confirmed by ^{1}H-NMR and FT-IR spectroscopies.

The model compound **4′-methoxylbiphenyl (*E*)-4-methoxycinnamate (3)** was synthesized from 4-methoxycinnamoyl chloride and 4-methoxy-4′-hydroxybiphenyl in 51% yield; mp 202 °C, *T*i > 300 °C. ^{1}H-NMR ($CDCl_3$): δ (ppm) 3.86 (s, 6H, Ph-OC*H*$_3$, Ph-Ph-OC*H*$_3$), 6.5-6.53 (d, J = 15.8 Hz, 1H, -CH=C*H*-Ph), 6.93-6.96 (m,2H, cinnamoyl-Ph), 6.97-6.99 (m, 4H, Ph-Ph), 7.2-7.21 (m,2H, cinnamoyl-Ph), 7.5-7.51 (m, 4H, Ph-Ph), 7.83-7.86 (d, J = 15.8 Hz, 1H, -C*H*=CH-Ph). IR (KBr): 2966, 1722, 1631, 1599, 1494, 1137, 830 cm^{-1}.

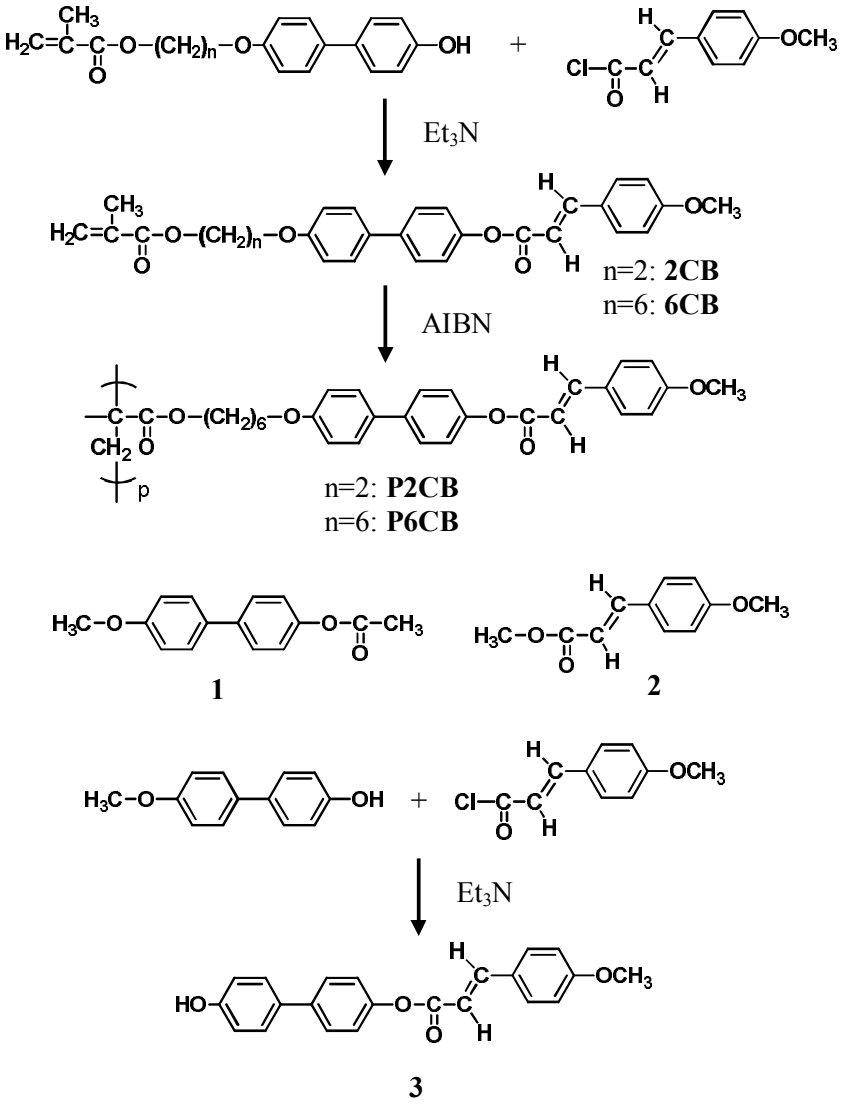

Scheme 2-1 Chemical structure and synthetic route to model compounds and polymer liquid crystals.

4′-(4-Methoxycinnamoyl)-4-phenylphenoxyalkyl methacrylates (**2CB** and **6CB**) were synthesized from 4′-hydroxy-4-phenylphenoxyalkyl methacrylate[27] and 4-methoxycinnamoyl chloride according to the usual method.[27] Yield, mp, NMR, and IR spectroscopic characteristics are as follows: **2CB:** yield 39%, mp 145 °C, ^{1}H-NMR ($CDCl_3$): δ (ppm) 1.96 (S, 3H, CH_2=C(CH_3)), 3.86 (s, 3H, Ph-OCH_3), 4.27 (t, J = 4.75 Hz, 2H, -COO-CH_2-), 4.52 (t, 2H, J = 4.75 Hz, -CH_2-O-Ph), 5.60 (s, 1H, CH_2=C(CH_3)), 6.16 (s, 1H, CH_2=C(CH_3)), 6.52 (d, J = 15.84 Hz, 1H, -CH=CH-Ph), 6.93-6.95 (m, 2H, cinnamoyl-Ph), 6.99-7.0 (m, 2H, Ph-Ph),

7.21-7.22 (m, 2H, cinnamoyl-Ph), 7.51-7.52 (m, 2H, Ph-Ph), 7.55-7.83 (m, 4H, Ph-Ph), 7.85 (d, J = 15.84 Hz, 1H, -C*H*=CH-Ph). IR (KBr): 2935, 1723, 1631, 1598, 1495, 1145, 829 cm^{-1}. **6CB:** yield 38%, mp 89 °C, ^1H NMR ($CDCl_3$): δ (ppm) 1.47-1.57 (m, 4H, -O-$(CH_2)_2$-(C*H*$_2)_2$-$(CH_2)_2$-O-), 1.70-1.88 (m, 4H, -O-CH_2-C*H*$_2$-$(CH_2)_2$-C*H*$_2$-CH_2-O-), 1.95 (s, 3H, CH_2=C(C*H*$_3$)), 3.86 (s, 3H, Ph-OC*H*$_3$), 4.00 (t, J = 6.6 Hz, 2H, -COO-C*H*$_2$-), 4.17 (t, J = 6.6 Hz, 2H, -C*H*$_2$-O-Ph), 5.55 (s, 1H, C*H*$_2$=C(CH_3)), 6.10 (s, 1H, C*H*$_2$=C(CH_3)), 6.52 (d, J = 15.8 Hz, 1H, -CH=C*H*-Ph), 6.93-6.95 (m, 4H, Ph), 6.99-7.2 (m, 2H, Ph), 7.21-7.22 (m, 2H, cinnamoyl-Ph), 7.51-7.52 (m, 2H, Ph-Ph), 7.55-7.83 (m, 2H, Ph-Ph), 7.85 (d, J = 15.8 Hz, 1H, -C*H*=CH-Ph). IR (KBr): 2935, 1722, 1632, 1599, 1500, 1145, 829 cm^{-1}.

2-2-2. Polymerization

The polymerization of methacrylate monomers **2CB** and **6CB** was performed by a free radical solution polymerization in tetrahydrofuran (THF) with 2,2′-azobis(isobutyronitrile) (AIBN) as the initiator. The concentration of monomers and AIBN were 10% (w/v) and 2 mol %, respectively. As an example of a general polymerization procedure, the synthesis of polymer **P6CB** is given below. **6CB** and AIBN were dissolved in THF, and the reaction mixture was treated with a gentle stream of nitrogen. After sealing, the mixture was heated to 60 °C for 24 h. The resulting homogeneous solution was added dropwise into excess amount of diethyl ether to precipitate the polymer. After two additional precipitations from a dichloromethane solution into diethyl ether, the polymer was extracted with diethyl ether for 1 day. The polymer was dried at 25 °C under vacuum for 48 h. In the case of the polymerization of **2CB**, the resultant polymer, **P2CB**, was precipitated during the polymerization because of its low solubility in THF at 60 °C. **Table 2-1** summarizes the yield, molecular weight, and thermal properties of synthesized PLCs. NMR and IR spectroscopic characteristics of **P2CB** and **P6CB** are as follows:

P2CB: ^1H-NMR ($CDCl_3$/hexafluoro-2-propanol) 1/1): δ (ppm) 1.0 (brs, 3H, CH_2-C(C*H*$_3$)), 1.26 (brs, 2H, C*H*$_2$-C(CH_3)), 4.12 (m, 2H, -COO-C*H*$_2$-), 4.50-4.51 (m, 2H, -C*H*$_2$-O-Ph), 6.37 (m, 1H, -CH=C*H*-Ph), 6.85-6.97 (m, 6H, Ph), 7.26-7.39 (m, 6H, Ph-Ph), 7.74 (m, 1H, -C*H*=CH-Ph). Signal of Ph-OC*H*$_3$ group is overlapped with the solvent. IR (KBr): 2930, 1723, 1632, 1600, 1495, 1245, 1134, 826 cm^{-1}. **P6CB:** ^1H-NMR ($CDCl_3$): δ (ppm) 1.47-1.57 (m, 6H, -O-$(CH_2)_2$-(C*H*$_2)_2$-$(CH_2)_2$-O- and C*H*$_2$-C(CH_3)), 1.70-1.88 (m, 4H, -OCH_2-C*H*$_2$-$(CH_2)_2$-C*H*$_2$-CH_2-O-), 1.74 (s, 3H, CH_2C(C*H*$_3$)), 3.51 (s, 3H, Ph-OC*H*$_3$), 3.64 (t, J) 6.6 Hz, 2H, -COO-C*H*$_2$-), 3.81 (t, J) 6.6 Hz, 2H, -C*H*$_2$-O-Ph), 6.41 (d, J) 15.8 Hz, 1H, -CH=C*H*-Ph),

6.93-6.96 (m, 2H, Ph), 7.0-7.2 (m, 4H, Ph), 7.42-7.49 (m, 4H, cinnamoyl-Ph), 7.51-7.52 (m, 2H, Ph), 7.85 (d, *J*) 15.8 Hz, 1H, -C*H*=CH-Ph). IR (KBr): 2930, 1723, 1632, 1599, 1495, 1245, 1145, 829 cm^{-1}.

2-2-3. Characterization

^{1}H-NMR spectra were measured with Bruker DRX-500 FT-NMR apparatus. As the synthesized polymers were hardly soluble in THF at room temperature, they were hydrolyzed before molecular weight determination by gel permeation chromatography (GPC). The hydrolysis was carried out by refluxing the polymers in 10/80/10 wt/wt/wt % sodium hydroxide/THF/water solution for 2 days, resulting in a polymer soluble in THF. By the ^{1}H -NMR analysis, the main part of the hydrolyzed polymer was poly(methacrylic acid), although further identification was not carried out to present. The molecular weight of these hydrolyzed polymers was measured by GPC (Tosoh HLC-8020 GPC system with Tosoh TSK gel column; eluent, THF) calibrated using polystyrene standards. Thermal properties were examined using a polarization optical microscope (Olympus BHA-P) equipped with a Linkam TH600PM heating and cooling stage in addition to differential scanning calorimetry (DSC; Seiko-I SSC5200H) analysis at a heating and cooling rate of 10 K/min. Polarization FTIR spectra were recorded through a JASCO FTIR-410 system with an attached wire-grid polarizer. Polarization UV-vis spectra were measured using a Hitachi U-3030 spectrometer equipped with Glan-Taylor polarizing prisms. The in-plane order parameter, *S*, is expressed in the form of eq 1:[23]

$$S = (A_p - A_s) / (A_{(large)} + 2A_{(small)}) \qquad (1)$$

where A_p and A_s are the absorbances parallel and perpendicular to **E**, respectively, while $A_{(large)}$ is taken to be the larger of A_p and A_s, while $A_{(small)}$ is taken to be the smaller. *S* was calculated by polarized UV-vis spectroscopy at a wavelength of 320 nm.

2-2-4. Photoirradiation

Thin films of **P*n*CB** were prepared by spin-coating a methylene chloride solution or a hexafluoro-2-propanol (6FP) solution of polymers (~5 wt %) onto a quartz or CaF_2 substrate. The film thickness was 0.2-0.5 μm, which was determined by the stylus contact method using Taly-Step (Rank Taylar Hobson). The film was set on a Linkam TH600PM heating stage and

irradiated by light from a 250 W high pressure Hg-UV lamp which passed through Glan-Taylor polarizing prisms with a cutoff filter under 290 nm. The light intensity was about 50 mW cm^{-2} at 313 nm. The optical anisotropy of the film was measured by polarizing microscopy and polarization UV-vis and FT-IR spectra.

2-2-5. Spectrum Analysis

Thin films of **P*n*CB**s were irradiated with UV light, and the absorption spectra were measured at intervals. The molar extinction coefficient of the *Z*-isomer and photo-Fries (*PF*) product of **3** at each wavelength were calculated using the determination of the *E/Z* and *E/PF* ratios by means of HPLC analysis. **Table 2-2** summarizes the results. Spectral analysis of **P*n*CB** was performed using the procedure given by Ichimura et al.[28] according to the following expression:

$$D_{315nm} = \varepsilon_{E(315nm)}[E] + \varepsilon_{Z(315nm)}[Z] + \varepsilon_{PF(315nm)}[PF]$$

$$D_{330nm} = \varepsilon_{E(330nm)}[E] + \varepsilon_{Z(330nm)}[Z] + \varepsilon_{PF(330nm)}[PF]$$

$$D_{365nm} = \varepsilon_{E(365nm)}[E] + \varepsilon_{E(365nm)}[Z] + \varepsilon_{PF(365nm)}[PF]$$

where D_{315nm}, D_{330nm}, and D_{365nm} are the absorbances during photolysis, $\varepsilon_{E(315nm)}$, $\varepsilon_{Z(330nm)}$, and $\varepsilon_{PF(365nm)}$ are the absorbance coefficients of *E*-isomer, *Z*-isomer, and photo-Fries products at the corresponding wavelength, and [*E*], [*Z*], and [*PF*] are their concentrations.

2-3. Results and Discussion

2-3-1. Photochemistry of PnCB Films

The synthesized PLCs exhibit a nematic liquid crystalline phase as summarized in **Table 2-1**. Both polymers are insoluble in THF at room temperature, while **P6CB** is soluble in chloroform, methylene chloride, and dimethylformamide. However, **P2CB** is insoluble in such solvents and only soluble in 6FP. Therefore, thin films were prepared by the spin-coating method from a methylene chloride solution for **P6CB** and from a 6FP solution for **P2CB**. To analyze the photoreaction of **P*n*CB** films, we initially examined the UV spectra of model compounds **1**-**3** in methylene chloride solution as shown in **Figure 2-1**. Model compound **3** has a mesogenic side group identical to that of **P*n*CB**, and the spectrum is similar to that of **P6CB**. It reveals that **3** exhibits several absorption peaks that could be considered as the

absorption bands for **1** and **2**. Since absorption of **2** is longer than 305 nm and does not overlap with that of **1**, the absorption of the cinnamate group in **3** could approximately be separated from the absorption of the biphenyl group. This may allow evaluation of the photoreaction of the cinnamate group of **3** using absorption bands longer than 305 nm. It is well-known that irradiation of phenyl cinnamate derivatives with UV light produces three types of photoproducts as shown in **Figure 2-2**, i.e., a photodimerized product (photodimer), a photoisomerized product (*Z*-isomer), and a product from photo-Fries (*PF*) rearrangement. [27,29]

Table 2-1 Yield, Molecular Weight and Thermal Properties of Synthesized PLCs.

	Yield (%)	Molecular Weight [a]		Thermal Property [b]		
		$M_w \times 10^{-3}$ (g/mol)	M_w/M_n	T_m (°C)	(Phase)	T_i (°C)
P2CB	60	78.6	2.9	153	N	>300
P6CB	51	67.8	3.1	116	N	>300

[a] Molecular weight of hydrolyzed polymer. Determined by GPC using polystyrene standard. THF was used for eluent. [b] Determined by polarization optical microscopy and DSC. T_m: Melting point, T_i: Clearing point, N: Nematic. Both polymer did not exhibit T_i up to 300 °C.

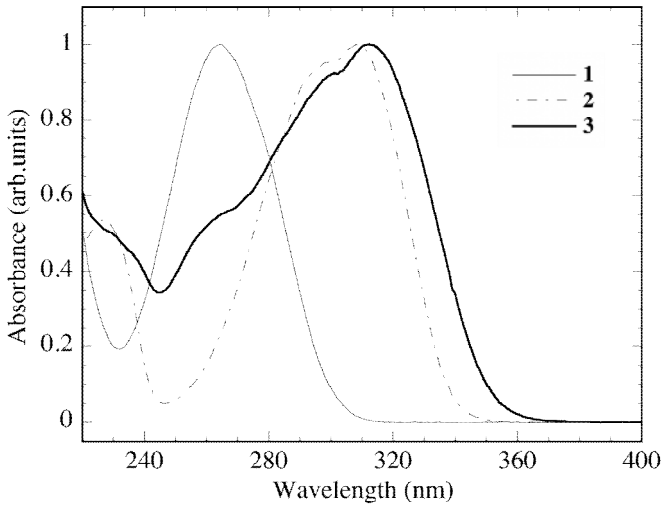

Figure 2-1 UV absorption spectra of model compounds **1-3** in a methylene chloride solution.

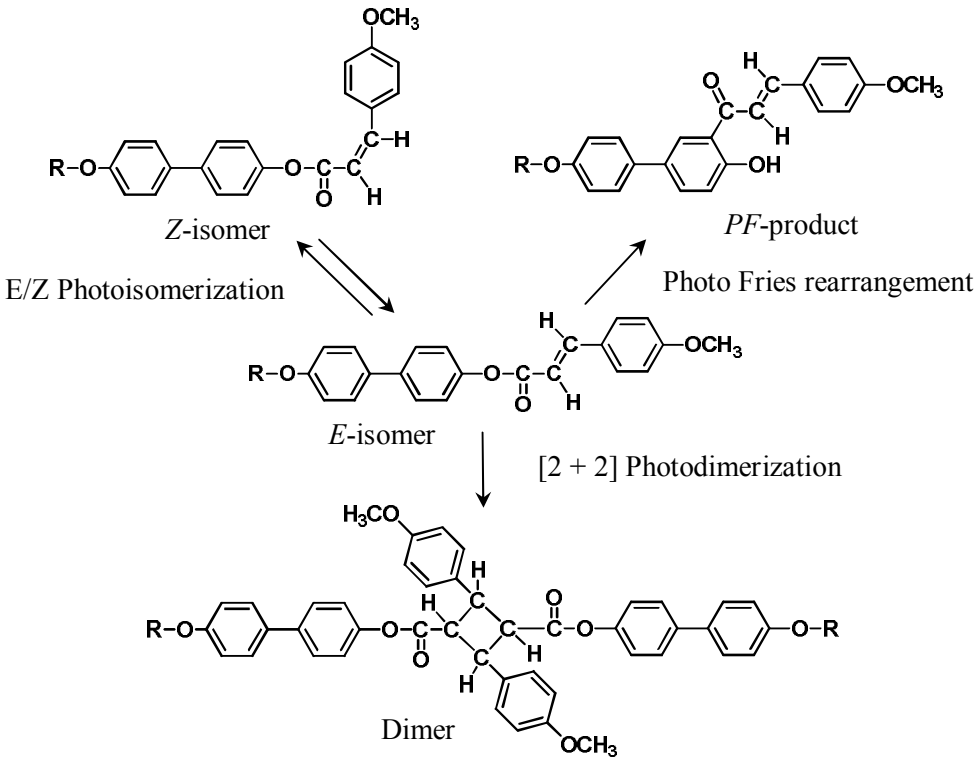

Figure 2-2 Posible types of photoreaction of the mesogenic group of 4-methoxycinnamoyloxybiphenyl.

Figure 2-3 illustrates the spectral change of **P6CB** film upon a quartz substrate. Film absorption was found to decrease monotonically, exhibiting a slight increase at longer wavelengths. This increase in the absorption at longer wavelengths is attributed to formation of a very small amount of *PF* product. The suppression of the photo-Fries rearrangement reaction in the film state when using a methacrylate polymer with 4-cinnamoyloxybiphenyl side groups was reported.[27] Therefore, the major photoproducts will come from photodimerization and photoisomerization reactions of the mesogenic group.

Spectral analysis was performed according to Ichimura's method using spectral parameters as listed in **Table 2-2**.[28] Results for the **P6CB** film plotted in **Figure 2-4** reveal both photodimerization and photoisomerization take place at an early stage of photoirradiation, although the amount of the photodimer produced is larger than that of the *Z*-isomer. Additionally, the amount of *Z*-isomer produced was found to have an upper limit of 18-20 % over a prolonged exposure. The formation of *PF* products amounts to less than 1 % over all exposure doses. Similar results were obtained for **P2CB** films. A greater degree of

photodimerization relative to photoisomerization had been reported for methacrylates with cinnamate side group having a para substituent.[28]

Table 2-2 Spectral Analysis of Model Compound **3**.

Wavelength (nm)	Absorption Coefficients (ε) [a]		
	E-isomer	*Z*-isomer	*PF*-Product
315	3.65×10^4	1.90×10^4	0.16×10^4
330	2.57×10^4	1.53×10^4	0.55×10^4
365	0	0	1.11×10^4

a) Absorption coefficients ($Lmol^{-1}cm^{-1}$) in methylene chloride solution.

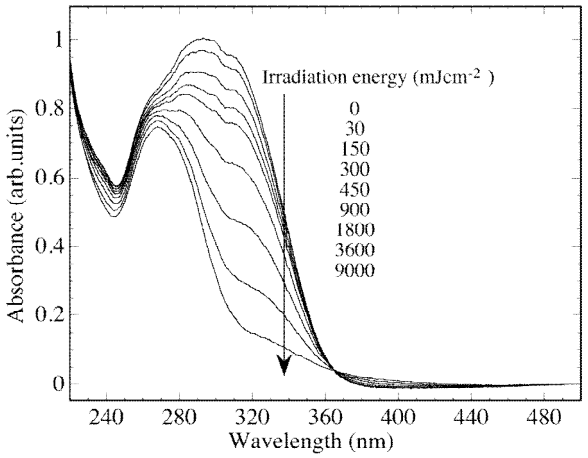

Figure 2-3 UV absorption Spectral changes in **P6CB** film during the course of irradiation with UV light.

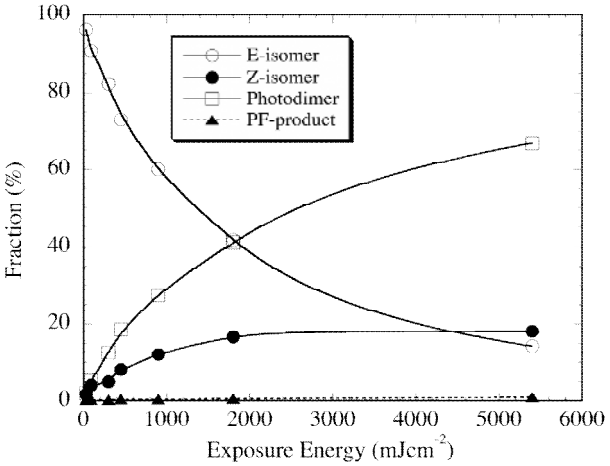

Figure 2-4 Fragments of *E*- (○) and *Z*- (●) isomers, photodimers (□), and photo-Fries products (▲) in thin films of **P6CB** as a function of exposure energy.

2-3-2. Enhancement and Reversion of Photoinduced Optical Anisotropy

Irradiation of a polymer containing cinnamoyl groups with LPUV light leads to negative optical anisotropy as a result of axis-selective [2 + 2] photodimerization as well as *E*-to-*Z* photoisomerization.[5,6,23,28,30] If a polymer with cinnamoyl groups exhibits a liquid crystalline phase, the photoinduced optical anisotropy generated in an amorphous state of the as-coated polymer film may change when the film is annealed at elevated temperatures due to its liquid crystalline nature.[5,20-23] Accordingly, for **P*n*CB**, irradiation with LPUV light generates a small negative ΔA, and subsequent annealing will yield a pronounced adjustment of spectral intensities.

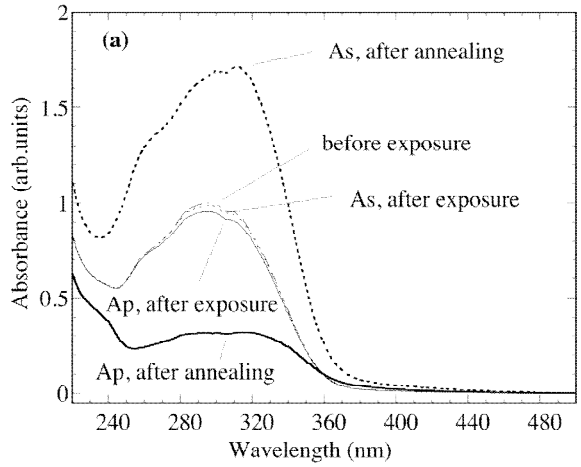

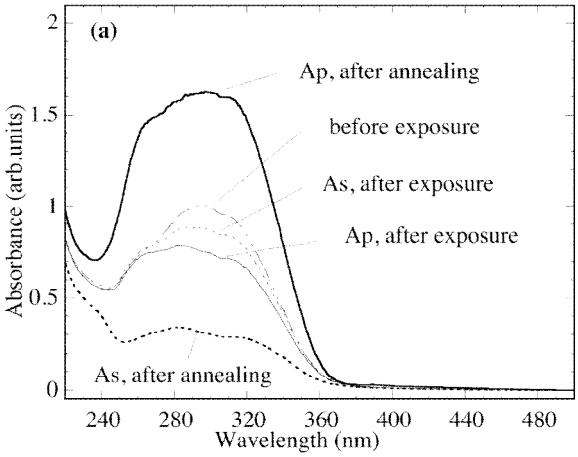

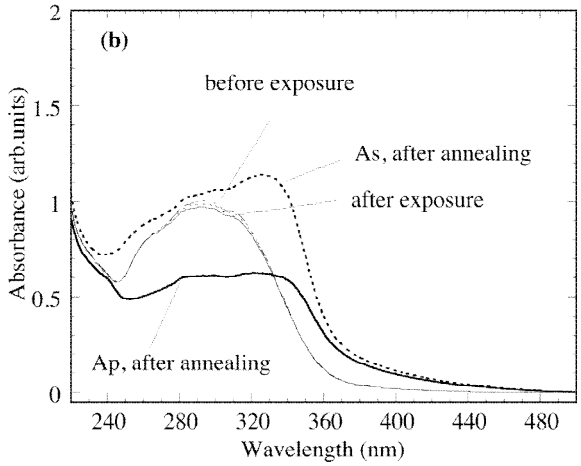

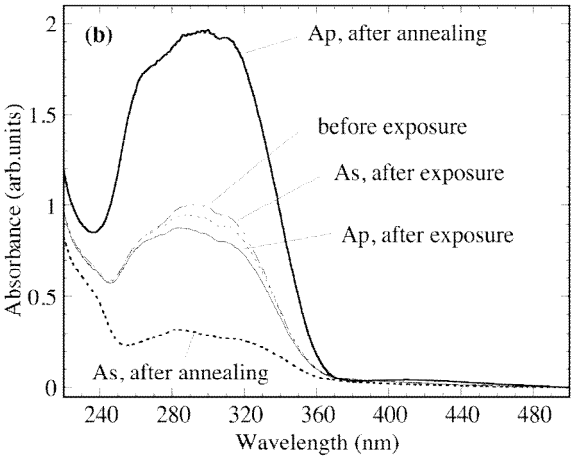

Figure 2-5 UV absorption Spectrum of **P*n*CB** films before photoirradiation, after irradiation with 30 mJ cm^{-2} doses (thin lines), and after subsequent annealing (thick lines). A_p is shown as the solid lines, and A_s is shown as the dotted lines. (a) **P2CB** film, annealed at 170 °C for 1min; (b) **P6CB** film, annealed at 130 °C for 1min.

Figure 2-6 UV polarization Spectrum of **P*n*CB** films before photoirradiation, after irradiation with 450 mJ cm^{-2} doses (thin lines), and after subsequent annealing (thick lines). A_p is shown as the solid lines, and A_s is shown as the dotted lines. (a) **P2CB** film, annealed at 180 °C for 1min; (b) **P6CB** film, annealed at 155 °C for 1min.

Figure 2-5(a) shows polarized UV-vis spectral differences between a **P2CB** film irradiated with 30 mJ cm^{-2} doses of LPUV light and that of a film following subsequent annealing at 170 °C for 1 min. After exposure, a small negative ΔA is generated as annealing induces enhancement of the negative anisotropy. The enhanced reorientation direction of mesogenic groups is perpendicular to **E** of LPUV light, and the orientational order parameter S is amplified from -0.009 to -0.61. The thermal enhancement of negative ΔA is also observed for PLCs with azobenzene side groups, where separate mechanisms have been elucidated with

respect to *E*-to-*Z* photoisomerization and thermal reorientation.[7-15] The first mechanism was clarified by using of a LP light at a wavelength of 436 nm, where the major component of the rod-shaped *E*-isomer of azobenzene lays in a direction perpendicular to **E** and amplifies the negative ΔA.[14] The second mechanism involves the generation of considerable amounts of the *Z*-isomer in a direction parallel to **E** by the use of 365 nm LPUV light which lowers the phase transition temperature by accelerating thermal motion of the azobenzene side groups.[15] In the case of **P2CB** irradiated with 30 mJ cm^{-2} doses, the photogenerated *Z*-isomer and the photodimer are 1.5 % and 1.9 %, respectively. Reorientation of the mesogenic groups during photoirradiation will scarcely occur as the mobility of the mesogenic groups at room temperature is quite low while the photoinduced ΔA is very small. Therefore, thermal enhancement of negative ΔA will be triggered by a small amount of *Z*-isomer and photo-cross-linked photodimer in a direction parallel to **E**, which may lower the T_m of the film analogously to the behavior of the polymer with azobenzene groups.[15] A detailed discussion is provided in section ***2-3-5***. In addition, the thermal enhancement of negative ΔA is also observed for films of **P6CB**, although a red shift of the absorption band takes place, as shown in **Figure 2-5(b)**. This red shift is a consequence of the *J*-aggregation of mesogenic groups caused by annealing and results in a lower ΔA in comparison with that of **P2CB**.

In contrast, reversion of the amplification of the thermal reorientation order is observed when the irradiation dose is 450 mJ cm^{-2}, as shown in **Figure 2-6**. In these cases, the amounts of photogenerated *Z*-isomer and photodimer are 7 % and 17 % for **P2CB** and 8 % and 17 % for **P6CB**, respectively. This shows that the photoinduced negative optical anisotropy after exposure is larger than in films with 30 mJ cm^{-2} doses because of the larger degree of axis-selective photoreaction. This strongly suggests that an efficient, axis-selective, photo-cross-linking reaction of the cinnamoyl group is occurring. After annealing, *S* is amplified from -0.05 to +0.60 for **P2CB** and from -0.03 to +0.68 for **P6CB**. This phenomenon is attributed to the thermally enhanced reorientation of unreacted mesogenic groups along the photo-cross-linked mesogenic groups in a direction parallel to **E**. The axis-selective irradiation decreases mobility of the photo-cross-linked mesogenic groups that can control the reorientational direction as reported previously,[20-22] while the greatest values of enhanced order parameters are obtained to date for photo-cross-linkable PLC films. The thermally enhanced optical anisotropy of **P2CB** is revealed to be smaller than that of **P6CB** in **Figure 2-6**. The mobility of mesogenic groups during thermal reorientation with a shorter methylene spacer will be limited. Additionally, aggregation is suppressed for **P6CB** as a certain amount

of photoreaction products will restrain molecular aggregation as a result of the decrease in liquid crystallinity of the PLC.

2-3-3 FT-IR Spectroscopy

The reversion of reorientation direction was further investigated by polarized FT-IR spectroscopy measurements. Parts **(a)** and **(b)** of **Figure 2-7** show FT-IR spectral differences of **P2CB** and **P6CB** films prior to irradiation with LPUV light and after irradiation with 30 mJ cm^{-2} doses and subsequent annealing. After irradiation, a slight decrease in the absorption of the cinnamoyl group at 1632 cm^{-1} (νC=C) is observed for **P2CB**, although differential spectra (Ap - As) reveal a very small dichroism, indicating that reorientation of the mesogenic groups can be negligible. A similar change is observed for **P6CB**. Large adjustment in absorbance appeared after annealing. For Ap of **P2CB** film, intensities of absorption bands at 1632 cm^{-1}, 1600 cm^{-1} (νPh-Ph), 1495 cm^{-1} (νPh), and 1245 cm^{-1} (νPh-O) are pronouncedly decreased, while a slight increase at 1723 cm^{-1} (νC=O) and around 2930 cm^{-1} (νC-H) can be observed. As absorption bands, however, exhibit opposite changes. The differential spectrum reveals clear enhancement of photoinduced dichroism in the same direction by annealing. This result indicates that mesogenic side groups thermally reorient in a direction perpendicular to **E**. *S* is amplified at 1495 cm^{-1} to -0.61, in good agreement with the value obtained by UV-vis spectra. For **P6CB** films, a similar tendency for adjustment in the absorption bands is observed, but the difference between Ap and As after annealing was found to be relatively small. This is a consequence of the aggregation of mesogenic groups as described in the above section.

When films are irradiated with 450 mJ cm^{-2} doses, there is a greater photoinduced dichroism than arises from 30 mJ cm^{-2} doses as shown in **Figure 2-8(a)**. In contrast to **Figure 2-7**, annealing leads to increases in absorption bands at 1632 cm^{-1}, 1600, 1495, and 1245 cm^{-1}, with decreases observed at 1723 cm^{-1} for Ap of both PLC films. However, As exhibits opposite adjustment to these absorption bands. The differential spectrum reveals these changes are entirely in the opposite direction as compared to films with 30 mJ cm^{-2} doses. In addition, absorption around 2930 cm^{-1} (*ν*C-H) in the differential spectrum in **Figure 2-8(b)** distinctly displays negative dichroism. These results suggest that mesogenic groups including methylene spacers reorient thermally in a direction parallel to **E**. Furthermore, *S* values at 1495 cm^{-1} are + 0.53 for **P2CB** and + 0.65 for **P6CB**. These values are also in good agreement with that obtained by UV-vis spectra.

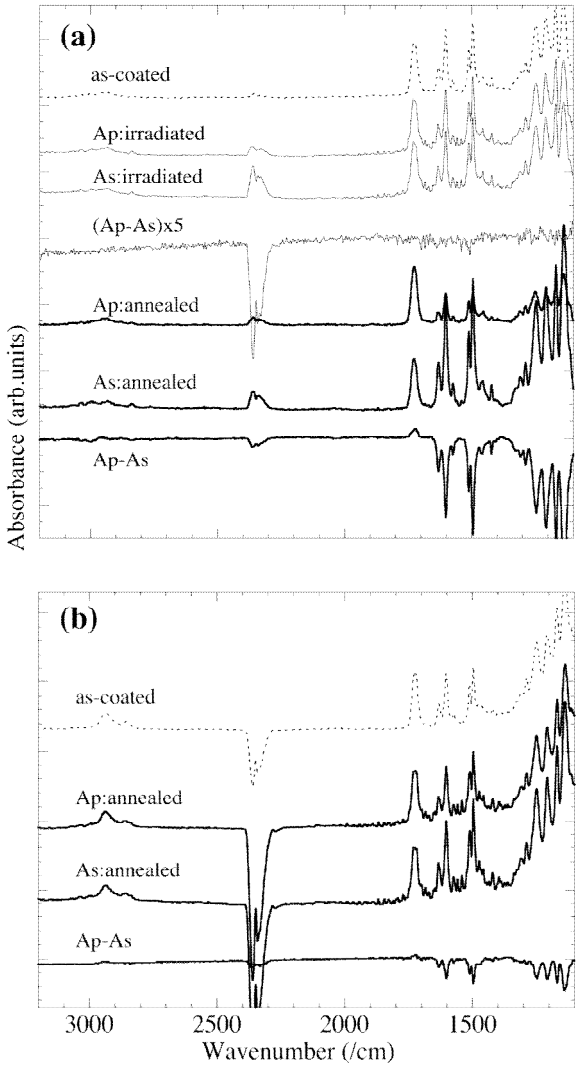

Figure 2-7 FT-IR spectra of **P*n*CB** films on CaF_2 substrates before photoirradiation (dotted lines), after irradiation with 30 mJ cm^{-2} doses (thin lines), and after subsequent annealing (thick lines). (a) **P2CB** film, annealed at 170 °C for 1min. (b) **P6CB** film, annealed at 130 °C for 1min.

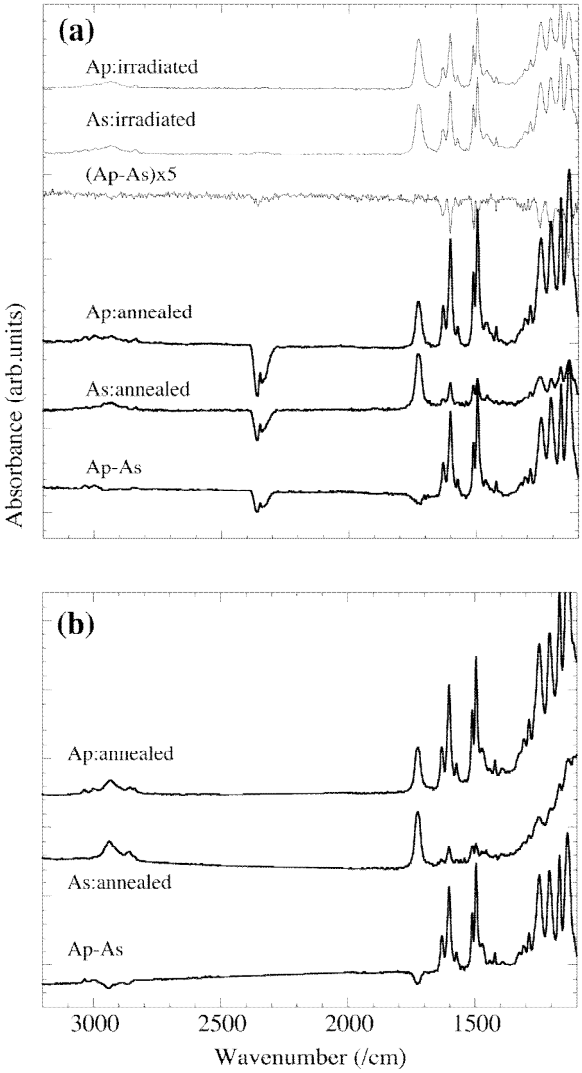

Figure 2-8 FT-IR spectra of **P*n*CB** films on CaF_2 substrates before photoirradiation (dotted lines), after irradiation with 450 mJ cm^{-2} doses (thin lines), and after subsequent annealing (thick lines). (a) **P2CB** film, annealed at 180 °C for 1min. (b) **P6CB** film, annealed at 155 °C for 1min.

2-3-4. Effect of the Exposure Energy

To elucidate the effect of exposure energy on the reversion of direction for thermally enhanced reorientation of mesogenic groups, films were irradiated with LPUV light at various exposure doses. Results are shown in **Figure 2-9** where a plot of the order parameter *S* after irradiation and after subsequent annealing as a function of exposure energy is given. All irradiated films of **P2CB** and **P6CB** were annealed at 180 and 155 °C for 1 min, respectively.

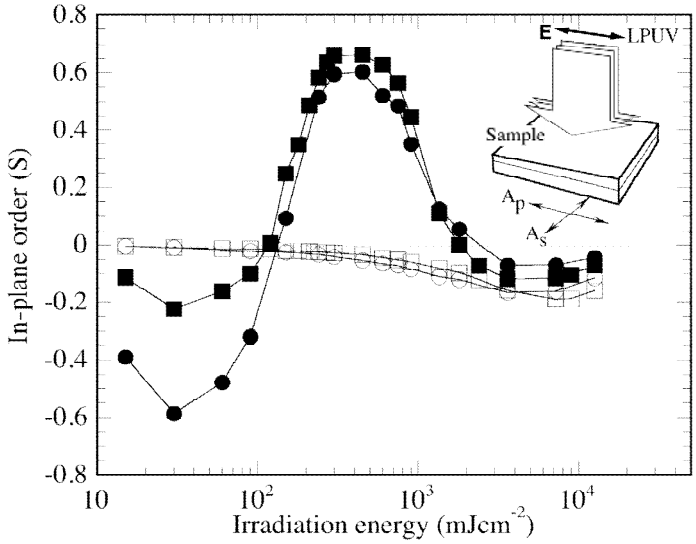

Figure 2-9 Difference in the order parameter *S* of **P*n*CB** films after irradiation with LPUV light (open points) and after subsequent annealing (closed points), as a function of the exposure energy. **P2CB** films were annealed at 180 °C for 1min. and **P6CB** films were annealed at 155 °C for 1min. for all cases. Circles and squares denotes *S* for films of **P2CB** and **P6CB**, respectively.

Figure 2-9 reveals the *S* value after irradiation is negative regardless of exposure dose and that increasing exposure doses for both PLCs results in increasing *S* values. This is due to the axis-selective photoreaction of the cinnamoyl group as described in section ***2-3-2***. When the exposure doses were less than 100 mJ cm^{-2}, annealing amplified the negative value of *S*, with a degree of photo-cross-linking of the side groups being less than about 13 % and with the amount of *Z*-isomer being less than about 5 %. Further irradiation inverts the reorientation direction after annealing. The maximum positive *S* is obtained when the degree of photo-cross-linking of the side groups was 15-20 %, and the amount of *Z*-isomer was 7-10 %. In addition, annealing of the films irradiated with doses of 2.0 J cm^{-2} scarcely enhanced molecular reorientation because a high degree of photo-cross-linking restricts mobilization of the mesogenic groups at elevated temperatures. These results suggest that the thermally enhanced reorientation behavior is strongly dependent on the degree of photoreaction and on the ratio of the type of photoreacted products, which may affect the thermal property of exposed film.

2-3-5. Effect of Annealing Temperature

As described above, thermally enhanced molecular reorientation is triggered by the

photoinduced optical anisotropy of the irradiated film. Therefore, mobility of the mesogenic side groups will depend on the annealing temperature. Accordingly, we evaluated the reorientational behavior of films annealed at various temperatures, using doses of 30, 90, and 450 mJ cm^{-2}. Results shown in parts **(a)** and **(b)** of **Figure 2-10** plot the order parameter *S* for both films as a function of the annealing temperature. For all cases, an explicit magnification of *S* appears when the annealing temperature is larger than T_m of the PLC. When films are annealed above T_m, the direction of reorientation is found to be perpendicular to **E** when irradiated with 30 mJ cm^{-2} or parallel for films subjected to 450 mJ cm^{-2} doses, respectively. *S* of **P2CB** films with 90 mJ cm^{-2} doses, however, are initially negatively enhanced and then positively increase upon increase of annealing temperature.

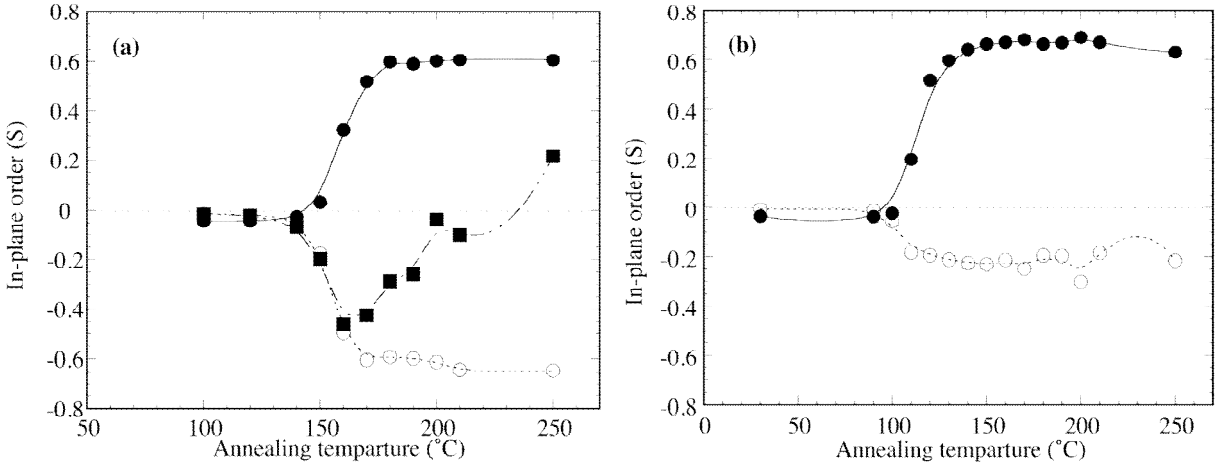

Figure 2-10 Change in in-plane order parameters (*S*) of **P*n*CB** films as a function of annealing temperature at various irradiation doses: ○, 30 mJ cm^{-2}; ●, 450 mJ cm^{-2}; ■, 90 mJ cm^{-2}, (a) **P2CB**; (b) **P6CB**.

Looking closely at **Figure 2-10**, the threshold temperature for thermal reorientation varies with exposure energy. **Table 2-3** summarizes the ratio of the thermally enhanced order parameter ($R = S_x/S_{(T_m+35)}$) with different exposure doses, where $S_{(T_m+35)}$ is taken as *S* at T_m + 35 (°C), and S_x is *S* annealed at T_m - 5, T_m, and T_m + 5 (°C) of the PLCs. For both PLCs irradiated with 30 mJ cm^{-2} doses, *R* values when annealed at T_m - 5 are close to that at T_m and at T_m + 5. This shows that thermally enhanced reorientation occurs below T_m of the PLC when the irradiation energy is 30 mJ cm^{-2}, indicating T_m of the PLC decreased after exposure as described in section ***2-3-2.***

Table 2-3 Ratio of Order Parameter *S* at Various Annealing Temperatures.

	Doses[b] (mJ cm^{-2})	$S_x/S(T_m + 35)$ [a]		
		$T_m - 5$[c]	T_m [c]	$T_m + 5$[c]
P2CB	30	0.71	1.0	1.01
	450	0.25	0.53	0.65
P6CB	30	0.70	0.81	0.82
	450	0.27	0.42	0.76

[a] Ration of order parameter annealed at T_x °C and at T_m + 35 °C.
[b] Irradiation energy. [C] Annealing temperature, °C.

In contrast, *R* values for PLC irradiated with 450 mJ cm^{-2} doses gradually increase with increasing annealing temperature, and *R* values at T_m - 5 are much lower than for films with 30 mJ cm^{-2} doses. It is suggested that the larger amount of photo-cross-linked side groups restrict the mobility of mesogenic side groups rather than lowering the T_m of the film; i.e., photo-cross-linked side groups control the thermally enhanced molecular reorientation in a direction parallel to **E**. For **P2CB** film irradiated for 90 mJ cm^{-2}, it is noteworthy that the enhanced negative value of *S* decreased with increasing annealing temperature and became positive with an annealing temperature of 250 °C. This indicates that reorientation in a direction perpendicular to **E** is generated by a similar manner with film irradiated at 30 mJ cm^{-2} when an annealing temperature of about T_m is used. However, immobile photo-cross-linked groups could act as the command group for thermal reorientation in a direction parallel to **E** when the annealing temperature is increased.

2-4. Conclusion

The reversion of in-plane reorientation of PLC films was investigated by irradiation with LPUV light and subsequent annealing, whereby a high orientational order in both directions was achieved. Spectral analysis of the films suggested that both photoisomerization and the photo-cross-linking reactions occurred in the mesogenic groups of the films, with the degree of the photo-cross-linking reaction occurring to a greater extent than that of other reactions and with the photo-Fries rearrangement occurring to the least extent. The mechanism of reversion of the orientational direction can be related to the degree and type of photoreaction

of the mesogenic groups, as illustrated in **Figure 2-11**. Thermal amplification of the perpendicular orientation of the films is induced by a small amount of photoproducts in a direction parallel to **E**, resulting in reorientation of the mesogenic groups perpendicular to **E**. On the other hand, when the degree of the photo-cross-linking becomes large enough in a direction parallel to **E**, reversion of orientation direction is generated because of the decrease in mobility at an elevated temperature in a direction parallel to **E**. Therefore, I anticipate these photoreactive PLC films may find application in new optical devices such as birefringent films for LCD, optical memory devices and photo-alignment layers for LCs. In this way, I describe the performance of **P6CB** as a photoalignment layer in following Chapter.

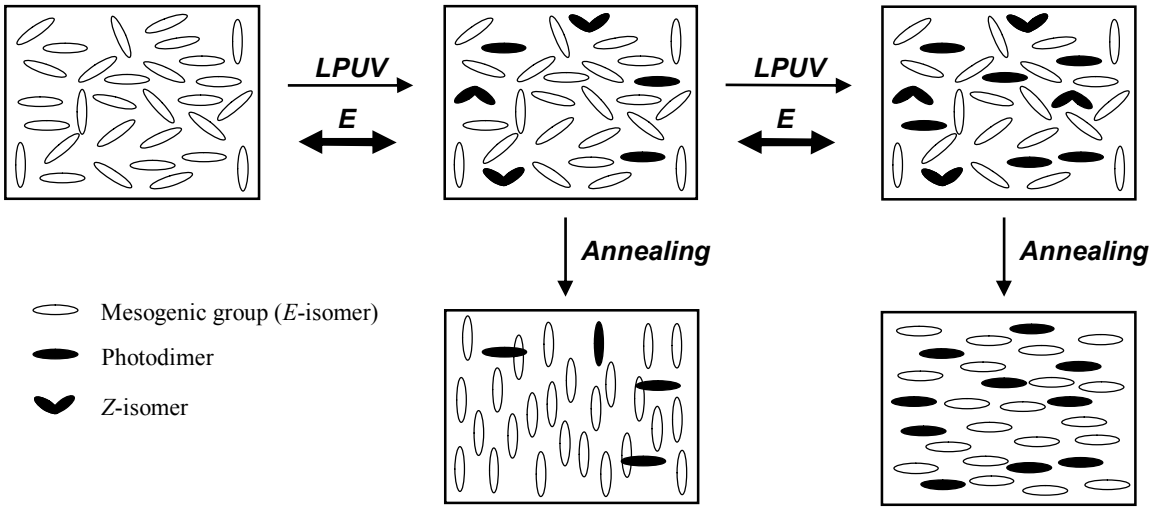

Figure 2-11 Model illustration of the reversion of thermally enhances in-plane reorientation of **PnCB** films.

2-5. References

(1) Shibaev, V. P.; Kostromin, S. G.; Ivanov, S. A. *Polymers as Electroactive and Photooptical Media*; Shibaev, V. P., Ed.; Springer: Berlin, **1996**; p 37.

(2) (a) MacArdle, C. B. *Applied Photochromic Polymer Systems*; MacArdle, C. B., Ed.; Blackie: New York, 1991; p 1. (b) Krongauz, V. *Applied Photochromic Polymer Systems*; Mac-Ardle, C. B., Ed.; Blackie: New York, **1991**; p 121.

(3) Anderle, K.; Birenheide, R.; Eich, M.; Wendrorff, J. H. *Makromol. Chem. Rapid Commun.* **1989**, *10*, 477.

(4) Benecke, C.; Seiberle, H.; Schadt, M. *Jpn. J. Appl. Phys.* **2000**, *39*, 525.

(5) Ichimura, K. *Chem. Rev.* **2000**, *100*, 1847.

(6) O'Neil, M.; Kelly, S. M. *J. Phys. D: Appl. Phys.* **2000**, *33*, R67.

(7) (a) Fischer, T.; La¨sker, L.; Stumpe, J. *J. Photochem. Photobiol. A: Chem.* **1994**, *80*, 453. (b) Andrews, S. R.; Williams, G.; La¨sker, L.; Stumpe, J. *Macromolecules* **1995**, *28*, 8863, (c) Fischer, T.; La¨sker, L.; Czapla, S.; Ru¨ bner, J.; Stumpe, J. *Mol. Cryst. Liq. Cryst.* **1997**, *298*, 213.

(8) (a) Holme, N. C. R.; Ramanujam, P. S.; Hvilsted, S. *Appl. Opt.* **1996**, *35*, 4622. (b) Ramanujam, P. S.; Holme, C.; Hvilsted, S.; Pedersen, M.; Andruzzi, F.; Paci, M.; Tassi, E.;Magagnini, P.; Hoffman, U.; Zebger, I.; Siesler, H. W. *Polym. Adv. Technol.* **1996**, *7*, 768.

(9) (a) Wu, Y.; Zhang, Q.; Kanazawa, A.; Shiono, T.; Ikeda, T. *Macromolecules* **1999**, *32*, 3951. (b) Wu, Y.; Demachi, Y.; Tsutsumi, O.; Kanazawa, A.; Shiono, T.; Ikeda, T. *Macromolecules* **1998**, *31*, 4457. (c) Wu, Y.; Demachi, Y.; Tsutsumi, O.; Kanazawa, A.; Shiono, T.; Ikeda, T. *Macromolecules* **1998**, *31*, 1104. (d) Wu, Y.; Demachi, Y.; Tsutsumi, O.; Kanazawa, A.; Shiono, T.; Ikeda, T. *Macromolecules* **1998**, *31*, 349.

(10) Meng, X.; Natansohn, A.; Rochon, P. *Supramol. Sci.* **1996**, *3*, 207.

(11) Labarthet, F.; Freiberg, S.; Pellerin, C.; Pe´zolet, M.; Natansohn, A.; Rochon, P. *Macromolecules* **2000**, *33*, 6815.

(12) Ruslim, C.; Ichimura, K. *Macromolecules* **1999**, *32*, 4254.

(13) Han, M.; Morino, S.; Ichimura, K. *Chem. Lett.* **1999**, 645.

(14) Han, M.; Ichimura, K. *Macromolecules* **2001**, *34*, 82.

(15) Han, M.; Ichimura, K. *Macromolecules* **2001**, *34*, 90.

(16) Han, M.; Morino, S.; Ichimura, K. *Macromolecules* **2000**, *33*, 6360.

(17) (a) Meier, J. G.; Ruhmann, R.; Stumpe, J. *Macromolecules* **2000**, *33*, 843. (b) Stumpe, J.; Fischer, T.; Rutloh, M.; Meier, J. G. *Proc. SPIE* **1999**, *3800*, 150.

(18) Kidowaki, M.; Fujiwara, T.; Morino, S.; Ichimura, K.; Stumpe, J. *Appl. Phys. Lett.* **2000**, *76*, 1377.

(19) Date, R. W.; Fawcett, A. H.; Geue, T.; Haferkorn, J.; Malcolm, R. K.; Stumpe, J. *Macromolecules* **1998**, *31*, 4935.

(20) Kawatsuki, N.; Takatsuka, H.; Yamamoto, T.; Sangen, O. *J. Polym. Sci., Part A:*

Polym. Chem. **1998**, *36*, 1521.

(21) (a) Kawatsuki, N.; Suehiro, C.; Yamamoto, T. *Macromolecules* **1998**, *31*, 5984. (b) Kawatsuki, N.; Matsuyoshi, K.; Yamamoto, T. *Macromolecules* **2000**, *33*, 1698.

(22) (a) Kawatsuki, N.; Suehiro, C.; Shindo, H.; Yamamoto, T.; Ono, H. *Macromol. Rapid Commun.* **1998**, *19*, 201. (b) Kawatsuki, N.; Yamamoto, T.; Ono, H. *Appl. Phys. Lett.* **1999**, *74*, 935.

(23) (a) Kawatsuki, N.; Ono, H.; Takatsuka, H.; Yamamoto, T.; Sangen, O. *Macromolecules* **1997**, *30*, 6680. (b) Kawatsuki, N.; Takatsuka, H.; Yamamoto, T.; Ono, H. *Jpn. J. Appl. Phys.***1997**, *36*, 6469.

(24) Obi, M.; Morino, S.; Ichimura, K. *Jpn. J. Appl. Phys.* **1999**, *38*, L145.

(25) (a) Obi, M.; Morino, S.; Ichimura, K. *Macromol. Rapid Commun.* **1998**, *19*, 643. (b) Obi, M.; Morino, S.; Ichimura, K. *Chem. Mater.* **1999**, *11*, 656.

(26) Kawatsuki, N.; Matsuyoshi, K.; Hayashi, M.; Takatsuka, H.; Yamamoto, T. *Chem. Mater.* **2000**, *12*, 1549.

(27) Kawatsuki, N.; Sakashita, S.; Takatani, K.; Yamamoto, T.; Sangen, O. *Macromol. Chem. Phys.* **1996**, *197*, 1919.

(28) Ichimura, K.; Akita, Y.; Akiyama, H.; Kudo, K.; Hayashi, Y. *Macromolecules* **1997**, *30*, 903.

(29) Turro, N. J. *Modern Molecular Photochemistry*; The Benjamin/Cummings Publishing: Menlo Park, 1978.

(30) Schadt, M.; Schmitt, K.; Kozinkov, V.; Chigrinov, V. *Jpn. J. Appl. Phys.* **1992**, *34*, 2155.

Chapter 3

Photoalignment Properties of Molecular Oriented Film for Liquid Crystals

3-1. Introduction

The fabrication of liquid crystal displays (LCDs) requires the uniform alignment of liquid crystal (LC) molecules. Since the mechanical rubbing of polyimide (PI) films, which is the most conventional technique for the LC alignment, causes some problems such as the generation of dust and static electricity, non contact techniques to align LC molecules have been widely explored.[1] Among them, photoalignment has received much attention from the viewpoints of theoretical and practical interests.[1,2] The photoalignment layer for LCs is usually fabricated by irradiating a photoreactive film using linearly polarized (LP) light.[1,2] The axis- or direction-selective photoreaction induces an optical anisotropy of the film,[3] which controls the homogeneous LC alignment direction.[4] One of the factors determining the LC alignment is the chemical interaction between the LC molecules and the photoalignment layer. For the poly(vinyl cinnamate) (PVCi) photoalignment layer, which exhibits a axis-selective photodimerization reaction under LP ultraviolet (UV) light, LC molecules are aligned perpendicular to the electric vector (**E**) of LPUV light.[4,5] In this case, nonphotoreacted and photodimerized molecules determine the LC alignment direction to be perpendicular to **E**, where the required degree of the photoreaction for the LC alignment is approximately 10 – 40 mol %. As most of the cinnamate molecules are randomly oriented, the azimuthal anchoring energy is relatively small compared with the conventional rubbed PI film. It is expected that photoalignment layers with a molecular-oriented structure exhibit higher azimuthal anchoring than those without it. Furthermore, it is suitable for the LC alignment of the photoalignment layer to be parallel to **E** for the tilt-angle formation by the use of the slantwise exposure technique.[6,7] Additionally, a photoalignment layer possessing high durability and photosensitivity is required for practical purposes. In this way, we have carried out systematic studies on the photoinduced reorientation of polymethacrylates comprising photoreactive mesogenic side groups by irradiation with LPUV light, and have studied their application to the photoalignment layer for LCs.[7–9] In addition, novel photoreactive material showing large orientational order has been developed as described in chapter 2. In this chapter, it is

described the development of a new photoalignment layer for LCs, **PLC1** which is a modified **P6CB** developed in chapter 2, exhibits high photosensitivity, high azimuthal anchoring, tilt-angle formation of LCs, and high thermal stability.

3-2. Experimental Section

3-2-1. Materials

The photoreactive polymer **PLC1** shown in **Figure 3-1(a)** was used as the photoalignment layer. The synthesis of **PLC1** is described elsewhere.[10] The number average molecular weight (M_n) of the polymer is 25,000. This polymer exhibits a nematic LC phase between 112 and 289 °C.

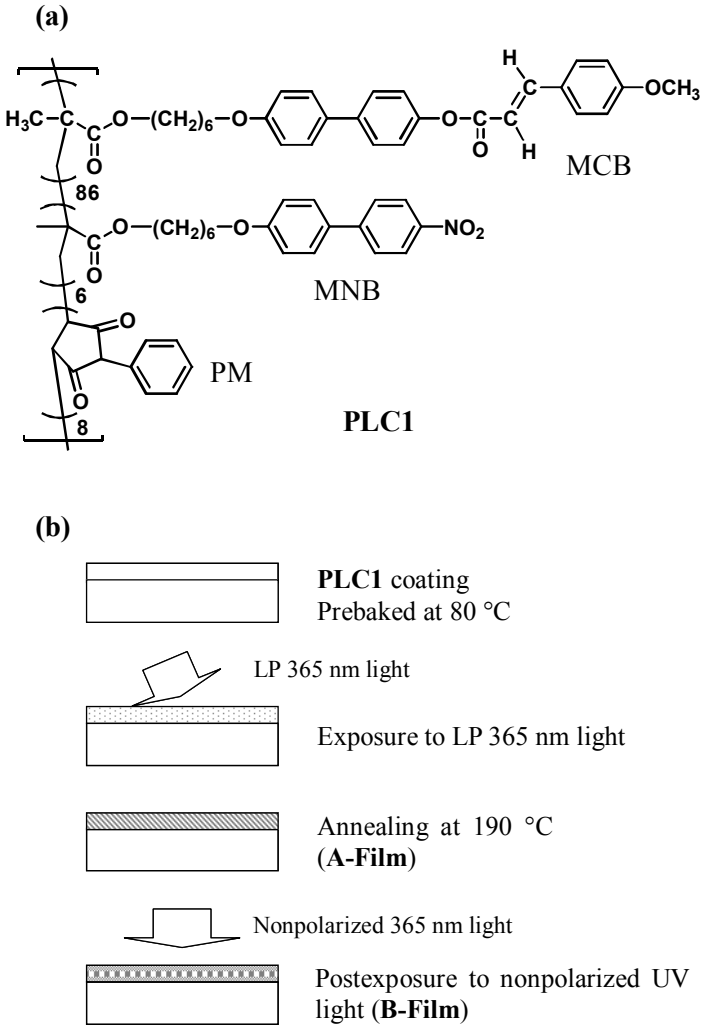

Figure 3-1 (a) Chemical structure of **PLC1** photoalignment layer.
(b) Fabrication process for the photoalignment layer.

3-2-2. Fabrication of PLC1 Alignment Layer

The fabrication process of the LC alignment layer is shown in **Figure 3-1(b)**. A 20 – 60 nm-thick **PLC1** film was spin-coated on quartz or glass substrates using a chloroform solution. After prebaking at 80 °C for 10 min, the film was exposed to a LP 365 nm light from a xenon-lamp (using a band-path filter at 365 nm) and subsequently annealed at 190 °C for 10 min (A-film). The A-film was further exposed to a nonpolarized (NP) 365 nm light (postexposure) to accomplish the photoreaction of the entire area (B-film).

3-2-3. Evaluation of Photoreaction and LC alignment

The axis-selective photoreaction and photoinduced optical anisotropy of the film were evaluated by polarization UV-vis spectroscopy. To evaluate the LC alignment behavior, an antiparallel LC cell was fabricated using two A- (or B-) films. The 12.5 μm-thick LC cell was filled with a nematic LC mixture (ZLI4792: Merck Japan, T_i . 102 °C) doped with 0.1 wt% dichroic dye (disperse blue 14 (DB14), Aldrich) at 110 °C and then cooled slowly. Homogeneous LC alignment order was evaluated by dichroic absorption measurement utilizing a guest-host effect. The in-plane order was evaluated using the order parameter, *S*, which is expressed as following eq.

$$S = (A_{\parallel} - A_{\perp}) / (A_{(\text{large})} + 2A_{(\text{small})})$$

This equation means that the reorientation direction of the LP 365 nm light is parallel to E for $S > 0$, and perpendicular for $S < 0$. Where $A_{\parallel}$ and $A_{\perp}$ are the absorbances parallel and perpendicular to **E**, respectively, and $A_{(\text{large})}$ is the larger value of $A_{\parallel}$ and $A_{\perp}$, and $A_{(\text{small})}$ is the smaller value. The azimuthal anchoring energy was evaluated by a torque balance method using a twisted nematic LC cell (4 μm-thick). To evaluate effect of NP 365 nm light postexposure for the azimuthal anchoring energy, 4 μm-thick anti-parallel LC cell using two A- and B-films was fabricated and the alignment quality of LC cells was observed before isotropic treatment with Polarization Microscope (POM).

3-3. Results and Discussion

3-3-1. Photoinduced Reorientation

The photoreactive polymer **PLC1** contains three functional components; MCB is a

photo-cross-linkable mesogen, MNB is a photosensitizing mesogen, and PM is a comonomer that inhibits the thermal aggregation of the mesogenic groups. On the basis of the polarization-preserved energy transfer from photoexcited MNB to MCB groups,[10] **PLC1** exhibits a high photoreactivity to LP 365 nm light, and the resultant film shows a small optical anisotropy. The photosensitivity improves by a factor of 50 times and by more than that without MNB groups. Since the axis-selective photoreacted MCB groups act as photo-cross-linked anchors, annealing at elevated temperatures enhances the optical anisotropy due to the LC nature of **PLC1**. Detailed photosensitizing and the molecular reorientation mechanisms are described in refs. 10 and 11. **Figure 3-2(a)** shows plots of thermally amplified *S* values measured at 270 nm (absorption band of biphenyl moiety) of A- and B-films as a function of the exposure energy of LP 365 nm light. For A-films, molecular reorientation parallel to **E** is generated when the exposure doses are 0.2 – 0.8 J cm^{-2}. After the postexposure (B-films), a decrease in the *S* value was observed. This is due to the decrease in the absorbance caused by the photoreaction of the MCB groups in the entire area.

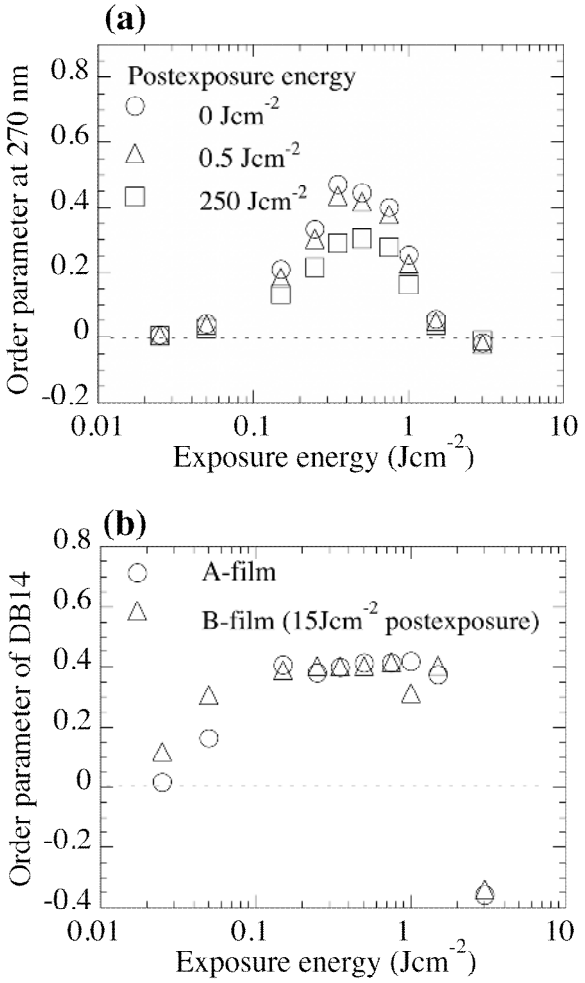

Figure 3-2 (a) Photoinduced in-plane order parameter of **PLC1** photoalignment layer at 270 nm as a function of exposure energy. (b) In-plane order parameter of dichroic dye (DB14) doped in the LC cell using various types of A- and B-films as a function of exposure energy.

3-3-2. LC Alignment

The LC alignment behavior on A- and B-films was evaluated using parallel LC cells. **Figure 3-2(b)** shows plots of the order parameter of DB14 in the LC cell measured at 584 nm using A- and B-films as a function of the exposure energy of LP 365 nm light. The figure

shows that a uniform LC alignment parallel to **E** is obtained when the exposure energy is 0.15 –1.5 J cm^{-2} for both A- and B-films, when the photoalignment layer exhibits a high in-plane molecular orientation (**Figure 3-2(a)**). This means that the molecular reorientation direction of the **PLC1** film determines the LC alignment direction, and the interaction between the LC molecules and the reoriented MCB and MNB side groups in the film plays an important role in the LC alignment. Because the postexposure decreases the amount of cinnamate groups, the interaction between the reoriented biphenyl moieties and the LCs controls the LC alignment direction for the B-films. In contrast, LCs align perpendicular to **E** when the exposure energy is 3.0 J cm^{-2}, when the molecular reorientation of the alignment layer does not occur. This is due to the interaction of unphotoreacted mesogenic side groups and LC molecules, as observed in other types of photoalignment layers.[4,5]

Table 3-1 shows a summary of the azimuthal anchoring energy of the **PLC1** and PVCi photoalignment layers fabricated under several conditions. The azimuthal anchoring energy for **PLC1** is approximately 10^{-4} N m^{-1} and increases slightly as postexposure energy increases. These values are one order larger than that of a conventional PVCi photoalignment layer. From this result, it is revealed that the high anchoring energy is leaded by the molecular-oriented structure of the photoalignment layer. Photographs of LC cells fabricated using two A- and B- films corresponding to the irradiation conditions for measurement of azimuthal anchoring energy are displayed in **Figure 3-3**. Although flow defect was observed in LC cell using two A-films caused by weak anchoring energy of alignment layer (**Figure 3-3(a)**), NP 365 nm postexposure improved alignment quality as postexposure energy increased (**Figure 3-3(b)-(c)**). This alignment behavior of LC on **PLC1** alignment layer corresponded to the measurement result of azimuthal anchoring energy.

Table 3-1 Anchoring energy of photoalignment layer under various fabrication conditions[a].

Material	LP (J cm^{-2})	NP[b] (J cm^{-2})	Anchoring Energy (N m^{-1})
PLC1	0.5	0	0.72×10^{-4}
PLC1	0.5	0.52	0.78×10^{-4}
PLC1	0.5	15	1.1×10^{-4}
PVCi	0.5	0	$< 10^{-5}$
PVCi	0.5	0.5	No alignment

a) Measured by torque balance method. Annealing was not carried out for the PVCi films because of the low T_g of the material.
b) Postexposure.

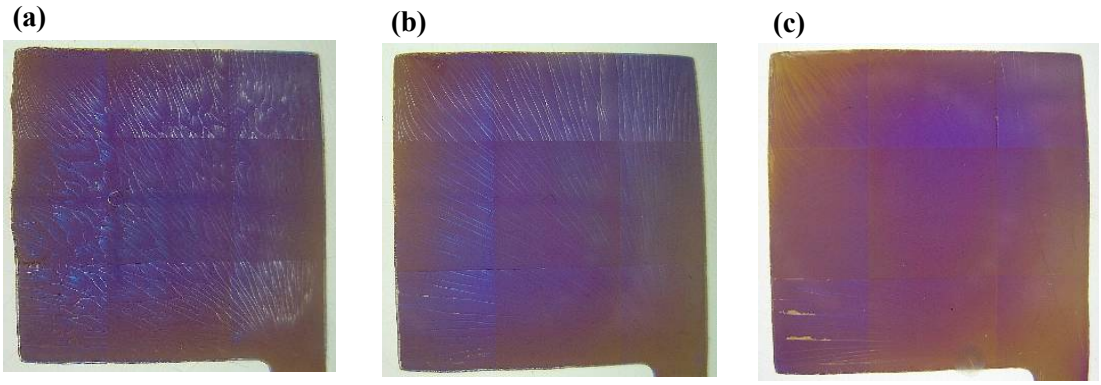

Figure 3-3 Photographs of LC cells, (a) fabricated using two A- films irradiated 0.5 J cm^{-2} of 365 nm LPUV light and annealed at 180 °C for 10min. (b): fabricated with two B-films irradiated 0.5 J cm^{-2} of 365 nm LPUV light and subsequently annealed at 180 °C for 10min and then further exposed to 365 nm 0.52 J cm^{-2}. (c): fabricated with two B- films irradiated 0.5 J cm^{-2} of 365 nm LPUV light and subsequently annealed at 180 °C for 10min and then further exposed to 365 nm 15 J cm^{-2}.

3-3-3. Thermal Stability of Molecularly Oriented Structure

For the effective LC alignment of **PLC1**, the degree of the anisotropic photoreaction must be approximately 10 mol %. The postexposure of the A-film to nonpolarized UV light generates a higher degree of the photo-cross-linked network, which affects the thermal stability of the film. **Figure 3-4** shows a plot of the in-plane order parameter of A- and B-films, after heating at elevated temperatures for 10 min, in order to evaluate the thermal stability. It shows that the *S* value of A-films does not change up to 250 °C, and the molecular orientation decreases at 270 °C. The film annealed at 270 °C does not align the LC molecules. This is a consequence of the disappearance of the molecular orientation of the alignment layer. In contrast, the initial *S* value for B-films gradually decreases at higher temperatures. Interestingly, LC molecules were uniformly aligned in case of the alignment layer that was annealed up to 280 °C, where the *S* value was

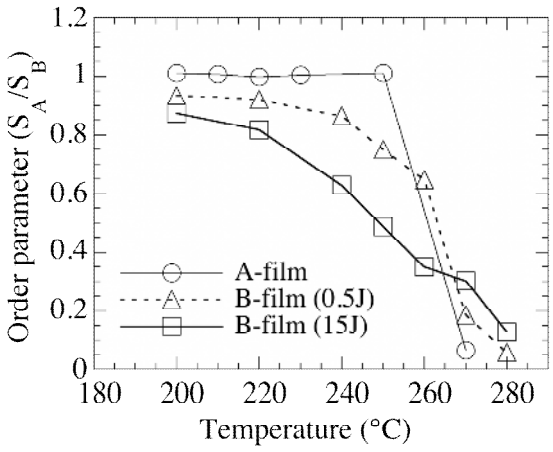

Figure 3-4 Order parameter (S_B/S_A) of A- and B-films when they were heated at elevated temperatures. S_A: *S* values after annealing, S_B : initial *S* values.

less than 0.15. The postexposure process generates a high degree of cross-linking which decreases the LC nature of the film, and allows the thermal motion of the mesogenic side groups in the network at lower temperatures. However, the network structure maintains a partial orientation of the biphenyl moieties parallel to **E**, which can control the LC alignment.

3-3-2. Formation of Pre-tilt angle

The formation of a tilt of LC alignment is conducted by the *p*-polarized slantwise exposure of **PLC1** films, as shown in **Figure 3-5(a)**. The exposure energy for each alignment layer was 0.5 J cm^{-2}. **Figure 3-5(b)** shows plots of the tilt angle of the LCs for antiparallel LC cells as a function of exposure angle. It shows that adjusting the angle of the *p*-polarized UV light controls the tilt angle by up to 4.5°. Because the slantwise *p*-polarized LPUV light exposure generates the slantwise molecular reorientation of the **PLC1** photoalignment layer, LC molecules align along the obliquely reoriented side groups to form tilt angles.

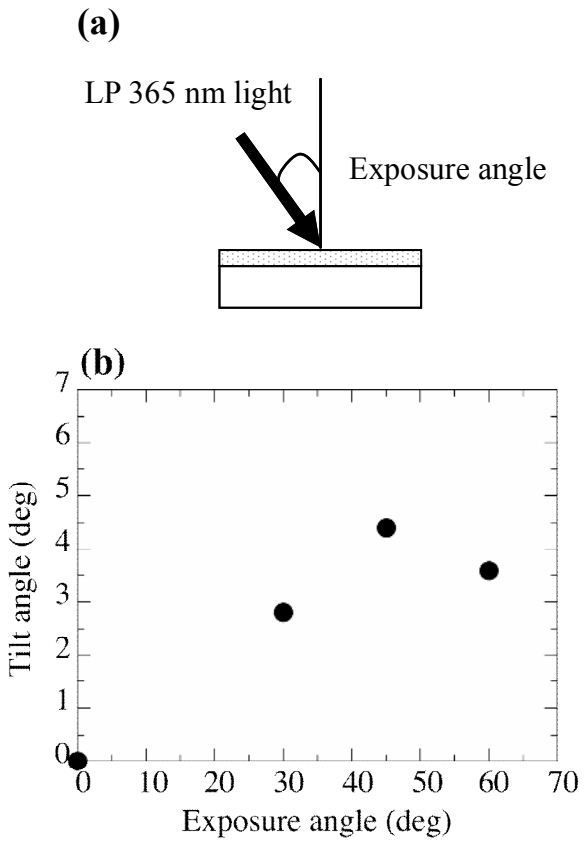

Figure 3-5. (a) Schematic illustration of slantwise *p*-polarized light exposure. (b) Tilt angle of LC cells as a function of exposure angle of *p*-polarized UV light. A-films were used for the anti-parallel LC cell fabrication.

3-4. Conclusion

A new photoalignment layer for LCs, which exhibits high thermal stability (up to 250 °C), is demonstrated. Since the LC alignment direction is controlled by the molecular orientation angle of the photoalignment layer, the azimuthal anchoring energy of the alignment layer is greater than that of the conventional PVCi photoalignment layer. The formation of the tilt angle of LCs is successfully achieved by adjusting the angle of the *p*-polarized UV light exposure. Further investigations of the electrooptical properties of the LC cell are underway.

3-5. References

1) M. O'Nell and S. M. Kelly: *J. Phys*., **2000**, *D 33*, R67.

2) K. Ichimura: *Chem*. *Rev*., **2000**, *100*, 1847.

3) V. A. Barachevsky: *Proc. SPIE 1559*, **1991**, 184.

4) M. Schadt, K. Schmitt, V. Kozinkov, and V. Chigrinov: *Jpn*. *J*. *Appl*. *Phys*., **1992**, *31*, 2155.

5) Y. Iimura, T. Saitoh, S. Kobayashi, and T. Hashimoto: *J*. *Photopolym*. *Sci*. *Technol*., **1995**, *8*, 257.

6) M. Schadt, H. Seiberle, and A. Schuster: *Nature*, **1996**, *381*, 212.

7) N. Kawatsuki, H. Ono, H. Takatsuka, T. Yamamoto, and O. Sangen: *Macromolecules*, **1997**, *30*, 6680.

8) N. Kawatsuki, H. Takatsuka, and T. Yamamoto: *Jpn*. *J*. *Appl*. *Phys*., **2000**, *39*, L230.

9) N. Kawatsuki, K. Matsuyoshi, M. Hayashi, H. Takatsuka, and T. Yamamoto: *Chem*. *Mater*., **2000**, *12*, 1549.

10) N. Kawatsuki, K. Kato, T. Shiraku, T. Tachibana, and H. Ono: *Macromolecules*, **2006**, *39*, 3245.

11) N. Kawatsuki, M. X. An, Y. Matsuura, T. Sakai, and H. Takatsuka: *Liq*. *Cryst*., **2004**, *31*, 55.

Chapter 4

Synthesis of Side Chain Liquid Crystalline Cinnamide Polymers Based on Post Polymer Reaction

4-1. Introduction

Introducing low molecular weight (LMW) functional materials into a simple polymer via polymer reaction or noncovarent bonding is a useful method because it can add electrical,[1] optical,[2,3] and photomechanical[4] properties originated from LMW materials. We have previously studied on the enhancement of processability of a π-conjugated LMW combined with photoreactive polymer liquid crystal (PLC) materials[5,6] and reported that fluorene derivatives can be aligned along the director of PLC film by using LC property[5] or hydrogen bonding.[6] PLCs induce a large photoinduced molecular reorientation when a thin film of these materials is exposed to linearly polarized UV (LPUV) light followed by annealing. PLCs also change their cross-linking density, acidity and dielectric properties just by tuning the polarization direction and exposing time of the actinic beam. Therefore, I focused on activated ester groups to enhance the reactivity and thermal stability for polymer functionalization. It can be connected to carboxylic molecular terminal and PLC can be functionalized by LMW compounds containing amine as end group due to its ability to convert to amide bonding by using amine compounds under a mild condition. In this chapter, I synthesized PLC containing activated ester as end group and explored their functionalization with primary phenyl amine derivatives and photoresponsive behavior.

4-2. Experimental Section

4-2-1. Materials and Monomer Synthesis

Figure 4-1 shows chemical structure of the polymers used in this study. We used phenyl amine to evaluate the effect of liquid crystal property on axis-selective photoreaction of cinnamide group. Synthetic route of the cinnamide polymers are described in **Scheme 4-1**. The photoreactive cinnamide was prepared from activated photoreactive polymer ester (**P6CAM-S**) and mixed with various liquid amines in order to convert to cinnamide derivatives (**P6CAM-A1, A2**). The cinnamic acid polymer (**P6CAM**) was synthesized

according to the literature as for example in reference 7.

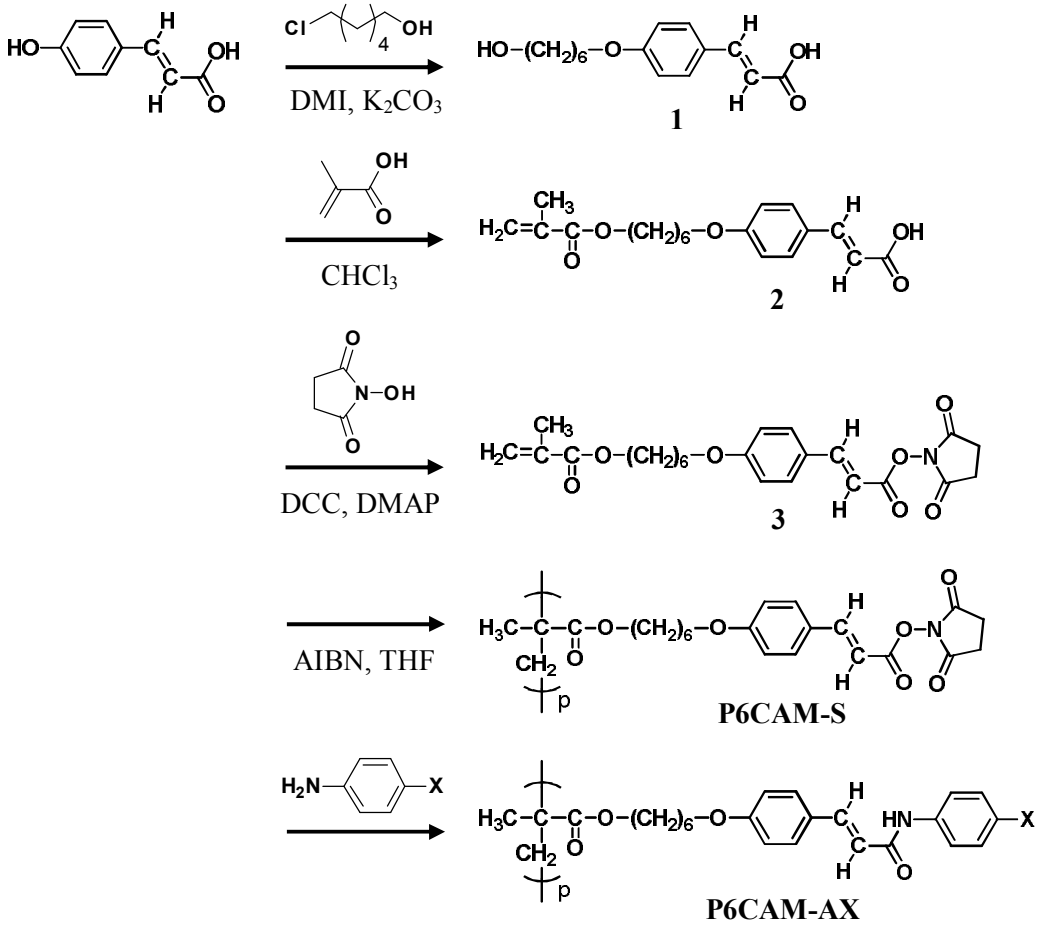

Scheme 4-1 Chemical structure and synthetic route to cinnamide polymer.

4-(6-Hydroxyhexyloxy) cinnamic Acid (1)

A mixture of *trans-p*-coumaric acid (25.0 g, 0.15 mol) and 6-chloro-1-hexanol (52 g, 0.38 mol) was dissolved in 25 g of N,N-dimethylimidazoridinone, potassium carbonate (25 g, 0.18 mol) and a trace amount of potassium iodide were added to the solution. The resulting solution was heated at 130 °C for 17 h. After the reaction mixture was cooled to 70 °C, 40 ml of water, 30 g (0.53 mol) of potassium hydroxide and 40 ml of methanol were added to the mixture and reflux for 1 h. The resultant solution was cooled to room temperature. After concentrated aqueous hydrochloric acid solution was added to the reaction mixture to give pH 3, the precipitated solid was collected and washed with water. The crude product was recrystalized from a mixture of *n*-hexane and tetrahydrofurane (THF) to give **1** (6.8 g, 22 mmol) in 47 % yield. ^{1}H-NMR (DMSO): δ(ppm) 1.34–1.36 (d, J = 6.6 Hz, 3H), 1.40–1.46 (m,

5H), 1.70–1.73 (t, J = 7.3 Hz, 3H), 4.01 (s, 2H), 4.38 (s, 1H), 6.36–6.39 (d, J = 16 Hz, 1H), 6.95–6.97 (d, J = 8.8 Hz, 2H), 7.53–7.56 (d, J = 16 Hz, 1H), 7.62–7.63 (d, J = 8.8 Hz, 2H)

4-(6-Methacryloyloxy-1-hexyloxy)-cinnamic Acid (2)

14 g (50 mmol) of **1** and 4.3 g (40 mmol) of *p*-toluene sulfonic acid was dispersed in a mixture of 5 ml of chloroform and 5.2 g of methacrylic acid (38 mmol). The mixture was refluxed at 85 °C for 4 h. After the resulting solution was cooled down to room temperature, 40 ml of diethyl ether was added and it was washed with water for 20 times. After the solvent was removed, a yellow solid obtained was purified by column chromatography on silica gel (chloroform) and recrystallized from ethyl acetate and methanol to give **2** (3.2 g, 6.6 mmol) in 19 % yield. ^{1}H-NMR (DMSO): δ(ppm) 1.40–1.45 (m, 4H), 1.63–1.66 (m, 2H), 1.72–1.74 (m, 2H), 1.89 (s, 3H), 4.01 (s, 2H), 4.10 (s, 2H), 5.66–5.67 (t, J =1.6 Hz, 1H), 6.02 (s, 1H) 6.36–6.39 (d, J = 16 Hz, 1H), 6.95–6.97 (d, J = 8.8 Hz, 2H), 7.52–7.56 (d, J = 16 Hz, 1H), 7.61–7.63 (d, J = 8.7 Hz, 2H)

4-(6-Methacryloyloxy-1-hexyloxy)-cinnamic Acid N-Succimide (3)

2.0 g (6.0 mmol) of **2**, 0.83 g (7.2 mmol) of N-hydroxysuccinimide, trace amount of 4-dimethylaminopyridine (DMAP), and 1.5 g (7.2 mmol) of dicyclohexyl carbodiimide (DCC) was put in 100 ml flask. Then, 40 mL of dried THF was slowly added. The reaction mixture was kept under stirring at room temperature for 19 h. The precipitate formed during the reaction was filtered off and the organic solution was washed with water. The mixture was dried over sodium sulfate and evaporated under vacuum. The crude product was purified by silica gel column chromatography (ethyl acetate: *n*-hexane = 7:3) and finally recrystallized from *n*-hexane/THF to give **3** (1.3 g, 0.22 mmol) in 50 % yield. ^{1}H-NMR ($CDCl_3$): δ(ppm) 1.49–1.56 (m, 4H), 1.63 (s, 2H), 1.73–1.76 (t, J = 7.2 Hz 2H), 1.83–1.86 (t, J = 7.3 Hz 3H), 1.96 (s, 4H), 2.91 (s, 4H), 4.03 (s, 2H), 4.18 (s, 2H), 5.57(s, 1H), 6,12 (s, 1H), 6.45–6.48 (d, J = 16 Hz, 1H), 6.93–6.94 (d, J = 8.7 Hz, 2H), 7.53–7.54 (d, J = 8.7 Hz, 2H), 7.89–7.91 (d, J = 16 Hz, 1H).

4-2-2. Polymerization of 3

0.8 g (1.9 mol) of **3** and 3.6 mg (0.022 mol) of AIBN were dissolved in chloroform and placed in a polymerization tube. The tube was sealed under nitrogen atmosphere after bubbling with nitrogen for 40 min. Then, the tube was kept at 60 °C for 24 h. The resulting

solution was cooled to room temperature and poured into diethylether with vigorously stirring to precipitate the polymer. The polymer obtained was purified by repeated reprecipitation from THF into a large excess of diethylether and dried under vacuum to yield 0.52 g of **P6CAM-S** in 65 wt% conversion. The number average molecular weight (M_n) of **P6CAM-S** determined by gel-permeation chromatography was about 29,000 and M_w/M_n = 3.7.

4-2-3. Polymer Functionalization

40 mg of **P6CAM-S** and 100 mg of phenylamine was mixed at room temperature for 3 h and washed with aqueous hydrochloric acid to afford **P6CAM-A1** or **P6CAM-A2**.

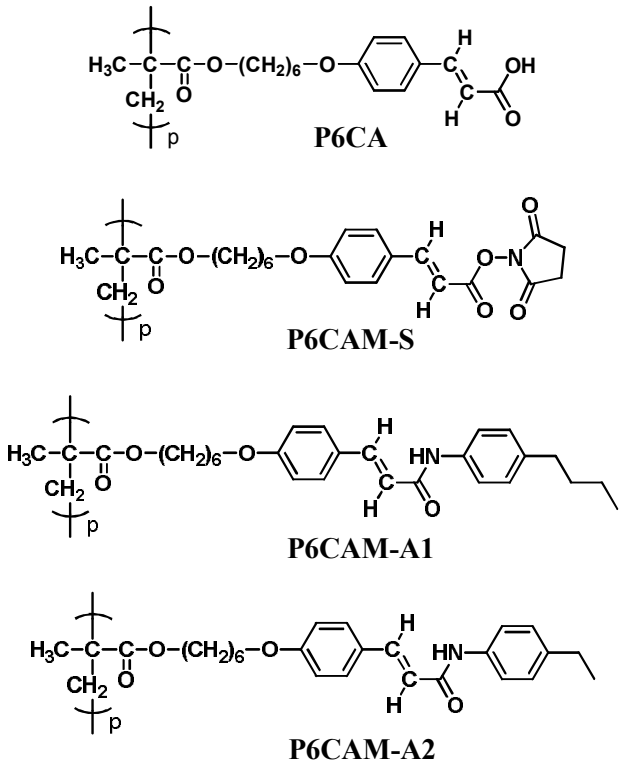

Figure 4-1 Chemical structure of cinnamide polymers used in this study.

4-2-4. Measurements

^{1}H-NMR spectra of synthesized compounds were taken on a Bruker DRX500. Thin films of cinnamic acid derivatives were prepared by spin-coating of polymer solutions onto a quartz substrate. The film was irradiated by UV-light from a 250 W high-pressure Hg-UV lamp (Ushio, spotcure UIS 20102) that was passed through Glan-Taylor polarizing prisms with a

cut-off filter below 290 nm. The light intensity was about 150 mW cm^{-2} at 365 nm. After exposing, the film was annealed at elevated temperatures for 10 min. The optical anisotropy of the film was evaluated with a polarizing microscope (POM: OLMPUS, BX-51P) and polarized absorption spectroscopy (Hitachi, U3010). Conversion of succimide into amide terminal was confirmed with ^{1}H-NMR, FT-IR spectrometer (Jasco, FT/IR-410) and ATR FT-IR spectrometer (Jasco, FT-IR-480 plus). The thermodynamic properties of the polymers were analyzed using differential scanning calorimetry (DSC; Seiko I&E SSC-5200 and DSC220C) at heating and cooling rates of 10 °C min^{-1}. The molecular weight of the polymer was determined by gel permeation chromatography (GPC; Sugai, U-620 column, Jasco UV-2075, RI-8020, TOSOH Gskgel 4000H, Gskgel α5000; eluent, chloroform) calibrated with standard polystyrenes.

4-3. Results and Discussion

4-3-1. Preparation of Cinnamide Group

In a previous work, Zhang *et al.* described a novel method for preparation of cross-linked liquid crystalline polymers by using N-hydroxysuccinimide carboxylate, an activated ester that can react with primary amines easily under mild reaction conditions.[8] In this work, we applied the activated ester structure for PLC. **Figure 4-2** shows IR spectra of the **P6CAM-S**, **P6CAM-A1** and **P6CAM-A2** respectively. It is clearly observed that peak around 1739 cm^{-1} for FT-IR spectrometry originating from imide group was reduced and 1700 – 1650 cm^{-1} was increased after the reaction.

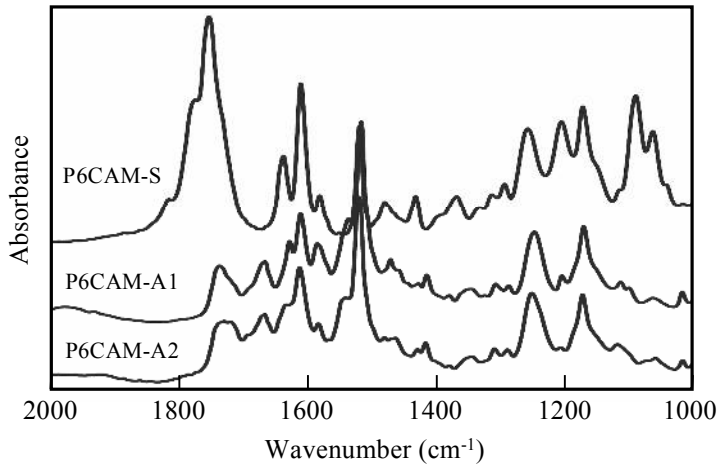

Figure 4-2 Change in FT-IR spectra of the activated ester by adding amine derivatives.

Moreover, the phenyl cinnamide group showed low solubility for chloroform, which can dissolve **P6CAM-S**, indicating that the activated ester converted amide group effectively in a polymer state. **Figure 4-3** shows DSC thermogram of the compounds. **P6CAM** and **P6CAM-A1** showed LC phase while the others showed no mesophase at relevant temperature. In addition, no obvious peak of glass transition was found in **P6CAM-A1** due to strong hydrogen bonding though it became viscous when they were heated above 100 °C. **Figure 4-4** displays absorption spectrum of the cinnamic acid derivatives used in this study. The absorbance was normalized in 314 nm, which corresponds to a peak of **P6CAM**. It was found that the peak red shifted for the succinimide group while it blue shifted correspond to amide group.

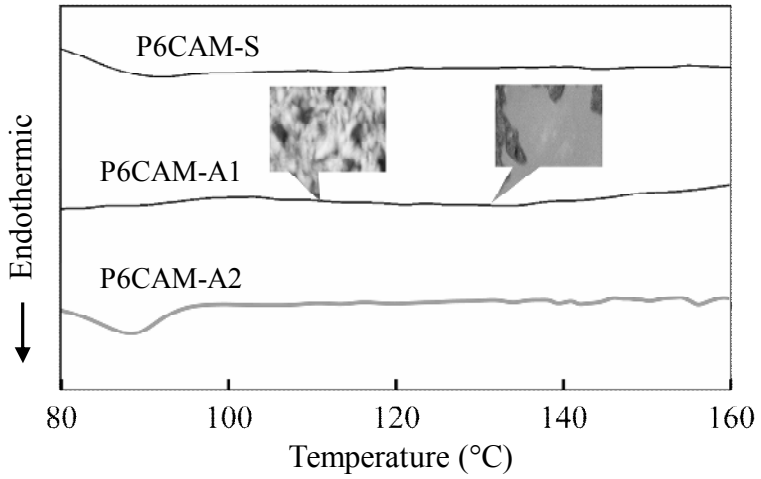

Figure 4-3 DSC thermogram of the polymers. The inset photograph represents the POM image of the **P6CAM-A1**.

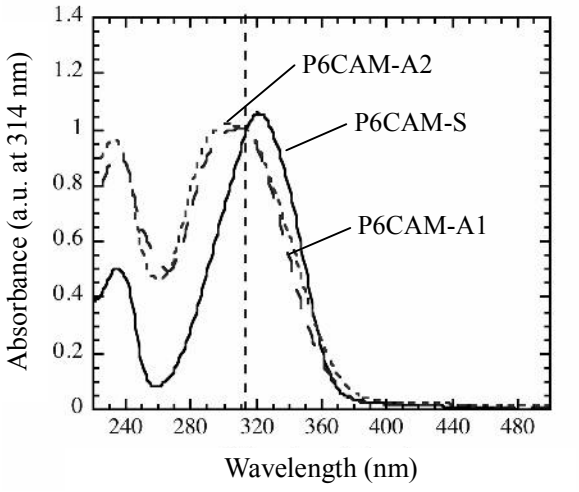

Figure 4-4 Comparison of absorption spectra of polymer films.

4-3-2. Photoreactivity of the Cinnamide Group

It was known that irradiating copolymer films comprising cinnamic acid groups and cinnamate-containing groups with LPUV light induced an axis-selective [2 + 2] photodimerization reaction, consequently, negative optical anisotropy is generated in the resultant films. Change in absorption spectrum of **P6CAM-A1** film and change in absorbance at 320 and 280 nm is displayed in **Figure 4-5**. A peak around 320 nm decreased upon exposure with UV light, the increase in absorbance at longer region (≈ 300 nm) owing to photo-Fries rearrangement was not observed in the polymers.[9] We defined degree of photoreaction by the following equation,

$$\Delta P = \frac{(A_{\parallel} + A_{\perp})_{\text{initial}} - (A_{\parallel} + A_{\perp})_{\text{exposure}}}{(A_{\parallel} + A_{\perp})_{\text{initial}}} \times 100$$

where $A_{\parallel}$ and $A_{\perp}$ are the absorbance at 314 nm parallel and perpendicular to electric vector of linearly polarized light, respectively. Degree of the photoreaction of cinnamic acid films as a function of exposure doses is described in **Figure 4-6**. It was found that the photoreaction of cinnamide groups use larger dose than that of **P6CAM** and **P6CAM-S** indicating that structure of molecular terminal strongly affected photoreactivity of PLCs. **Figure 4-7** plots the photoinduced dichoroism, $\Delta A = A_{\parallel} - A_{\perp}$, of cinnamic acid and their derivative films as a function of the exposure doses. All films show a generation of a negative ΔA due to the axis-selective photoreaction though **P6CAM-S** showed small dichoroism. It is well known that the annealing process enhanced the photoinduced optical anisotropy of cinnamic LC polymers.

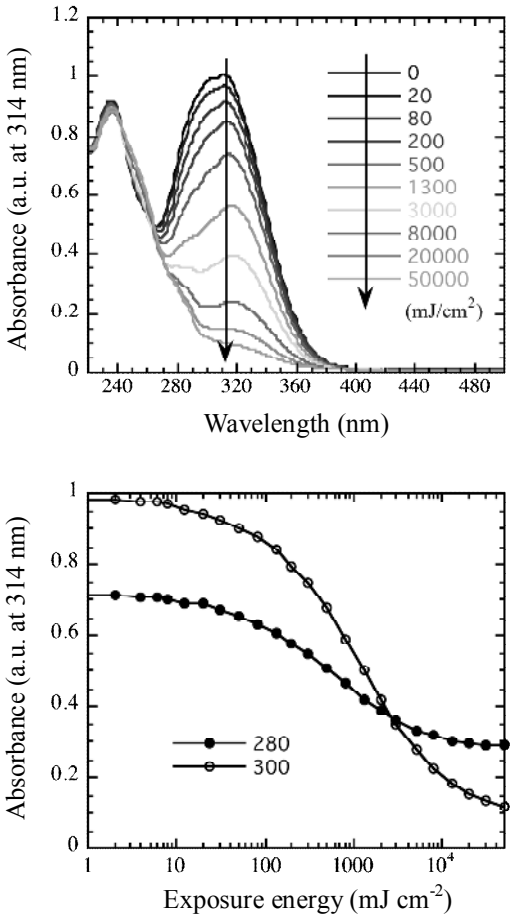

Figure 4-5 Change in absorption spectra of the **P6CAM-A1** film (a) and absorbance of **P6CAM-A1** film at 280 nm and 380 nm exposed with LPUV light (b).

Figure 4-8 shows polarized absorption spectrum of PLC films before and after photoirradiation and subsequent annealing. In this case, the degree of the photoreaction was fixed to 3 % (30 mJ cm^{-2}) that induces the largest value for **P6CAM** under thermal amplification. It was found that the optical anisotropy between $A_{\parallel}$ and $A_{\perp}$ became larger on annealing. Additionally, the absorption of $A_{\parallel}$ and $A_{\perp}$ after annealing was smaller than that after exposure. These results indicate that the cooperative effect in **P6CAM-A1** is not large enough to reorient the mesogenic side group in the in-plane direction after the annealing procedure even though it showed LC phase and containing hydrogen bonding.

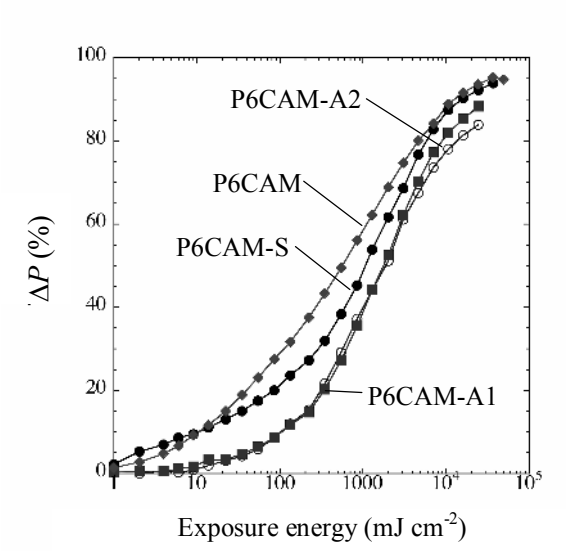

Figure 4-6 Change in degree of photoreaction of the polymers as a function of exposure energy.

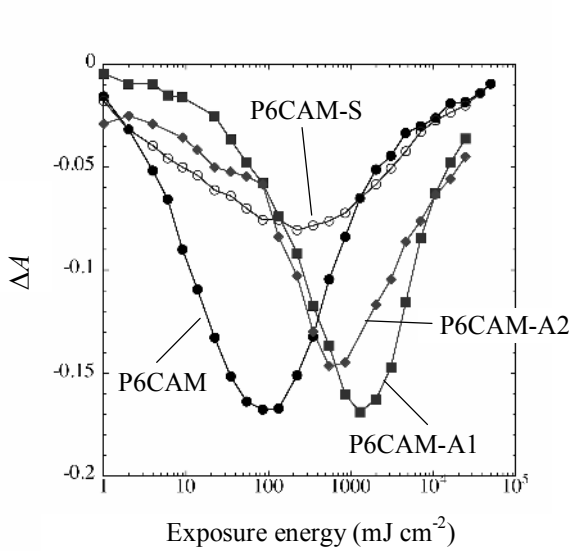

Figure 4-7 Change in photoinduced optical anisotropy of polymers.

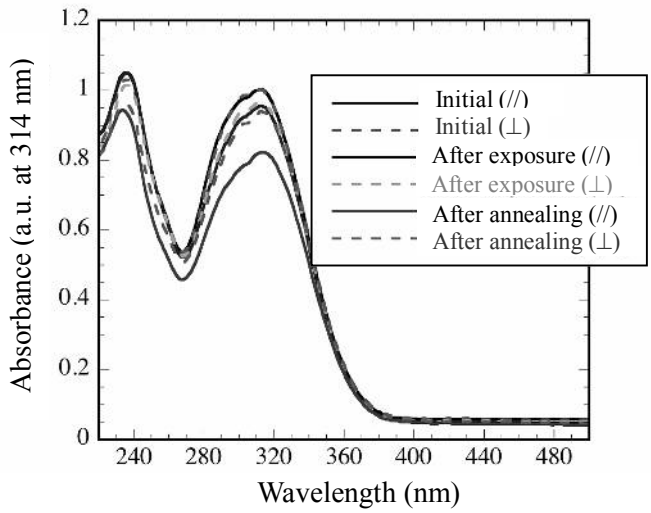

Figure 4-8 Polarized absorption spectra of **P6CAM-A1** film.

The annealing temperature affects the efficiency of the thermal amplification of the molecular alignment of the film. The amplified molecular alignment is evaluated using the following equation,

$$S = (A_{\parallel} - A_{\perp}) / (A_{(\text{large})} + 2A_{(\text{small})})$$

$A_{(\text{large})}$ is the larger value of $A_{\parallel}$ and $A_{\perp}$, and $A_{(\text{small})}$ is the smaller one.

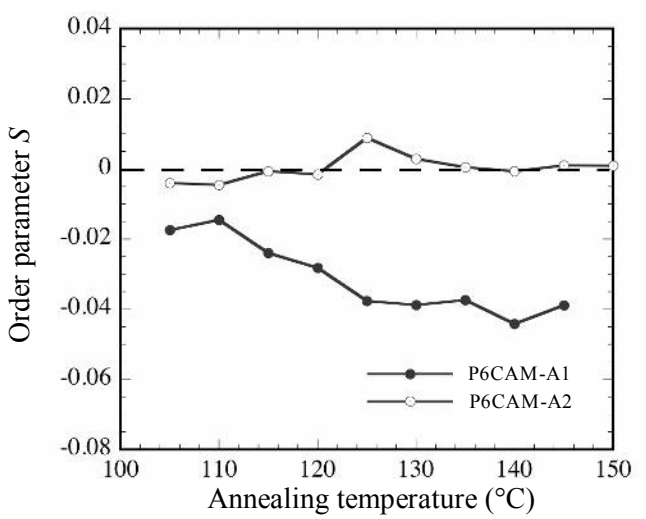

Figure 4-9 Thermally enhanced in-plane order parameter of polymer films containing cinnamide groups as a function of annealing temperature. The degree of photoreaction was fixed in 3 %.film.

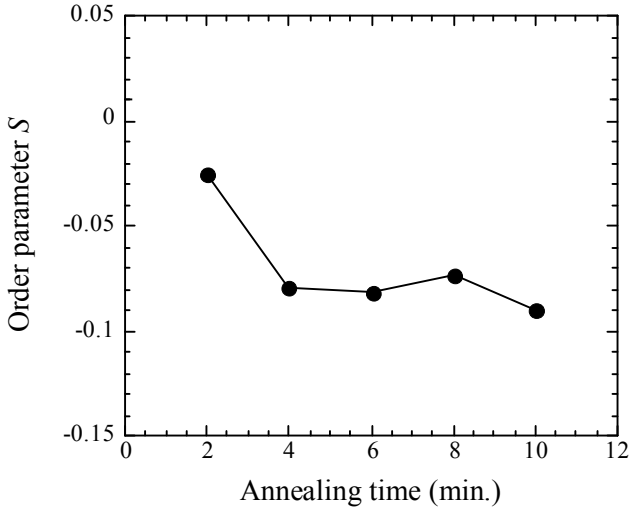

Figure 4-10 Thermally enhanced *S* value of **P6CAM-A1** film when the annealing time is varied.

Figure 4-9 represents the amplified *S* values of the **P6CAM-A1** and **A2**, when the exposed film is annealed at various temperatures. It is observed that the amplification occurred for **P6CAM-A1** films when the annealing temperature was between 130 and 150 °C while **P6CAM-A2** showed no amplification. Although the amplification in **P6CAM-A1** film was induced when the film was heated over 4 minutes, we fixed the annealing time in order to unify the experimental condition to the previous work (**Figure 4-10**). Additionally, the amplified value was smaller than that of, previous work, **P6CAM**. It can be presumed that the hydrogen bonding perpendicular to the director axis affects the reorientation behavior.

Finally, we dipped **P6CAM-S** film into liquid 4-alkylaniline in order to study whether cinnamide group directly convert from succiimide film. **P6CAM-S** showed a strong peak at 1739 cm^{-1}, correspond to the C=O bond of succinic imide. On the other hand, the peak decreased and new broad peaks around 1700 – 1650 cm^{-1} were detected alternatively when the reaction proceeded similar to reaction in the powder state. These peaks correspond to phenylamide ring, and indicate that the imide group converted to amide group in a film state (**Figure 4-11**).

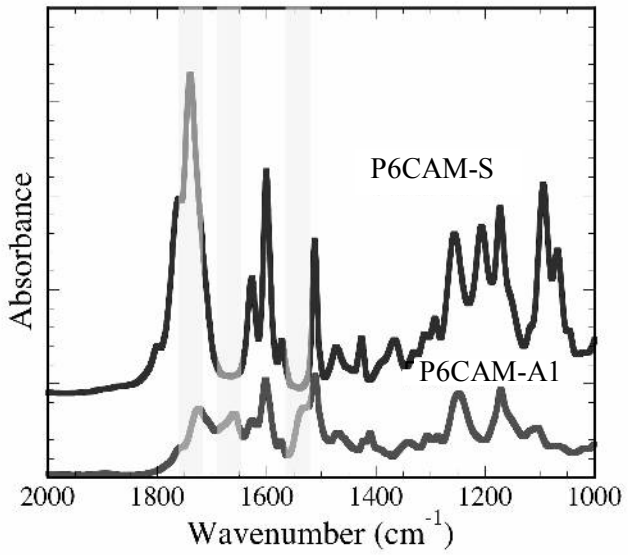

Figure 4-11 ATR-IR spectra of the **P6CAM-S** and **P6CAM-A1** film.

4-4.Conclusion

A novel photoreactive LC polymer via polymer reaction was prepared. The cinnamic acid activated ester easily converted to amide by mixing with amine derivative and the solubility of the polymer reduced due to hydrogen bonding. Upon exposure to UV light and subsequent

annealing, the LC cinnamide exhibited axis selective photoreaction and this was followed by thermally amplification of molecular orientation. However, photoreactivity, LC stability and thermal amplification behavior of the cinnamide group were limited compared to that of original cinnamic acid group, suggesting that the lateral hydrogen bonding disturbs molecular reorientation behavior.

4-5. References

1) B. J. Rancatore, C. E. Mauldin, S. H. Tung, C. Wang, A. Hxemer, J. Strzalka, J. M. J. Fr´echet, T. Xu: *ACS Nano*, **2000**, *4*, 2721.

2) M. Kondo, J. Miyake, K. Tada, N. Kawatsuki: *Chem. Lett.*, **2011**, *40*, 264.

3) G. Yaning, H. Fang, L. Xi, Z. Zhiqiang, Z. Wang, X. Wang: *Chem. Mater.*, **2007**, *19*, 3877.

4) J. He, Y. Zhao, Y. Zhao: *Soft. Matter.*, **2009**, *5*, 308.

5) N. Kawatsuki, R. Ando, R. Ishida, M. Kondo, Y. Minami: *Macromol. Chem. Phys.,* **2010***, 211*, 1741.

6) N. Kawatsuki, A. Hiraiwa, K. Tada, M. Kondo, H. Ono: *Jpn. J. Appl. Phys.*, **2009**, *48*, 120208.

7) E. Uchida, N. Kawatsuki: *Macromolecules*, **2006**, *39*, 9357.

8) X. X. Li, R. Wen, Y. Zhang, L. Zhu, B. Zhang, H. Zhang: *J. Mater. Chem.*, **2009**, *19*, 236.

9) N. Kawatsuki, T. Neko, M. Kurita, A. Nishiyama, M. Kondo: *Macromolecules*, **2011**, *44*, 5736.

Chapter 5

Photoreaction and Photoalignment Behavior of Novel Polyamic-Ester Derivatives Containing a Photo-Cross-Linkable Group

5-1. Introduction

To fabricate liquid crystal displays (LCDs), an uniform LC alignment is required. Mechanical rubbing of a polyimide film, although it is the most common process for the LC alignment in LCD industries, involves some problems such as non-uniformity in large size LC alignment, and the presence of dust and scratches upon rubbing. To overcome these problems, photoinduced alignment of nematic LCs has recently received much attention because it is the most promising candidate for realizing large scale LC alignment without any defects. This technique is based on the anisotropic photoreaction of the alignment films by the use of polarized light.[1,2] Additionally, the key technologies of photoalignment involve photosensitive materials and fabrication process. High photosensitivity of alignment materials is strongly required in order to put photoalignment to mass-production.

A wide range of photoreactive polymers including azobenzene-containing compounds,[3,4] polyvinyl cinnamate derivatives,[5] and polyimides (PIs)[6-9] have been investigated for the LC photoalignment layer. Among them, PI showed best properties as the LC alignment layer, exhibiting good alignment ability and electric properties, and high thermal stability. However, large exposure energy is generally required in order to achieve sufficient LC alignment quality on PI films. This is because the photoinduced optical anisotropy of PI films is based on the photodegradation of the materials.

In contrast, polyvinyl polymers containing photo-cross-linkable side groups, such as cinnamate, coumarin, and chalcone moieties show high photosensitivity compared to photodecomposition of PI, and can be used as the LC photoalignment layer using linearly polarized ultraviolet (LPUV) light.[10,11] Additionally, photosensitive PIs with photo-cross-linkable side groups have been synthesized.[12,13]

In this Chapter, I describe a new photoreactive polyamic-ester (**PAE**) derivative containing *p*-phenylene diacrylate for LC photoalignment layer. The influence of the exposure condition on the photoreactivity as well as LC alignment behavior were investigated.

5-2. Experimental Section

5-2-1. Materials and Characterization

Chemical structure of **PAE** is depicted in **Figure 5-1**. **PAE** was prepared by the poly-condensation reaction with 2,2-bis (4-aminophenyl)-hexafluoropropane, *p*-phenylene diacrylic acid chloride and 2,5-bis (ethoxycarbonyl) terephthalic acid chloride in dry N-Methyl-2-pyrrolidone (NMP). Polymer composition was measured by ^{1}H-NMR. The number average molecular weight (M_n) of **PAE** determined by gel-permeation chromatography was about 31,000. Heat imidization reaction of **PAE**, detected using FT-IR spectroscopy, started around 190 °C.

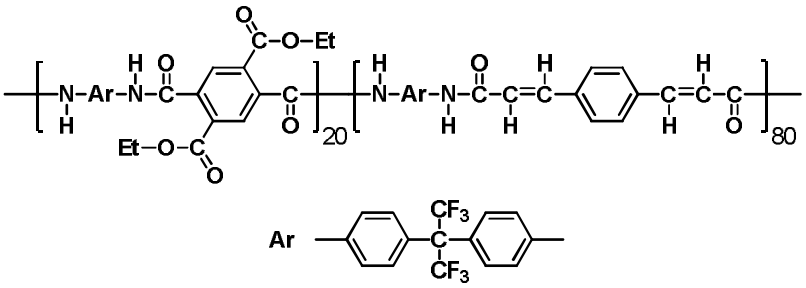

Figure 5-1 Chemical structure of **PAE**.

5-2-2. Photoreaction

Three processes for fabricating the alignment layer are illustrated in **Figure 5-2(a)-(c)**. To prepare the alignment layer, **PAE** was dissolved in NMP / Butyl-cellosolve (BCS) mixed solvent and then spin-coated onto quartz or ITO glass substrates. After pre-baking at 80 °C for 5 min, film thickness was controlled at 30-50 nm. The photoreaction was performed under several conditions (**Figure 5-2**) using an ultrahigh-pressure Hg lamp equipped with Glan-Taylor polarizing prisms and cut filter under 290 nm to obtain LPUV light with an intensity of 14 m Wcm^{-1} at 365 nm. The degree of photoreaction was estimated by monitoring the decrease in absorbance at 340 nm using UV spectroscopy. The photoinduced optical anisotropy, ΔA, which was evaluated using the polarization absorption spectra, is expressed in the following eq.

$$\Delta A = A_{\parallel} - A_{\perp}$$

where $A_{\parallel}$ and $A_{\perp}$ are the absorbances parallel and perpendicular to the polarization (**E**) of the

LPUV light.

To evaluate LC alignment behavior, an anti-parallel LC cell was fabricated using two photoreacted films. The 12.5 μm-thick LC cell was filled with a nematic LC mixture (ZLI-4792: Merck Japan, T_i = 102 °C) doped with 0.1 wt% of dichroic dye of DB14 (Ardrich) at 110 °C and then cooled slowly. The alignment direction of the dye was measured by a polarized UV-vis spectroscopy and LC alignment quality was evaluated by polarized optical microscopy (POM) observation of the LC cell.

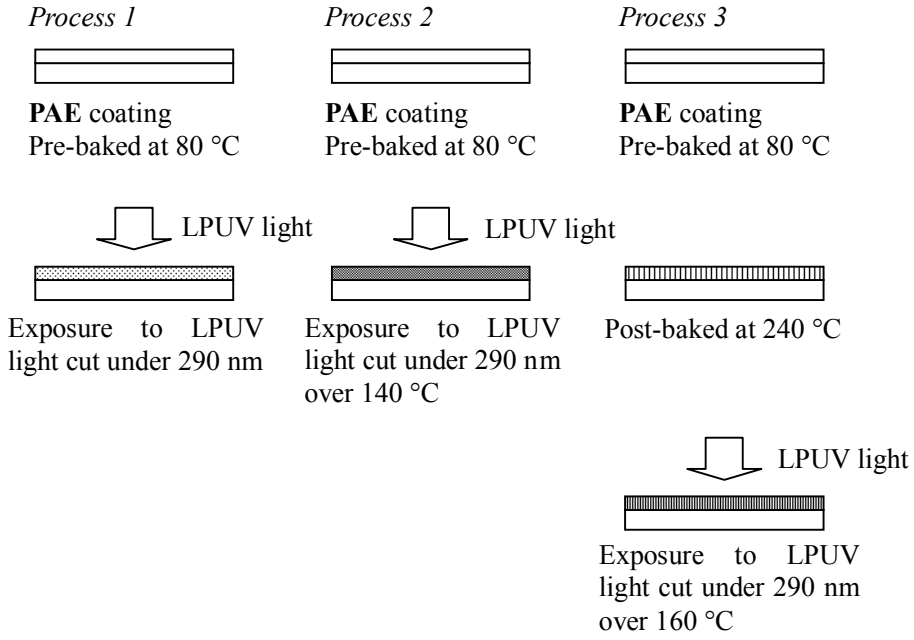

Figure 5-2 Three types of fabrication process for the photoalignment layer.

5-3. Results and Discussion

5-3-1. Photoreaction of PAE

Figure 5-3(a) shows the changes in the absorption spectrum of a **PAE** film upon irradiating with LPUV light at r.t. (*Process 1*). It reveals that the absorption around 340 nm gradually decreases when exposure dose increases. A new absorption band around 270 nm appeared, which increased until the exposure dose was 3.0 J cm^{-2}. After additional exposure over 3.0 J cm^{-2}, absorption band around 250 nm increased. Additionally, two isosbectic points at 300 nm and 270 nm were observed, which appeared during the course of irradiation with varying exposure dose. This indicates that the [2 + 2] photodimerization of the *p*-phenylene diacrylate

group firstly proceeds from one side and then to the other side of the diacrylate group stepwise as exposure dose increased.

Since the photoreaction of the *p*-phenylene diacrylate group occurred axis-selectively,[14] a photoinduced negative optical anisotropy of the film appeared as shown in **Figure 5-3(b)**. In the early stage of photoreaction until film was irradiated 3.0 J cm^{-2}, the negative dichroism was observed around 340 nm. Further exposure to the film led to blue shift of ΔA that also might be due to the stepwise photoreaction of *p*-phenylene diacrylate group.

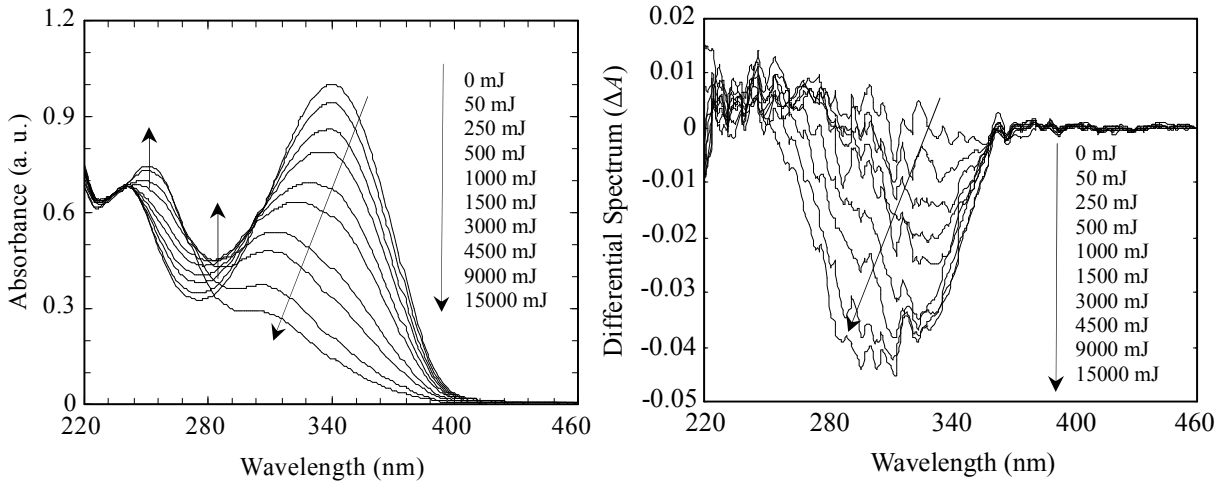

Figure 5-3 (a) Absorption spectral changes of **PAE** film irradiated with UV light at r.t. as a function of exposure dose. (b) Differential spectrum after LPUV irradiation at r.t. as a function of exposure dose.

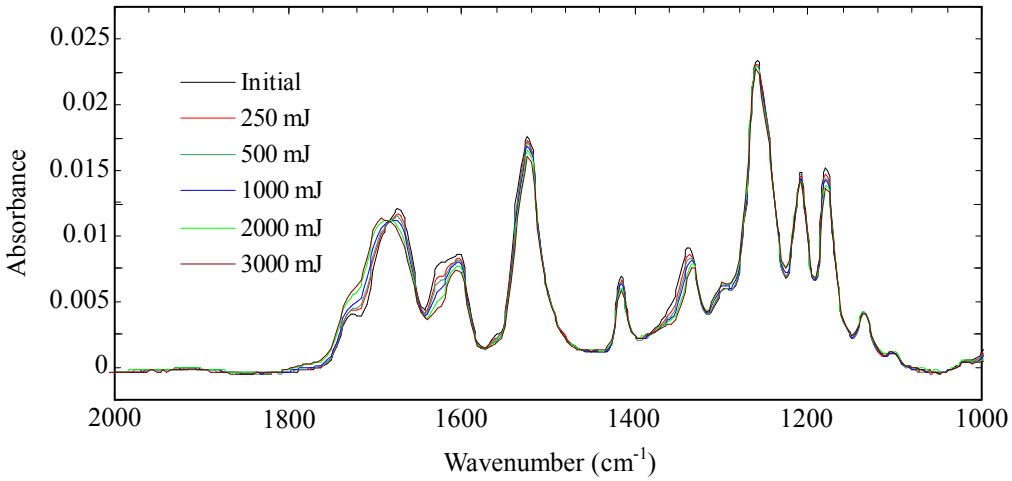

Figure 5-4 Changes in FT-IR spectrum of **PAE** film on ITO glass substrate irradiating with UV light at room temperature. Thickness: 100 nm.

The photoreaction of a **PAE** film was further elucidated by FT-IR spectroscopy. **Figure 5-4** shows the changes in the FT-IR spectrum of a **PAE** film before and after irradiating with LPUV light at room temperature (*Process 1*). The absorption bands at 1730, 1670 and 1628 cm^{-1} before irradiation are assigned to C=O stretching of ethyl-ester, C=O stretching of NH−C=O−C=C and C=C stretching, respectively. After exposure, the absorption band at 1628 cm^{-1} decreased as consequence of the photo-cross-linking reaction. C=O stretching at 1670 cm^{-1} decreased and shifted to long wavenumbers, and a new shoulder absorption appeared around 1730 cm^{-1}. These changes mean a loss of the conjugation for the carbonyl group due to the photo-cross-linking reaction of *p*-phenylene diacrylate goup.

The effect of irradiation temperature on photoreaction behavior of **PAE** was investigated by irradiating films under heating at various temperatures. **Figure 5-5** plots the degree of the photoreaction and induced ΔA as a function of exposure temperature when films were irradiated with 250 mJ cm^{-2} (*Process 2*). The photoreaction of **PAE** accelerated drastically when the irradiation temperature was 140 °C and then proceeded gradually as exposure temperature increased. The estimated photosensitivity improves by 8 times at 240 °C, as compared to that at r.t. Since the mobility of **PAE** main chain improves at elevated temperatures, exposing at elevated temperatures accelerate the photodimerization of **PAE** film. Furthermore, the photoinduced negative ΔA at 340 nm increased when the irradiation temperature increased,

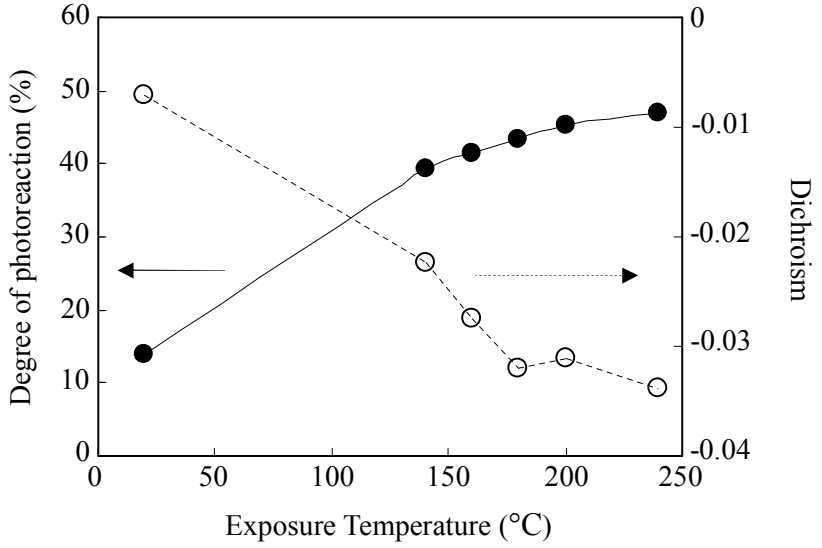

Figure 5-5 The degree of photoreaction of the *p*-phenylene diacrylate group (black circles), and dichroism ($A_{\parallel} - A_{\perp}$) at 340 nm after LPUV irradiation as a function of exposure temperature (white circles).

especially at 180 °C and higher. The maximum Δ*A* increased from -0.0097 at r.t. to -0.0323 at 240 °C.

Figure 5-6 shows a comparison of the photoinduced Δ*A* between the films that were irradiated at r.t. and at 240 °C. In case of exposing at 240 °C, the maximum Δ*A* was obtained when the film was irradiated with 250 mJ cm^{-2}. However, the value of Δ*A* was almost equal to that of exposing 3000 mJ cm^{-2} to the film at r.t. This means that irradiating films under heating process is not suitable for increasing photoinduced optical anisotropy in spite of the accelerating photoreaction due to improvement mobility of **PAE** main chain at elevated temperature. Additionally, further exposure to the film led to blue shift and spread of Δ*A* wavelength band as in the case of photoreaction at r.t., that might be attributed to the stepwise photoreaction of *p*-phenylene diacrylate group.

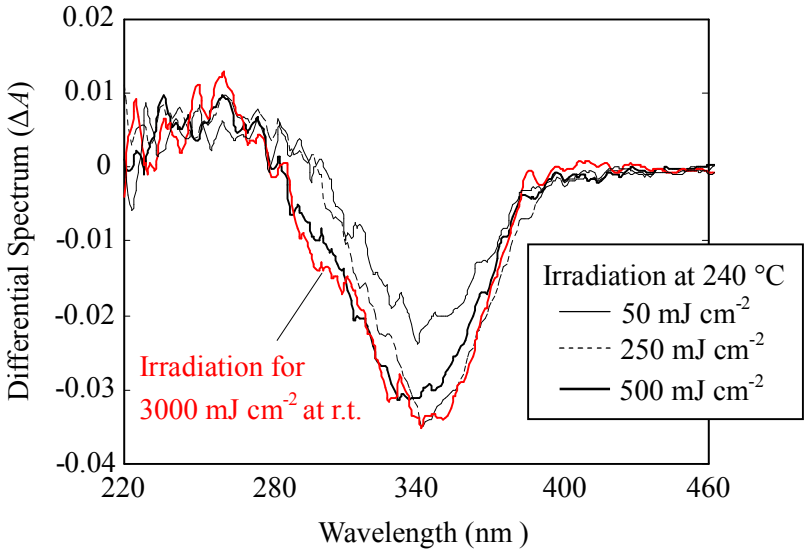

Figure 5-6 Differential spectrum after LPUV irradiation at 240 °C as a function of exposure dose.

5-3-2. LC Alignment

The LC alignment behavior on **PAE** film was evaluated using parallel LC cells. **Figures 5-7(a)-(c)** display the POM image of LC cells using alignment layer of **PAE** irradiated with 50 mJ cm^{-2}, 250 mJ cm^{-2} and 500 mJ cm^{-2} at r.t., respectively (*Process 1*). Since irradiating a **PAE** film with LPUV at r.t. leads to a negative optical anisotropy due to the axis-selective [2 + 2] photodimerization, LC alignment direction is perpendicular to **E** of LPUV light. This is caused by a decreased interaction between LC molecules and photo-cross-linked main chain

parallel to **E**. However, LC alignment obtained using alignment layer fabricated by *process 1* was not uniform regardless of the exposure energy as shown in **Figures 5-7(a)-(c)**, where the disclination lines were observed. In contrast, improved LC alignment quality was observed when using alignment layers fabricated by *Process 2*. **Figures 5-7(d)-(f)** display the POM image of LC cells using alignment layer of **PAE** irradiated with 50 mJ cm^{-2}, 250 mJ cm^{-2} and 500 mJ cm^{-2} at 240 °C respectively. Especially, uniform LC alignment was obtained when the **PAE** film was irradiated for 500 mJ cm^{-2} (**Figure 5-7(f)**).

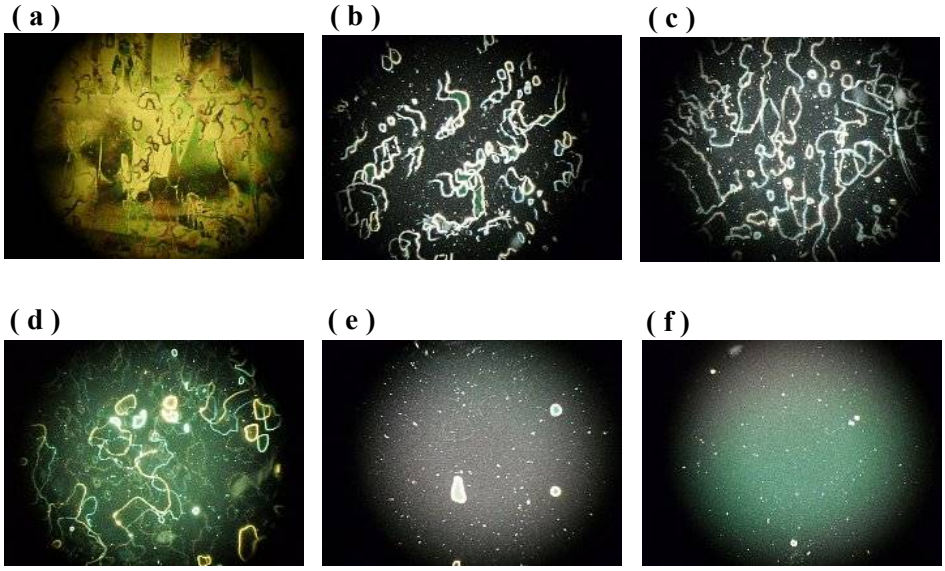

Figure 5-7 POM photograph of LC cells using **PAE** film irradiated with LPUV at different exposure doses, (a) **PAE** irradiated for 50 mJ cm^{-2} at r.t., (b) **PAE** irradiated for 250 mJ cm^{-2} at r.t., (c) **PAE** irradiated for 500 mJ cm^{-2} at r.t. (d) **PAE** irradiated for 50 mJ cm^{-2} at 240 °C, (e) **PAE** irradiated for 250 mJ cm^{-2} at 240 °C, (f) **PAE** irradiated for 500 mJ cm^{-2} at 240 °C.

Additionally, influence of the exposure temperature on the LC alignment quality was investigated. **Figures 5-8(a)-(c)** display POM photographs of LC cells when the **PAE** films were exposed for 250 mJ cm^{-2} at various temperatures. The LC alignment became uniform when the exposure temperature was higher than 160 °C. This also suggests that the increased photoinduced optical anisotropy of **PAE** films accompanied by the increased photoreactivity at elevated temperatures played an important role in the improvement of the LC alignment quality. However, uniform LC alignment was not achieved when the **PAE** films were exposed to LPUV with 250 mJ cm^{-2} at 160 °C after the imidization reaction (*Process 3*) as shown in

Figure 5-9(a). This is because *Process 3* could not increase the photoinduced optical anisotropy compared to *Process 2*. This is caused by the elimination of main chain mobility by the thermal imidization reaction (**Figure 5-9(b)**).

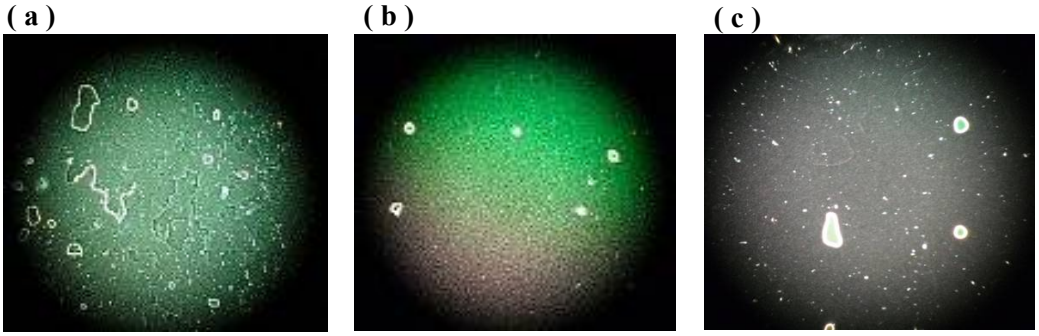

Figure 5-8 POM photograph of LC cells using **PAE** film irradiated for 250 mJ cm^{-2} at different temperatures, (a) **PAE** irradiated at 140 °C, (b) PAE irradiated at 160 °C, (c) **PAE** irradiated at 240 °C.

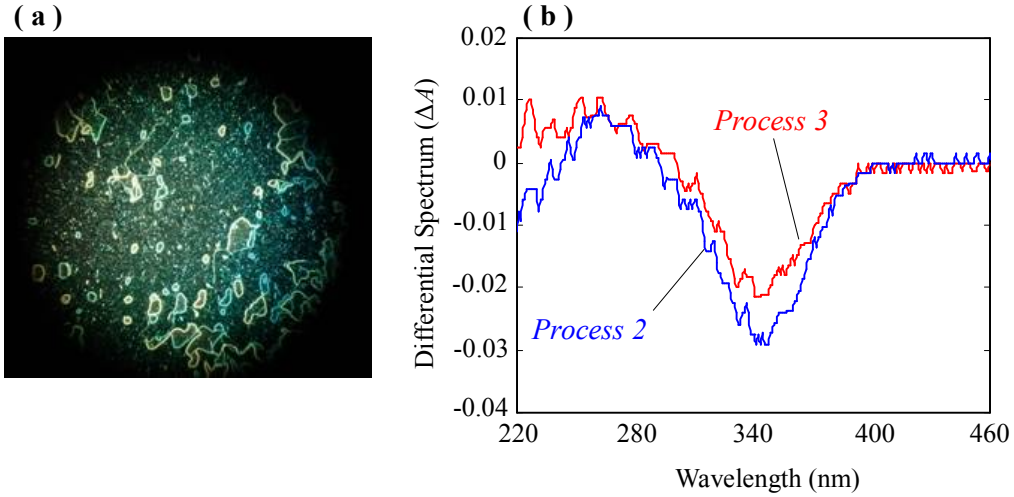

Figure 5-9 (a) POM photograph of LC cells using **PAE** irradiated for 250 mJ cm^{-2} at 160 °C after post-baked at 240 °C. (b) Comparison of differential spectrum of films irradiated for 250 mJ cm^{-2} at 160 °C (*Process 2*) and irradiated for 250 mJ cm^{-2} at 160 °C after post-baked at 240 °C (*Process 3*).

5-4. Conclusion

In summary, a new photo-cross-linkable polyamic-ester derivative containing *p*-phenylene diacrylate for photoalignment layer was developed. Since the degree of photoreaction of **PAE**

film was controlled by varying the exposure temperature of the film, an improvement of LC alignment quality using low irradiation dose of LPUV was achieved due to the improved mobility of polymer chain before the imidization reaction. This result indicates that this irradiation process can be very useful for improvement of the throughput of alignment process in mass production of photo-cross-linkable high performance polymers.

5-5. References

1) M. O'Nell and S. M. Kelly: *J. Phys. D: Appl. Phys.*, **2000**, *33*, R67.

2) V. G. Chigrinov, V. M. Kozenkov and H. S. Kwok, *Photoalignment of Liquid Crystalline Materials: Physics and Applications*, Willy, **2008**

3) K. Ichimura: *Chem. Rev.*, **2000**, *100*, 1847.

4) W. M. Gibbons, P. J. Shannon, S. T. Sun and B. J. Swetlin: *Nature*. **1988**, 4, 351, 49.

5) M. Schadt, K. Schmitt, V. Kozinkov and V. Chigrinov: *Jpn. J. Appl. Phys.*, **1992**, *31*, 2155.

6) H. Endo, Y. Miyama, T. Nihira, H. Fukuro, E. Akiyama and Y. Nagase: *J. Photopolym. Sci.*, **2000**, *13*, 277.

7) M. Nishikawa, T. Kosa and J. L. West: *Jpn. J. Appl. Phys.*, **1999**, *38*, L334.

8) C. J. Newsome and M. O'Neill: *J. Appl. Phys.*, **2000**, *88(12)*, 7328.

9) S. -K. Park, U. -S. Jung, S. –B. Kwon, M. Yi, Ahn, J. –S. Kim, Y. Kurioz and Y. Reznikov, *J. Soc. Inf. Disp.*, **2010**, *18/3*, 199.

10) N. Kawatsuki: *Chem. Lett.*, **2011**, *40*, 548.

11) O. Yaroshchuck and Y. Reznikov: *J. Mater. Chem.*, **2012**, *22*, 286

12) S. W. Lee, T. Chang and M. Lee: *Macromol. Rapid Commun.*, **2001**, *22*, 941.

13) W. C. Lee, C. S. H and S. T. Wu: *Jpn. J. Appl. Phys.*, **2000**, *39*, L471.

14) N. Kawatsuki, A. Kikai, R. Fukae, T. Yamamoto and O. Sangen: *J. Polym. Sci., Part A Polym. Chem.*, **1997**, *35*, 1849.

15) N. Kawatsuki, C. Suehiro, H. Shindo, T. Yamamoto and H. Ono: *Macromol. Rapid Commun.*, **1988**, *19*, 201.

Chapter 6

Application of Molecular Oriented Film to a Photoalignment Layer for In Plane Switching Mode LCD

6-1. Introduction

The fabrication of high resolution and high contrast In Plane Switching (IPS) mode liquid crystal display (LCD) requires an uniform and stable fine-pitch LC alignment. Mechanical rubbing of a polyimide film, which is the most conventional process for the LC alignment in LCD industries, involves several problems such as non-uniformity in large size LC alignment, the generation of dust and scratches upon rubbing. To overcome these problems, photoalignment technique has received much attention from the view point of practical interest.

Photoalignment is based on an anisotropic photoreaction of photosensitive polymeric layers by the use of polarized light.[1-5] After widely exploring of photo-reactive material for the LC alignment layers (ALs), it can be concluded that photosensitive polyimides show the best properties as the photo-alignment layer for IPS LCD at present, as they exhibit good alignment stability and consequently reduces image sticking of IPS LCD strongly. [6-9] Since photoinduced optical anisotropy of polyimide (PI) film is based on the photodegradation of the materials along parallel direction to the polarization of LPUV light, optical anisotropy on film surface seems to be quite large as in the case of mechanical rubbed film. I consider that this large optical anisotropy of PI surface induces strong interaction between LC molecules and photoalignment layer, which lead to good alignment stability of LC. However, a large exposure energy is generally required to achieve sufficient LC alignment stability on PI films because it needs sufficient amount of axis-selective photodegradation of the materials. Therefore, alignment materials which can induce large optical anisotropy with high photosensitivity are strongly required.

In this way, photoalignment layers revealing high photosensitivity and the resultant molecularly oriented structure should establish good image sticking property for IPS LCD. In this context, I describe LC photoalignment properties of photoalignment layers comprising of photoreactive polymer liquid crystals (PLCs) in this chapter. Since PLC

exhibits photoinduced molecular reorientation, excellent properties for the practical use of IPS LCD can be attained.

6-2. Experimental Section

6-2-1. Materials

The schematic illustrated structure of **PLC1** used in this study is depicted in **Figure 6-1**. **PLC1** exhibits LC phase between 133 °C and 197 °C. For the reference of the LC ALs used in this work are summarized in **Table 6-1**. **A1** is **PI** for the photoalignment IPS-LCD and **A2** and **A2'** are for the mechanical rubbing IPS-LCD,[10] respectively. **A1**, **A2** and **A2'** are supplied from Nissan chemical industries, LTD. The number average molecular weight (M_n) of **PLC1** determined by gel-permeation chromatography was approximately 17000.

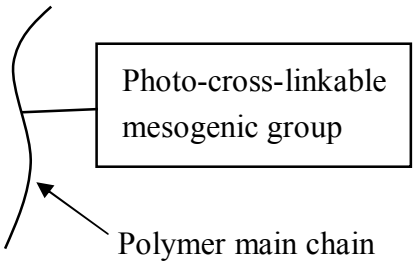

Figure 6-1 Schematic illustration of **PLC1**.

Table 6-1. Characteristics of used reference ALs in this study.

Reference Material	Conventional PI
A1	For photoalignment IPS LCD
A2, A2'	For rubbing type IPS LCD

6-2-2. Fabrication of Alignment Layer and Characterization

100 nm-thick polymer films were prepared by spin-coating on quartz, glass substrate with ITO and glass substrate with comb-like electrode. The photoreactions were performed using an ultrahigh-pressure Hg lamp equipped with band-pass filter for each wavelength and UV polarizer made of a multicoated dielectric film to obtain LPUV light of 254 or 313 nm with intensity of 2.5 and 10 mW cm^{-2}, respectively. The degree of photoreaction was estimated by monitoring the decrease in absorbance at 313 nm using UV spectroscopy. The photoinduced

optical anisotropy, ΔA, which was evaluated using the polarization absorption spectra, is expressed by the following eq.

$$\Delta A = A_{\parallel} - A_{\perp}$$

where $A_{\parallel}$ and $A_{\perp}$ are the absorbances parallel and perpendicular to the polarization (**E**) of the LPUV light. The thermally enhanced molecular reorientation was carried out by annealing exposed PLC films at elevated temperature for 10 min. The in-plane order was evaluated using the order parameter, S, and is expressed as following Eq.

$$S = (A_{(\text{large})} - A_{(\text{small})}) / (A_{(\text{large})} + 2A_{(\text{small})})$$

where $A_{(\text{large})}$ is the larger value of $A_{\parallel}$ and $A_{\perp}$ and $A_{(\text{small})}$ is smaller one. $A_{\parallel}$ and $A_{\perp}$ are the absorbances parallel and perpendicular to **E** of LPUV light, respectively.

6-2-3. Evaluation of LC Cell

6-2-3-1. LC Alignment

To evaluate LC alignmentability, an anti-parallel LC cell was fabricated using two ITO substrates with alignment treated films. One of the alignment treatment consists of irradiation of 254 or 313 nm LPUV light and subsequent annealing at LC temperature range of alignment materials in the case it is necessary. Another consist of mechanical rubbing. The 6 μm-thick LC cell was filled with a nematic LC mixture (MLC-2041: Merck Japan, T_i = 80 °C). LC alignment quality was evaluated by polarized optical microscopy observation (POM) of the LC cell.

6-2-3-2. IPS Cell Fabrication

In order to evaluate image-sticking property led by alignment stability and electric properties, an anti-parallel LC cell was fabricated using comb-like patterned substrates with alignment treated films. Schematic illustration of IPS cell is shown in **Figure 6-2**. After the 4 μm-thick IPS LC cell was filled with a

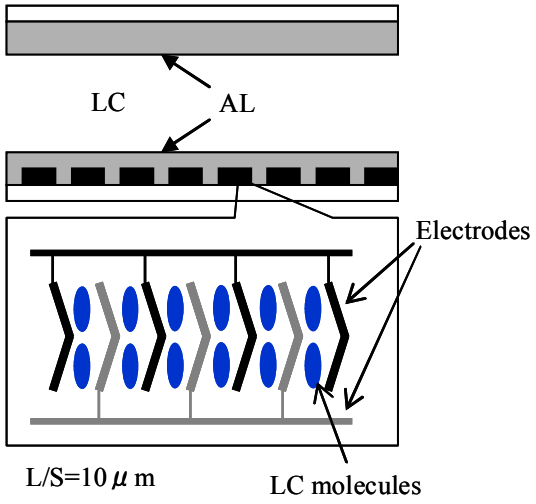

Figure 6-2 Rough sketch of IPS mode test cell.

nematic LC mixture (MLC-2041: Merck Japan), it was annealed at 120 °C for 60 min. and then, gradually cooled to room temperature in order to obtain uniform LC alignment.

6-2-3-3. Evaluation of Image Sticking due to Anchoring Energy

IPS LC cells with two pixels were prepared as described above. Image sticking property was evaluated by measuring the azimuthal deviation of the LC director from the easy axis (= $\Delta\theta$) after AC driving (30 Hz, 16 V_{pp}) for 300 h at 60 °C as described in the literature. [11, 12] Measurement principal of $\Delta\theta$ is shown in **Figure 6-3**.

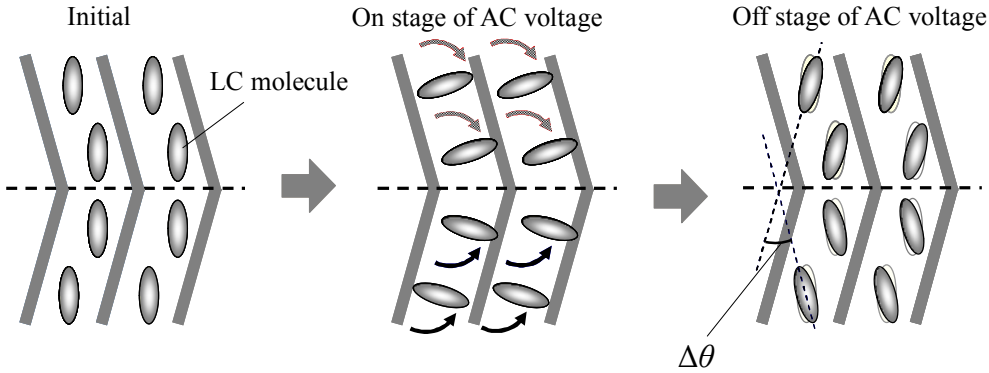

Figure 6-3 Rough sketch of measurement of principal LC director deviation after AC driving.

6-2-3-4. Black Level Measurement

Black level of IPS LC cell was evaluated by measuring pixel luminance of LC cells with CCD camera and polarized optical microscopy observation (POM) of LC cells.

6-2-3-5. Electric Properties of LC Cell

Voltage Holding Ratio (VHR) of LC cells was measured using a conventional method at various temperatures.[13]

6-3. Results and Discussion

6-3-1. Photoreaction and Photo induced Reorientation

As the photoreactive polymer liquid crystal **PLC1** contains photo-cross-linkable side groups which goes under axis-selective photoreaction, the resultant film shows a small optical

anisotropy. **Figure 6-4** plots the degree of the photoreaction and induced ΔA as a function of exposure energy. Photoreaction of **PLC1** proceeds rapidly as exposure energy increase and reaches 15 % with 20 mJ cm^{-2} irradiation. Optical anisotropy is also induced just with a low dose of LPUV under 20 mJ cm^{-2}.

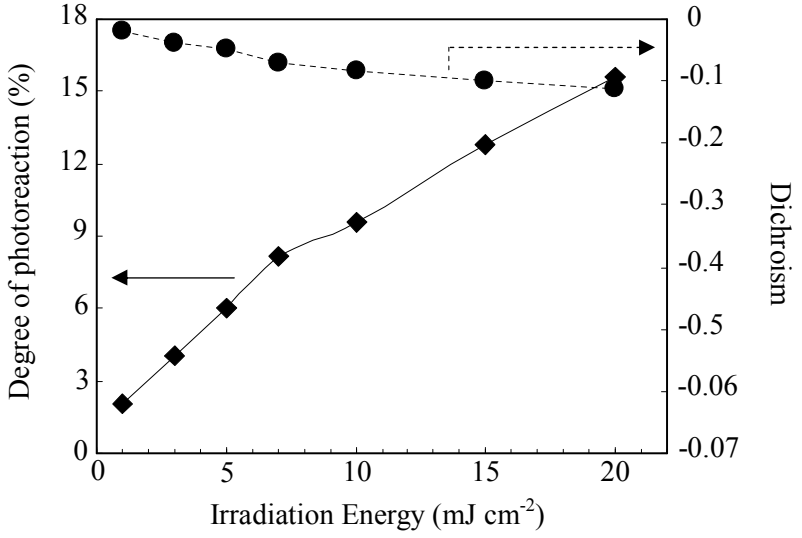

Figure 6-4 The degree of photoreaction (black squares) and UV dichroism (black circles) of **PLC1** as a function of exposure energy.

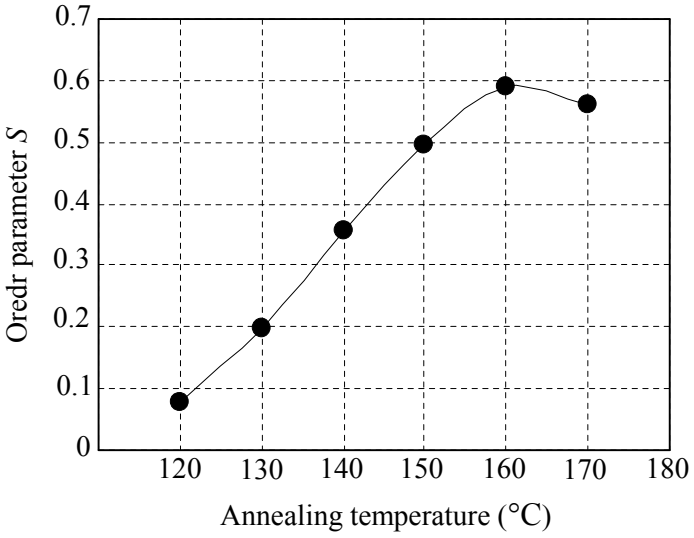

Figure 6-5 Order parameter *S* of **PLC1** film as a function of annealing temperature.

Since the axis-selectively photoreacted groups acts as the trigger, annealing at elevated temperatures enhances the optical anisotropy due to its LC characteristics. Detail of the molecular orientation mechanisms are described in chapter 2 and literature 14. **Figure 6-5** Plots thermally amplified *S* values measured at 313 nm of **PLC1** film irradiated with 5 mJ cm^{-2} as a function of annealing temperature. Molecular reorientation perpendicular to **E** is generated over the LC transition temperature of **PLC1** and *S* value increased after T_m and reached the maximum at 160 °C.

6-3-2. LC Alignment

LC alignment behavior on **PLC1** films was evaluated using anti-parallel cells. **Figure 6-6** displays the photo images of LC cells using alignment layer of **PLC1** treated under different conditions, which correspond to affording the minimum and maximum *S* value respectively. **PLC1** alignment layer was fabricated by irradiating with 5 mJ cm^{-2} and subsequent annealing at 120 and 160 °C for 10 min. For the **PLC1** annealed at 120 °C, although LC alignment direction perpendicular to **E** was obtained, alignment defects attributed to weak azimuthal anchoring energy is observed in **Figure 6-6 (a)**. This was caused by small optical anisotropy of alignment layer since significant thermally enhanced reorientation did not occur when the film was annealed at around T_m. In contrast, due to molecular reorientation of PLC film, improved LC alignment quality was observed when exposed **PLC1** film was annealed at its LC temperature range (**Figure 6-6 (b)**). Since alignment direction of LCs corresponded to the direction its

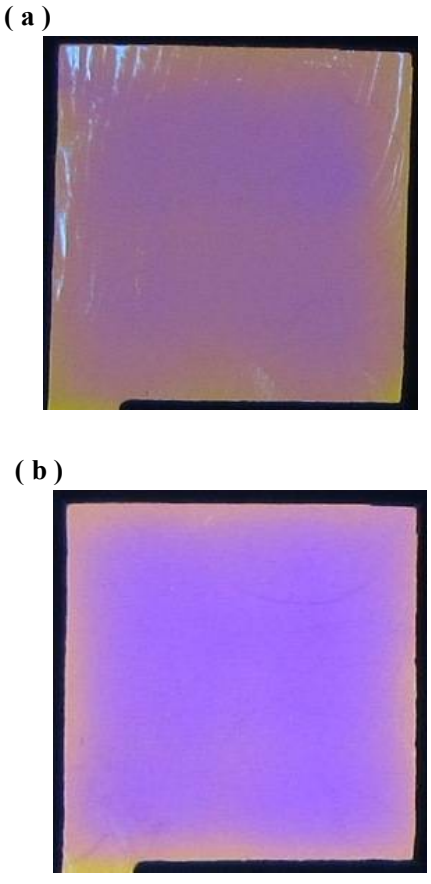

Figure 6-6 Photographs of LC cells using **PLC1**. (a) **PLC1** annealed at 120 °C after irradiating for 5 mJ cm^{-2}, (b) **PLC1** annealed at 160 °C after irradiating for 5 mJ cm^{-2}.

orientation direction of mesogenic group in PLC films, LCs on **PLC1** film aligned perpendicular to **E**. This result means that molecular orientation direction of PLC films determines the LC alignment direction and the number of mesogenic groups aligned uni-directionally is important in order to increase azimuthal anchoring energy strongly.

6-3-3. Image Sticking properties of PLC films

It is well-known that azimuthal deviation of the LC director from the easy axis after driving becomes large if azimuthal anchoring energy is weak. **Figure 6-7** shows a comparison of azimuthal deviations of the LC director on **PLC1**, **A1**, **A2** and **A2'** alignment layers fabricated under several conditions. Since **A2** and **A2'** are rubbing type materials which are currently used for mass-production, if $\Delta\theta$ of **PLC1** is smaller than **A2'**, it is expected that it would show good image-sticking performance on an IPS actual panel. In fact, $\Delta\theta$ for exposed **PLC1** film annealed at 160 °C is 0.08 °. This $\Delta\theta$ is smaller than that of **A1** (= 0.14 °) and **A2'** (= 0.1 °) which are the conventional PIs for photoalignment and rubbing. This is the first result in which a smaller azimuthal deviation of the LC director can be successfully realized by photoalignment layer fabricated with 313 nm LPUV light, compared to **A1** and **A2'**, from the view point of practical use.

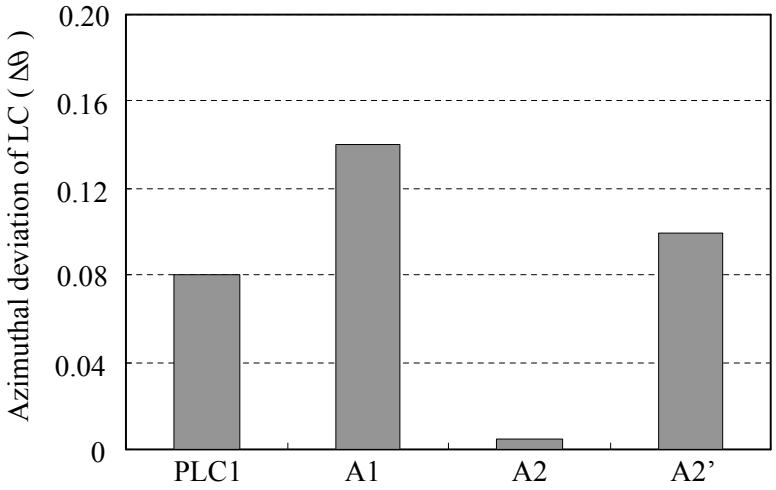

Figure 6-7 Azimuthal deviation of LC director from easy axis of **PLC1**, **A1**, **A2** and **A2'** films. **PLC1** : annealed at 160 °C for 10 min. after irradiating for 5 mJ cm^{-2} with 313 nm LPUV light, **A1** : irradiated for 1800 mJ cm^{-2} with 254 nm LPUV light after post baking at 230 °C 30 min., **A2** : rubbed after post baking at 230 °C 30 min., **A2'** : rubbed after post baking at 230 °C 30 min.

Since molecular reorientation of PLC was performed by self-organizing its LC characteristics, it is considered that the molecularly reoriented state of PLC is a stable state for the mesogenic groups. In fact, LC molecules on PLC alignment layer return to its original position regardless how high stress was applied to PLC films in the driving test. From this result, it is considered that **PLC1** would receive much interest from the view point of mass production because it can combine super high photosensitivity and good image sticking property. In the following section, I describe the IPS LC cell properties using **PLC1** from the view point of practical use.

6-3-4. Black Level of IPS LC Cell using PLC1

Black level of IPS LC cell was evaluated. **Figure 6-8** shows relative value of pixel luminance of LC cell. Luminance value of LC cells fabricated by photoalignment were 30 % darker than that of rubbing because of there is less photo leakage derived from rubbing scratches, alignment defect due to un-uniformity of rubbing around electrode, etc. In addition, the luminance value of **PLC1** was almost equal or improved compared to **A1** regardless both cells are fabricated by photoalignment. It is considered that black level will be attributed to the molecular oriented order on the film surface. Therefore, further detailed investigation for molecular oriented order of film surface is expected.

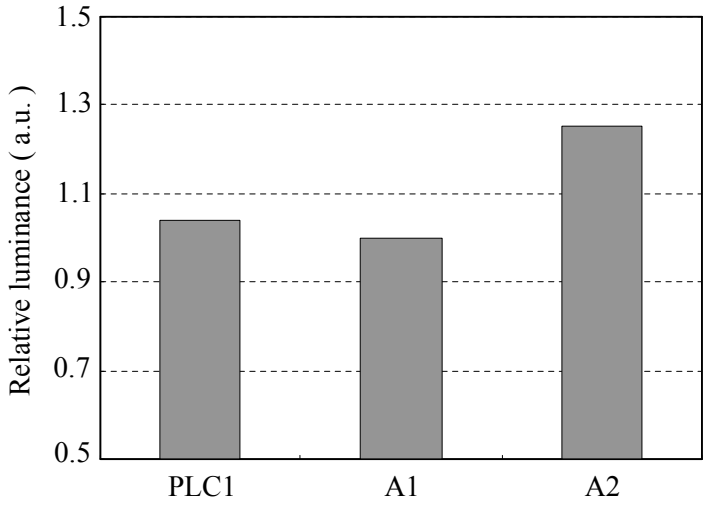

Figure 6-8 Relative value of pixel luminance of IPS LC cells fabricated with **PLC1**, **A1** and **A2** films. **PLC1** : annealed at 160 °C for 10 min. after irradiating for 5 mJ cm^{-2} with 313 nm LPUV light, **A1** : irradiated for 1800 mJ cm^{-2} with 254 nm LPUV light after post baking at 230 °C 30 min., **A2** : rubbed after post baking at 230 °C 30 min.

6-3-5. Other Properties of PLC1

It is proved from our investigation that **PLC1** has good potential for realizing less image sticking due to strong azimuthal anchoring energy with high photosensitivity using 313 nm LPUV light in IPS LCD. On the other hand, satisfying several properties at the same time is required for photoalignment materials besides improving image sticking property. Some of these properties are, for instance, good electric properties, wide process window, etc. Among them, electric properties, especially VHR, are important in order to obtain significant reliability for actual panel applications. The comparison of VHR between both of photoalignment layers **PLC1** and **A1** is summarized in **Table 6-2**. Since it is concerned that VHR of **PLC1** is lower than **A1**, further study to improve it is necessary for practical use.

Table 6-2 Comparison of VHR of photoalignment materials.

	VHR * (%)	
	23 ℃	60 ℃
PLC1	97.2	95.5
A1	98.5	98.1

*Applied voltage 4 V_{pp}, 30 Hz

Table 6-3 Process performance of **PLC1** photoalignment

Solvent selectivity	Soluble in amide-type, ketone type and some kind of glycol type solvent.
Storage stability	Stable over half year at 5 ℃ in dark place and going.
Coating	Flexo printing, and ink jet printing
Cleaning of alignment layer	Free or with DIW

Finally, process performance of **PLC1** photoalignment material for LCD industry is summarized in **Table 6-3**. With respect to solvent system of alignment layer, N-Methyl-2-pyrrolidone (NMP) and Gamma-Butyrolactone (GBL) are currently used because PI is the only suitable material of alignment layer for LCD so far. On the other hand, since **PLC1** can be dissolved in some types of solvent besides NMP and GBL, solvent selectivity is

extended and it is useful to the development of photoalignment materials for flexible LC devices using plastic substrates. Additionally, other process performances of **PLC1** are almost compatible with PI alignment layer. In conclusion, it is expected that **PLC1** which has a molecular oriented structure in its resultant film could change the situation of photoalignment technology.

6-4. Conclusion

In this chapter, I demonstrated a photoalignment layer with high photosensitivity at 313 nm LPUV light, which exhibits good image sticking property due to azimuthal anchoring energy. Since molecular orientation can improve alignment stability of LC molecules by increasing interaction between alignment layer and LC molecules, photoreactive polymer liquid crystal is suitable for the practical use of IPS LCD. In addition, it is revealed that **PLC1** photoalignment material shows good process performance for the practical use in the LCD industry.

6-5. References

1) M. O'Nell and S. M. Kelly: *J. Phys. D: Appl. Phys.* **2000**, *33*, R67.

2) O. Yaroshchuck and Y. Reznikov: *J. Mater. Chem*. **2012**, *22*, 286

3) K. Ichimura: *Chem. Rev.* **2000**, *100*, 1847.

4) M. Schadt, K. Schmitt, V. Kozinkov and V. Chigrinov: *Jpn. J. Appl. Phys.* **1992**, *31*, 2155.

5) W. M. Gibbons, P. J. Shannon, S. T. Sun and B. J. Swetlin: *Nature*. **1991**, 351, 49.

6) H. Endo, Y. Miyama, T. Nihira, H. Fukuro, E. Akiyama and Y. Nagase: *J. Photopolym. Sci.* **2000**, *13*, 277.

7) M. Nishikawa, T. Kosa and J. L. West: *Jpn. J. Appl. Phys*. **1999**, *38*, L334.

8) C. J. Newsome and M. O'Neill: *J. Appl. Phys*. **2000**, *88(12)*, 7328.

9) S. -K. Park, U. -S. Jung, S. –B. Kwon, M. Yi, Ahn, J. –S. Kim, Y. Kurioz and Y. Reznikov: *J. Soc. Inf. Disp*. **2010**, *18/3*, 199.

10) K. Tsutsui, T. Sakai, K. Goto, K. Sawahata, M. Ishikawa and H. Fukuro: *Dig. Tech. Pap*.

SID., **2003**, *38*. 2.

11) T. Suzuki, J. Matsushima, Y. Sasaki, M. Sugimoto, H. Tanalka, C. Mizoguchi, S. Onda, K. Mimura, K. Sumiyoshi: *IDW/AD'05*, **2005**, 57.

12) Y. Momoi, K. Furuta, T. Koda, S. Haneba, K. Yonetake: *proceeding of JLCS conference*, **2010**, 1a03.

13) T. shimazaki, S. mizushima, S. Minesaki, K. Yano, M. Masukawa: *proceeding of JLCS conference*, **1988**, *No. 2B110*, 78.

14) E. Uchida and N. Kawatsuki: *Macromolecules*. **2006,** *39*, 9357.

Conclusions

In chapter 1, a new type of photo-cross-linkable methacrylate polymer liquid crystal (PLC) with a coumarin containing mesogenic side group was synthesized and applied as a photoalignment layer for low molecular mass nematic liquid crystals. For these evaluations, linearly polarized ultraviolet (LPUV) light was directed onto a thin film of PLC under various exposure conditions. When a film was irradiated at room temperature, a small negative optical anisotropy was generated due to angular-selective photo-cross-linking. In contrast, when the film was exposed near the clearing temperature of the PLC, the induced anisotropy was positive due to thermally enhanced photoinduced reorientation of the side groups. The aggregation of the mesogenic groups was also observed when the irradiation was carried out in the liquid crystalline temperature range of the PLC. The LC alignment on the photoreacted film was greatly dependent on these irradiation conditions. As a conclusion, It was made clear that the LC alignment was regulated by the interaction among the LC, the photo-cross-linked side groups and the remaining mesogenic side groups, and that aggregated mesogenic groups inhibited the LC alignment.

In chapter 2, a large orientational order and reversion of the in-plane reorientation direction of mesogenic groups was observed for the first time in novel polymethacrylate liquid crystal films substituted with a 4-methoxycinnamoyloxybiphenyl side group. The reversion was generated by irradiation with LPUV light and a subsequent annealing. Irradiation with LPUV light induces negative optical anisotropy of the films as a result of an axis-selective photoreaction of the side groups. The direction of the thermally enhanced reorientation is dependent on the degree of photoreaction and the distribution of photoproducts, while the induced orientational order in both directions, S, was larger than 0.5. In addition, the distribution of photoproducts in PLC films was analyzed in order to elucidate their contribution to the thermally enhanced reorientation behavior. Initially upon photoreaction, thermal enhancement of the photoinduced negative optical anisotropy was observed. However, when the degree of photodimerization was 15 % or greater, the direction of the thermally enhanced reorientation was found to be parallel to the polarization direction (**E**) of LPUV light. It is concluded that a small amount of photoproduct plays a role in the thermal amplification of the photoinduced negative optical anisotropy in a manner identical to that of PLC with azobenzene side groups. In contrast, photodimerized mesogenic groups generated a reversion of the orientational direction and an enhancement of positive optical anisotropy of

the film through annealing.

In chapter 3, the fabrication of a durable photoalignment layer for LC with high azimuthal anchoring and controllability of the tilt angle, by modifying a PLC reported in chapter 2 was described. A film is irradiated using LPUV light followed by annealing, which induces the molecular orientation of the photoalignment layer. In this way, the nematic LC aligned parallel to the electric vector of the LPUV light, and the alignment layer showed high thermal stability of the orientational characteristics up to 250 °C.

In chapter 4, the novel photoreactive liquid crystalline polymer comprising cinnnamic acid activated ester, which can be easily converted to amide group, through polymer reaction was synthesized. The thermally amplification of mesogenic groups was achieved by exposing films to linearly polarized ultraviolet light and subsequent annealing. However, photoreactivity, LC stability and thermal amplification behavior of the cinnamide group were limited compared to that of original cinnamic acid group, suggesting that the lateral hydrogen bonding disturbs molecular reorientation behavior.

In chapter 5, the photoalignment behavior of LCs on a photoalignment layer containing a novel photosensitive polyamic-ester derivative (PAE) under several fabricating conditions was described. In this way, irradiating PAE films with a LPUV light at temperatures over 160 °C dramatically accelerated the photoreaction and photoinduced optical anisotropy. Furthermore, an improvement of the LC alignment quality was observed on PAE films when films were irradiated over 160 °C.

In chapter 6, photoalignment layers showing high photosensitivity at LP 313 nm light were described. In this way, irradiation of as low as 10 mJ cm^{-2} LP 313 nm light followed by annealing induced a molecularly oriented structure of the photoalignment layers, which showed excellent image sticking property due to strong azimuthal anchoring energy of the IPS LC cell using them. Therefore, it was revealed that enhanced optical anisotropy and its stability induced by molecular orientation, due to its LC characteristics, play an important role in the improvement of image sticking property.

In this thesis, I studied the photoalignment mechanism of LCs on several photo-cross-linkable polymer systems in order to design and synthesize new photo-cross-linkable polymers. Since controllable large and reversible orientation of molecules may prove to be useful in many optical devices as well as LC photoalignment layer, I firstly developed a new type of photo-cross-linkable polymer liquid crystal which showed greatly enhancement of mesogenic groups. Using these molecular oriented films as a

photoalignment layer, enhancement of optical anisotropy and its stability which led to better image sticking property, due to strong azimuthal anchoring energy, of IPS LCD were achieved. This is the first report in which good image sticking property is achieved due to strong azimuthal anchoring energy of a photoreactive polymer liquid crystal from the view point of practical use. By optimizing chemical structure and / or composition of alignment materials, it is expected that photoreactive polymer liquid crystal will be used as photoalignment layer for IPS LCD. In addition, I demonstrated the importance of fabrication process on photoalignment as described in chapter 5. In conclusion, the combination of materials and fabrication process is the key for the photoalignment technology.

List of Publications

1) Photoinduced Anisotropy and Photoalignment of Nematic Liquid Crystals by a Novel Polymer Liquid Crystal with a Coumarin-Containing Side Group.
Nobuhiro Kawatsuki, Kohei Goto and Tohei Yamamoto.
Liquid Crystals, **2001**, *Volume 28*, No. 8, Page 1171-1176.

2) Reversion of Alignment Direction in the Thermally Enhanced Photoorientation of Photo-Cross-Linkable Polymer Liquid Crystal Films.
Nobuhiro Kawatsuki, Kohei Goto, Tetsuro Kawakami and Tohei Yamamoto.
Macromolecules, **2002**, *Volume 35*, Page 706-713.

3) Molecular-Oriented Photoalignment Layer for Liquid Crystals.
Nobuhiro Lawatsuki, Katsuya Hamano, Hiroshi Ono, Tomoyuki Sakai and Kohei Goto.
Japanese Journal of Applied Physics, **2007**, *Volume 46*, No. 1, Page 339-341.

4) Synthesis of Side-Chain Liquid-Crystalline Polymers Based on Post Polymer Reaction
Mizuho Kondo, Yoshiyuki Dozono, Kohei Goto and Nobuhiro Kawatsuki
Molecular Crystals and Liquid Crystals, **2012**, *Volume 563*, Page 121-130.

5) Photoreaction and Photoalignment Behavior of Novel Polyamic-Ester Derivative Containing a Photo-Cross-Linkable Group.
Kohei Goto, Osamu Takeuchi, Mizuho Kondo, Hideyuki Endo and Nobuhiro Kawatsuki.
Molecular Crystals and Liquid Crystals, **2012**, *Volume 563*, Page 139-145.

6) Novel Photoalignment Layer for In Plane Switching Mode LCD Using 313 nm Ultraviolet Light.
Kohei Goto, Hirokazu Yamanouchi, Ryoichi Ashizawa, Atsuhiko Mandai, Tatsuya Nagi, Satoshi Minami, Kimiaki Tsutsui, Motoaki Ishikawa, Mizuho Kondo and Nobuhiro Kawatsuki.

SID 2013 Digest, Page, 537-540 (**2013**) *(Journal of the Society for Information Display*, **2013**, (Now in submitting)

Acknowledgements

This study was carried out at the Department of Materials Science and Chemistry Graduate School of Engineering, Himeji Institute of Technology, University of Hyogo and Electronic Materials Research Laboratories Nissan Chemical Industries, LTD. from April 1999 to March 2002, on year 2007 and from October 2010 to September 2013.

I wish to express my sincere gratitude to Professor Dr. Nobuhiro Kawatsuki, University of Hyogo, for his constant guidance, stimulating valuable discussion, valuable suggestions and encouragement in the course of this study. I gratefully acknowledge Professor Dr. Shinji Matsui, Professor Dr. Takeshi Kawase and Professor Dr. Naoto Matsuo for reviewing the draft of this thesis. I gratefully thank to Dr. Mizuho Kondo, University of Hyogo, for his helpful suggestions. I am grateful to Dr. Hiroyoshi Fukuro, the head of Electronic Materials Research Laboratories Nissan Chemical Industries, LTD., for permitting the publication of a part of this work. And I also wish to express my deepest appreciate to Hideyuki Endo, Motoaki Ishikawa, Dr. Takayasu Nihira, Dr. Kimiaki Tsutsui and Dr. Antonio Daniel Sahade, Nissan Chemical Industries, LTD., for helpful advices and encouragement. Furthermore, I appreciate the active collaboration of Mr. Hirokazu Yamanouchi, Mr. Ryoichi Ashizawa, Mr. Atsuhiro Mandai, Mr. Tatsuya Nagi, Mr. Satoshi Minami, Mr. Tetsuro Kawakami, Mr. Osamu Takeuchi and Mr. Katsuya Hamano and I also thank all other members of the research group of Professor Nobuhiro Kawatsuki.

Finally, I would like to express my gratitude to my parents, Mr. Takeshi Goto and Mrs. Hatsumi Goto, my wife, Noriko Goto, and my son, Kenta Goto, for their constant understanding, encouragement and financial support.

Kohei Goto
Department of Materials Science and Chemistry
Graduate School of Engineering
University of Hyogo
2013